INVESTIGATION OF MINIMUM FLOW CONDITIONS FOR MILK PRODUCTS IN FALLING-FILM EVAPORATORS

A THESIS PRESENTED IN PARTIAL FULFILMENT OF THE REQUIREMENTS
FOR THE DEGREE OF MASTER OF TECHNOLOGY

at

Institute of Technology and Engineering
Massey University
Palmerston North
New Zealand

Shabeshe Paramalingam
2001

SUMMARY

A daily nuisance in the processing of milk in evaporators is *fouling*, an undesirable deposit formed on the heating surface. Breakdown of the liquid film in the evaporator tubes is a major cause of this fouling, which can generally be avoided if the flow of milk is above the minimum peripheral flow. With knowledge of the minimum flow, the plant running time can be extended resulting in reduced cleaning time or frequency. Also, the plant efficiency can be increased without causing film break-up.

There are few models in the literature to estimate minimum peripheral flow (Chung & Bankoff, 1979; Hoke & Chen, 1992; Hartley & Murgatroyd, 1964; Zuber & Staub, 1966) most of which are strongly dependent on the physical properties of the liquid. For many milk products, however these physical properties are not available in the literature.

This thesis presents a standard force-balance theory to determine at what flow rate a stable dry patch will occur. Methods of estimating the required physical properties of milk products are then presented. These cover density, viscosity, contact angle and surface tension over a range of total solids content and temperatures encountered in milk evaporation. These are then used to estimate the minimum peripheral flow within an industrial falling-film evaporator set for given milk products at normal operating conditions. These values are used in testing the minimum flows after each pass in the Powder 3 Plant of Kiwi Co-op Dairies Ltd, at Hawera.

The current operating flows and total solids after each pass in the Powder 3 Plant were tested for minimum flow violation with different milk products and at different times during a run. The milk products are evaporated close to the advancing minimum flow and violate it in certain passes of the evaporation unit. The steady state model of the Powder 3 Plant was validated against these experimental results. The model predicted well the total solids and the outlet flows from passes (except for the first two passes) early in a run but showed deviation after several hours. The deviations were likely due

to constant heat transfer coefficients in the model. Therefore, the steady state model was only used to find flows and total solids after each pass close to start-up.

The validity of the minimum peripheral flow estimation was judged by two different methods. The first involved analysis of the heat transfer coefficients within an industrial evaporator set. The second investigated past operational data from an industrial evaporator set to determine where fouling had occurred and what the peripheral flows were at the time.

ACKNOWLEDGMENTS

I wish to express my sincere appreciation to my supervisor, Dr. Huub Bakker, for his guidance, encouragement and friendship throughout this project. Without his committed attitude, help and advice this project would never have succeeded.

Thanks to Dr. Hong Chen, Kiwi Co-op Dairies Ltd., for providing the place and information necessary to complete my project. He was very helpful and friendly during my time at Hawera. He solved many problems, which I encountered in the operation of evaporators. I really appreciate his encouragement and helpful attitude. Also, I thank him for having lent me his bicycle when I had problems with my car.

The Powder 3 plant operators provided me with help in several ways while I was conducting the experiments at the plant. Also, I would like to thank other staff members who helped me at the plant during my time at Kiwi Co-op Dairies Ltd.

My thanks go also to James Winchester for giving me his mathematical models of Powder-3 falling film evaporators. The models, which he gave me, were very useful in estimating the physical properties of milk. I appreciate his patience in answering my questions while he was busy with both his thesis preparation and work at his farm. Also, I appreciate Dr. Clive Marsh's hospitality when I visited James to gain a better understanding of his model.

I am indebted to the staff of the Institute of Technology and Engineering, Massey University, New Zealand, for assistance with this work and for the facilities provided. I am grateful to the Ministry of Foreign Affairs and Trade, New Zealand, for giving me this opportunity and supporting my study in New Zealand.

I would like to thank also Neil and Helen Walker for accommodating me at their house and treating me like one of their family members. Finally, I would like to express my special thanks to my wife for her encouragement, patience and moral support.

CONTENTS

Summary i

Acknowledgment iii

1. Introduction 1

2. Background 3

2.1 Introduction 3
2.2 Evaporators 3
2.3 Evaporators at Kiwi Co-op Dairies Ltd 4
2.4 Mathematical model 7
2.5 Wetting constraint 10
2.6 Fouling 11
2.7 Hartley and Murgatroyd force criteria 12
2.8 Hoke and Chen force criteria 14

3. Methodology 16

3.1 Introduction 16
3.2 Advancing contact angle and surface tension 17
3.3 Experimental measurement of density 19
3.4 Experimental measurement of viscosity 20
3.5 Minimum flow and Heat transfer coefficient test at Powder 3A Plant 21

4. Theoretical estimation of minimum flow 23

4.1 Introduction 23
4.2 Density 23
4.3 Viscosity 25

4.4 Advancing contact angle and Surface tension 27
4.5 Minimum flow from proposed models 29

5. Tests for minimum flow at the Kiwi, Powder-3 plant 33

5.1 Introduction 33
5.2 Measurements 33
5.3 Actual flow rates and total solids at the end of passes 34
5.4 Validation of Steady state model prediction 36

6. Time-variant heat transfer coefficient **41**

6.1 Introduction 41
6.2 Heat transfer coefficient of Whole milk 41
6.3 Effect of cleanliness of the surface on the HTC 43

7. Historical data check for minimum flow violation **45**

7.1 Introduction 45
7.2 Film break-up and heat transfer coefficient of water 45
7.3 Minimum flow violations with milk products 50

8. Conclusion **58**

9. Recommendations and areas for future work **60**

10. Nomenclature **63**

11. References **65**

12. Appendix **68**

Appendix A : Experimental data for contact angle and surface tension 69
Appendix B : Density 88
Appendix C : Viscosity 90
Appendix D : Contact angle and surface tension 92
Appendix E : Minimum flow 94
Appendix F : Experimental data and results at Powder plant 96
Appendix G : Heat transfer coefficients 101

1. INTRODUCTION

Multiple-effect evaporators are widely used in dairy industries to concentrate milk, which will be further processed in spray driers to produce powder. Compared to the evaporation stage the drying stage consumes a lot of energy. So, from an energy-saving point of view it is important to remove as much water as possible in the evaporation stage. In producing milk powder about 90% of the water removal takes place in the evaporating stage. The operational conditions must be satisfied within the falling film evaporators in order to have continuous production. One of the constraints to the optimisation of the falling-film evaporator is found to be the minimum peripheral flow (Brenmuhl, 1999). Violation of this constraint could cause fouling due to film break-up within the evaporator tubes.

Fouling due to film break-up is a major concern in the operation of falling-film evaporators (Brenmuhl, 1999; Winchester, 2000; Paramalingam et al., 2000). Insufficient flow is found to be the cause of film break-up (Hartley & Murgatroyd, 1964; Chung and Bankoff, 1979; Paramalingam, 1999; Hughes & Bott, 1991). To avoid fouling due to film break-up the flow rate along the tubes should not be less than a minimum flow necessary to sweep off the dry patches. This flow is known as the *advancing minimum flow*, where the flow can no longer advance to cover a dry area. For the safe operation of falling-film evaporators it is also important to know the minimum flow below which film break-up occurs. This minimum flow is known as the *retarding minimum flow*, where the flow can no longer support a full film and the film retards leaving a dry area. The purpose of this study is to determine the minimum flows for milk products and for water. To this end two models are used, proposed by Hartley and Murgatroyd (1964) and Hoke and Chen (1992) to predict film break-up and therefore minimum flows.

Both the Hartley and Murgatroyd (1964) and Hoke and Chen (1992) models were based on the force analysis at the apex of a stable dry patch. The Hartley and Murgatroyd model is suggested for milk products at low total solids and for water, due to its simplicity and because the weight force at the stagnation of a dry patch for

these liquids is not significant. The Hoke and Chen model is suitable for milk products with high total solids and to the high viscosity liquids-as the weight force becomes significant for these liquids. To predict the minimum flows within the evaporator tubes using the models proposed, the physical properties of milk should be known. These include density, viscosity, advancing contact angle, retarding contact angle and the surface tension over the range of operating temperatures and product concentrations.

In chapter 2, the composition and temperature based models (Winchester, 2000) used in estimating the density and the viscosity of milk products are described. The experimental technique from previous studies (Paramalingam, 1999) carried out to find the advancing contact angle and surface tension of milk products and of water is briefly explained in chapter 3. In Chapter 4 the theoretical estimation of both advancing and retarding minimum flows for different milk products and for water are shown.

Chapter 5 presents the testing of current operating flows at Kiwi Co-op Dairies Ltd. Powder 3A Plant with milk products and with water for minimum flow violation. The accuracy of the steady sate model of Powder 3A plant predictions is also presented.

The importance of the heat transfer coefficient of milk products and of water in the falling film evaporators and its variation during runs are explained in chapter 6. In chapter 7, the operational data from Powder 3 Plant were analysed for minimum flow violations and for possible fouling. The data from this plant operating on water are used to infer the occurrences of film break-up and stable dry patches at low flows at evaporator operating conditions. Many situations with milk products where the inter-pass flows violate the minimum flow requirements are also shown in this chapter.

2. BACKGROUND

2.1 Introduction

This section provides a brief overview of evaporators, the evaporation process and the mathematical model developed by Winchester (2000). Also it outlines the wetting constraint in falling film evaporators.

2.2 Evaporators

Evaporation is the process of concentrating a solution containing dissolved or suspended solids by boiling off the solvent. There are a variety of evaporators that are being used by process industries, however the predominant users of evaporators are the food industry.

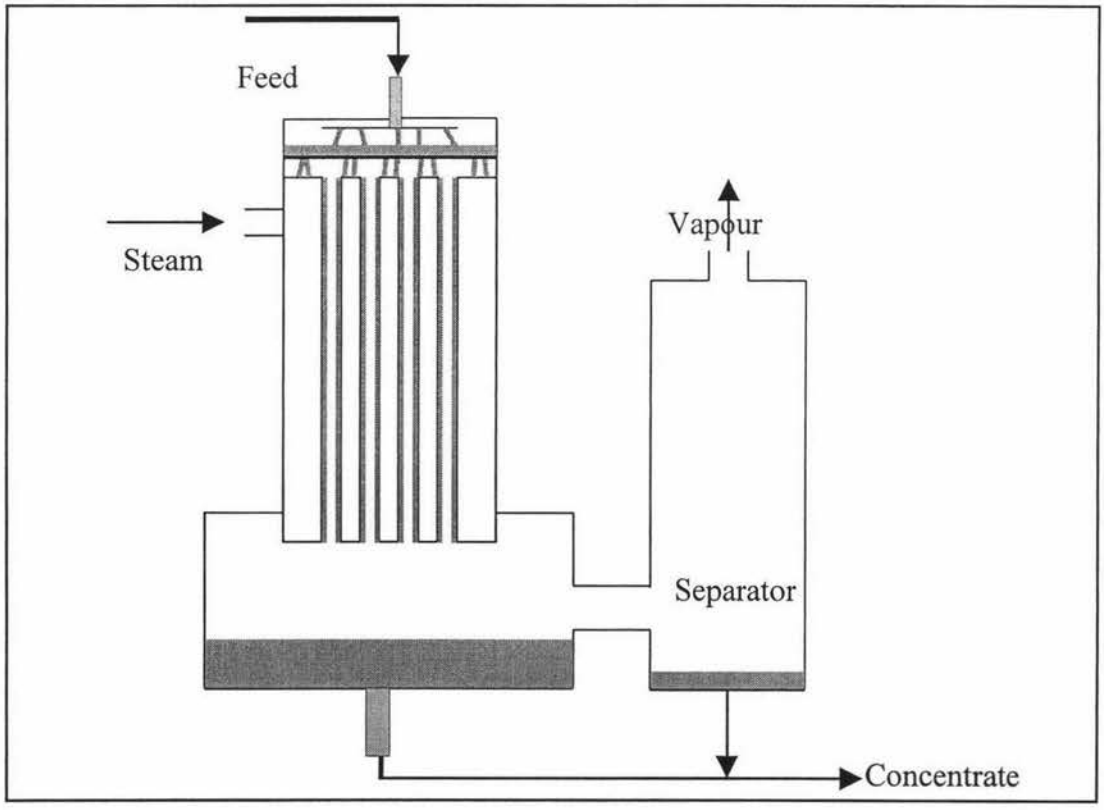

Figure 1: Single effect Falling film evaporator

Among all types of evaporators available, falling-film evaporators are in widespread use within the food industry due to their simplicity in design, high heat

transfer area and short residence time. The major elements of a falling film evaporator effect are the vertical tube bundle with surrounding heating jacket (calandria), the distribution device at the top of the calandria and a separation vessel at the base (Figure 1). The modern falling film evaporators are multi-effect falling film evaporators.

2.3 Evaporators at Kiwi Co-op Dairies Ltd

The evaporators at Kiwi Co-op Dairies Ltd. are three-effect, eight-pass, falling film evaporators. This means that the vapour is collected at three points and reused (three effects). However the liquid contacts the collected vapour in each effect more than once (eight passes). Multiple effect evaporators are more energy efficient than single effect models. This is due to reuse of energy in the evaporated water. It has been shown from the energy balance calculations (Winchester, 2000) that the higher the number of effects in the evaporation unit the higher the energy efficiency of the evaporator. The whole evaporation unit at Kiwi Co-op Dairies Ltd. can be divided into three sections: the MVR (Mechanical Vapour Recompression) section, the TVR (Thermal Vapour Recompression) section and the preheat section. The MVR and TVR sections have five and three passes respectively.

MVR Evaporator section

Mechanical vapour recompression effects use a Mechanical system, such as a compressor, driven with an electric motor. Nearly 90% of the water removed in evaporators is evaporated in this section. The vapour leaving the separator is compressed mechanically to the pressure that corresponds thermodynamically to the saturation temperature required on the steam side of the heat exchanger. The single effect MVR has two calendria and a preheat condenser. There are two passes in the 1st calendria and three passes in the 2nd calendria, giving a total of five passes for milk in the MVR section. The Preheat Condenser helps in maintaining the temperature of milk feed to the MVR section. The MVR operates at around 65°C and the driving force for heat transfer is normally 3°C. Figure 2

shows the schematic diagram of the MVR section of Powder 3 Plant at Kiwi Co-op Dairies Ltd.

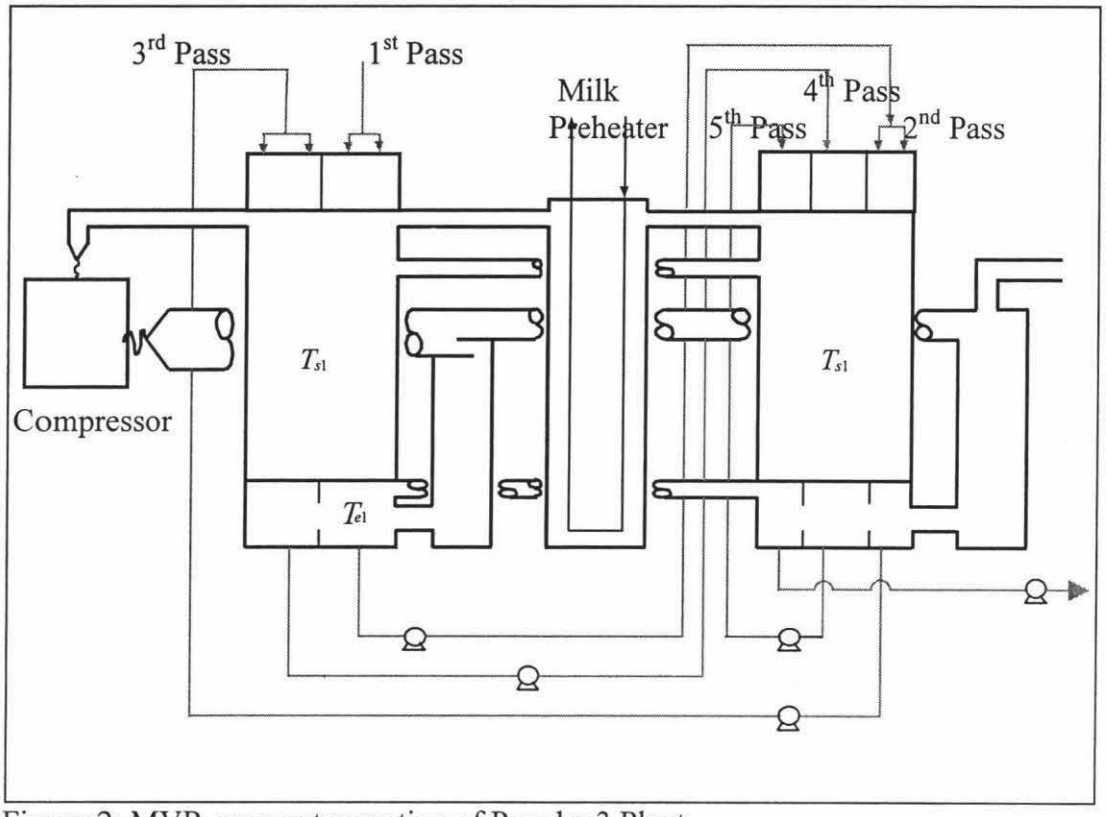

Figure 2: MVR evaporator section of Powder 3 Plant.

As shown in Paramalingam (1999) the efficiency of the MVR section increases with decreasing the feed flow rate to this section. Winchester (2000) showed that the energy cost to evaporate 1kg of water in the MVR is much less compared to the TVR (Thermal Vapour Recompression) and spray drier sections. This leads to the study of optimising the MVR section (Brenmuhl, 1999).

TVR Evaporator section

Thermal Vapour recompression unit is a steam jet ejector designed to increase the pressure of vacuum steam with high-pressure steam in a venturi. The water evaporated in this section is to refine the product from the evaporation unit. Steam at high pressure is used to compress water vapour. This section has two effects, with one pass in the 1st effect and two passes in the 2nd effect. The 1st effect operates at 60°C and the second operates at 55°C. The vacuum condenser attached to this section maintains the pressure within the TVR section and thus the

temperature in the last effect. Cooling water circulates between the vacuum condenser and the plate heat exchanger. Figure 3 shows the diagram of the TVR section of the Powder 3 Plant at Kiwi Co-op Dairies Ltd..

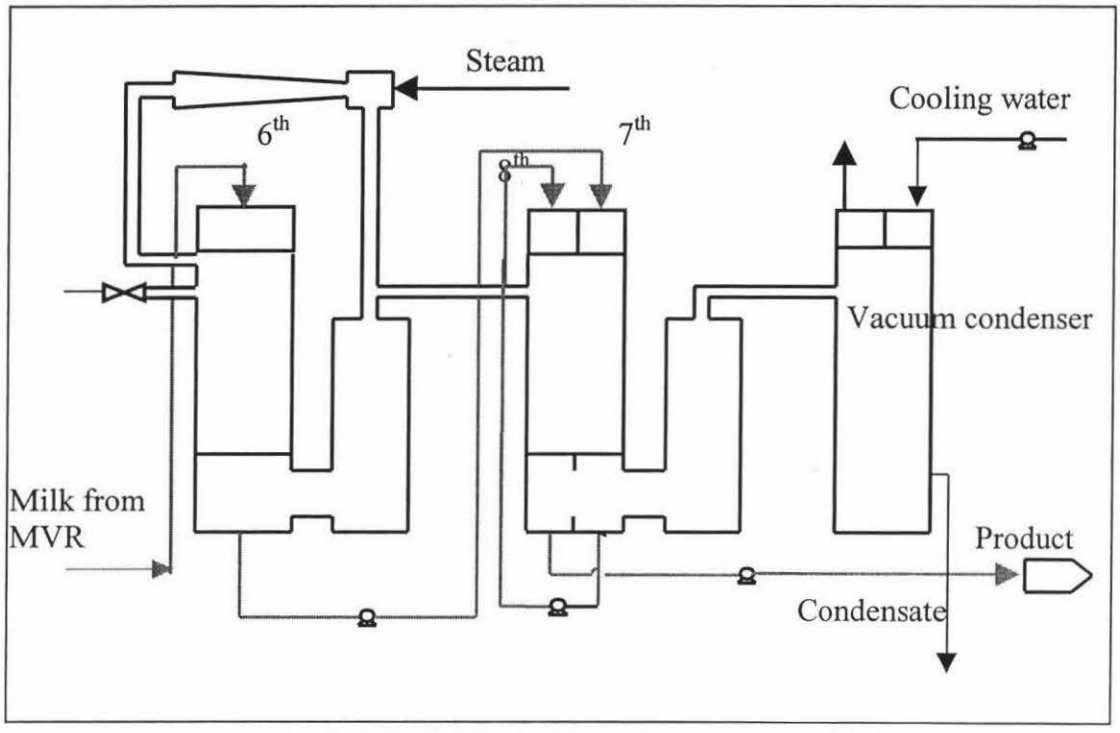

Figure 3: TVR Evaporator section in Powder-3 A Plant.

The Spray Drier, which converts the concentrated milk into powder, has a limitation for the inlet milk viscosity and temperature. This is one of the constraints to product concentration from the TVR unit. Since the energy cost to evaporate 1kg of water in the TVR is higher than that in the MVR, the process is operated such that most water is evaporated in the MVR and the rest is evaporated in the TVR.

Process description

The schematic flow diagram of the Powder 3 Plant at Kiwi Co-op Dairies Ltd. is shown in Figure 4. First, milk enters the plate heat exchanger, where it is preheated by hot condensate from the MVR and the TVR shell and cooling water from the Vacuum condenser before it enters the preheat condenser in the MVR section. After it has passed through the Preheat condenser, milk is pumped into the DSI (Direct Steam Injection unit), where steam is injected directly into the milk.

Then the milk is held within the holding tubes at almost DSI temperature for whey protein denaturation. The holding time varies from product to product, and depends

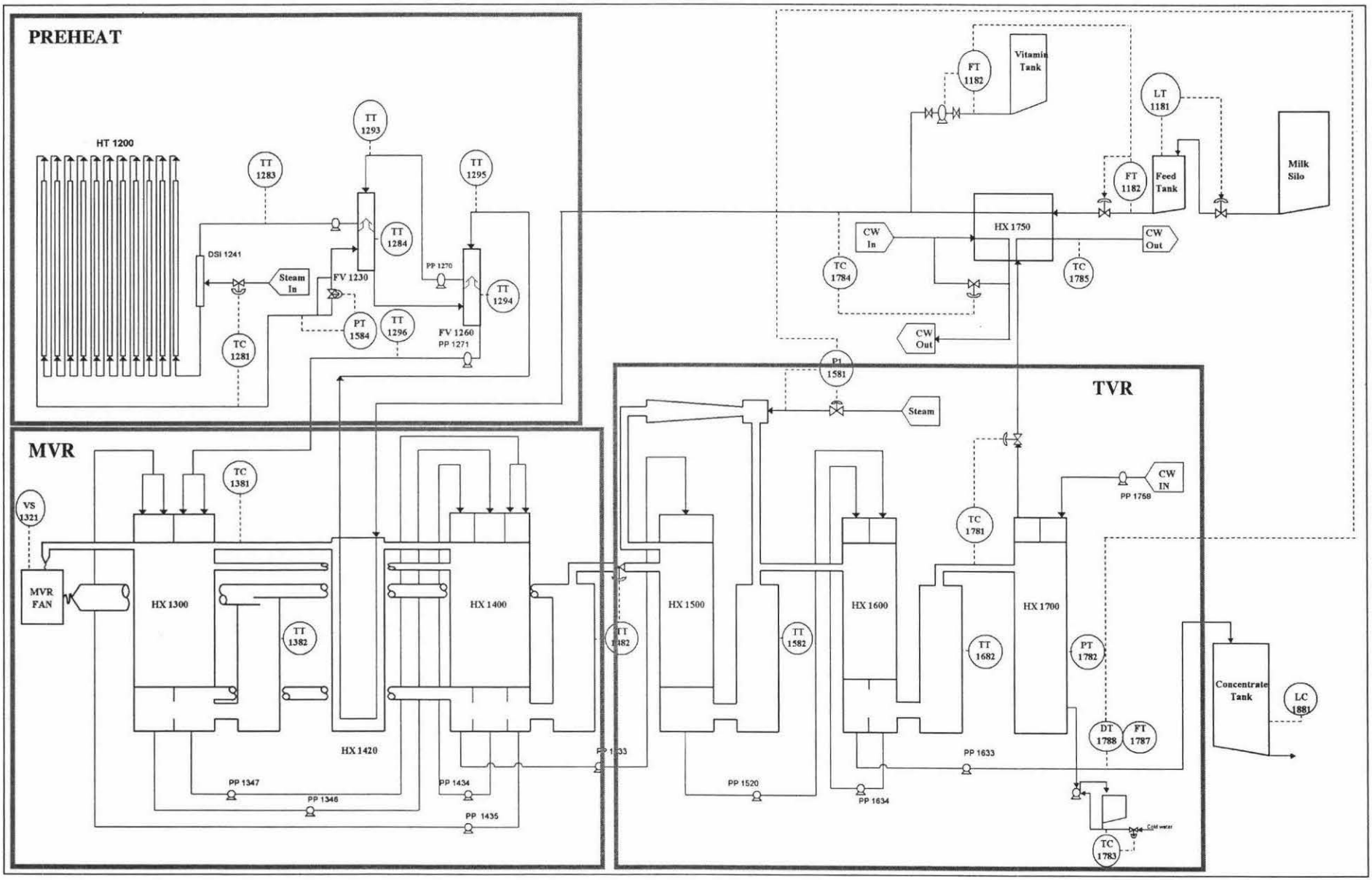

Figure 4: Evaporator A plant at Kiwi Coop Dairies.

upon the WPNI (Whey Protein Nitrogen Index) requirement of the product. After this, the milk is passed through the flash vessels before it is pumped into the first pass of the MVR section.

All three effects run at low pressure in order to lower the evaporating temperature, as the protein deforms in temperatures above 70°C. The initial heat source to the MVR shell is steam. After the plant comes to steady state the evaporated water in all five passes in the MVR is compressed and used as the heat source in the calendria instead of steam. After five passes in the MVR, milk is pumped into the TVR section, where the water vapour is thermally compressed and used in the calendria as the heat source. Steam at high pressure is used for this purpose. After three passes in the TVR, milk is pumped to a storage tank from where milk is supplied to the spray drier.

2.4 Mathematical model

Winchester (2000) developed a mathematical model for the Powder 3 Plant at Kiwi Co-op Dairies Ltd. from the basic principles of heat and mass transfer. It includes both a steady state model and a dynamic model of the Powder 3 Plant, and models for estimating both the density and the viscosity of milk products. The steady state model was developed for the optimisation of operation parameters with respect to energy cost, fouling and milk quality. The dynamic model was developed to investigate the controllability of the plant for disturbance rejection.

Winchester (2000) used the steady state model to estimate the flow rate of milk and the total solids after each and every pass, and the shell and effect temperatures. With these estimates he identified the heat transfer coefficients for different milk products. The steady state model was also used to estimate the static Relative Gain Array (RGA) in controllability studies. The dynamic model was

used to estimate the dynamic RGA and to analyse the decentralised control loops in the first and in the third effect.

The steady state model of the plant is used here to estimate the flow rates and total solids of milk products after each pass. The steady state model prediction and the actual measurement values are compared in section 6.4. The viscosity and density models are used here to estimate the viscosity and density of milk products at different operating conditions. These values are used in minimum flow calculations in chapter 4. The models used and the modifications made are described here.

Density

"Dairy products" densities, which depend mainly on their composition and temperature, are very important in processing and handling. These depend mainly upon its composition and the temperature at which it is measured. The composition of the product changes with time, and from point to point along the processing of that product. The method proposed to estimate density in previous studies (Paramalingam, 1999) was not close enough to the real plant values. This may be due to the fact that the changes in composition were not incorporated in the density model (Equations 3 & 4). Therefore, in the density model, the experimental values from Winchester's (2000) work in Appendix B are used for model constants instead of constants calculated from its composition. The model uses a regression equation based on temperature and the density of the components as shown below,

$$\rho_{water} = A_{water} + B_{water}T + C_{water}T^2 \tag{1}$$

$$\rho_i = a_i + b_i T \tag{2}$$

$$\rho = \frac{\rho_{water}}{(1 - a_{TS}.w_{TS})} \tag{3}$$

And

$$a_{TS} = 1 - \frac{\rho_{water}}{\rho_{lact}}.x_{lact} - \frac{\rho_{water}}{\rho_{prot}}.x_{prot} - \frac{\rho_{water}}{\rho_{fat}}.x_{fat} - \frac{\rho_{water}}{\rho_{salt}}.x_{salt} \tag{4}$$

Where, w_{TS} -Dry matter concentration of milk product.

ρ -Density (kgm^{-3}).

a_{TS} -Density model coefficient

ρ_{water} -Density of water (kgm^{-3})

A_{water} , B_{water} , C_{water} , a and b are constants

Viscosity

It is well known that the viscosity of milk is very complex and changes with a number of factors (Bloore & Boag, 1981; Snoeren et al., 1982; Kruif et al., 1985), important ones being temperature and composition. This property of milk is one of the most important process input variables in the manufacture of milk powders. Total solids, heat treatment, composition, holding time and the temperature all affect the viscosity of the concentrate milk.

The viscosity of milk has a complex relationship with the properties of its constituents and with the temperature. The composition of milk changes along the process and also with time. There were no models in general literature incorporating these changes in viscosity prediction. Winchester (2000) proposed a model that can predict the viscosity of milk from its constituent volume fractions (Appendix-C, Table-1) and the viscosity of water as shown below. This model can be solved both numerically and analytically for viscosity of milk.

$$\Phi = \mu_{TS}.w_{TS}.\rho \tag{5}$$

$$\mu_{TS} = \nu_{cas}.x_{cas} + \nu_{whey}.x_{whey} + \nu_{fat}.x_{fat} \tag{6}$$

$$\mu = \mu_{water}\left[1 + d_1.w_{TS}\right]\left[1 + \frac{1.25\mu_{TS}.w_{TS}.\rho_{water}}{1 - \left(a_{TS} + \frac{\mu_{TS}.\rho_{water}}{\Phi_{\max}}\right)w_{TS}}\right]^2 \tag{7}$$

Where,

w_{TS} -total solids content of the milk.(kg/kg)

μ_{TS} -viscosity model coefficient (m^3/kg)

μ -Viscosity (kg/m.s)

ρ -ratio of the concentrate density to milk density (-)

ν -specific volume of mixture component (m^3/kg)

d_1 -linear coefficient for lactose and mineral salt contribution to viscosity

a_{TS} -density model coefficient

Φ -volume fraction of the dispersed phase

Estimation of Flows and total solids after each passes

Winchester's (2000) combined steady state model for the Powder 3 Plant was used to infer theoretically the flows and concentration after each pass. This was developed from the basic principles of thermodynamics and heat and mass transfer. Here all variables that have a direct effect on the product quality are considered. Feed flow rate, feed concentration, feed temperature and compressor speeds all have a direct effect, while coolant flow, coolant temperature and ambient temperature have an indirect effect on product quality. These are the key input variables to the steady state model.

The model was basically developed in two steps. Firstly the effect and shell temperatures were determined from the energy balance equations across all parts in the evaporation unit. This is because the temperature difference is the driving force in the evaporation. Then, secondly, from the mass balance equations and from the results in step one, the flows and concentration after each pass were estimated.

2.5 Wetting Constraint

Because of the higher evaporation costs associated with the TVR and the fact that most of the water is removed in the MVR, the optimisation study was carried out to increase the amount of evaporation in the MVR section. This will reduce the evaporation in the TVR and thus it will require less steam.

The mass flow rates of milk feed and product (M_f and M_p) and their respective dry mass fractions (w_f and w_p) are related by $M_f w_f = M_p w_p$. Since $M_f = M_p + M_{evap}$,

where M_{evap} is the mass of water evaporated, the concentration ratio of the evaporator can be expressed as,

$$\frac{w_p}{w_f} = 1 + \frac{M_{evap}}{M_p} \tag{8}$$

So, to maximise the concentration ratio for fixed evaporative capacity (M_{evap}), one should seek to minimise M_p and hence the wetting constraint becomes active. At flow rates below a minimum flow there is an incomplete film on the evaporator tubes and a

breakdown of the film occurs. This formation of rivulets on the tube wall may lead to fouling.

2.6 Fouling

In order to remove the deposit from fouling, a frequent shutdown of the production processes is required for cleaning, which of course requires time, work, materials and energy. In other words cleaning is a costly affair. The reductions in cleaning time and frequency will lengthen the production time and thus will increase the plant's net profit. The 1998/1999 cost model of Powder 3 plant emphasises the importance of reducing the cleaning time. It has been shown by Emily (2000) that if a 10% reduction in cleaning cost could be achieved, the total cost saving in Powder 3 plant would be several thousands of dollars per season.

Fouling is caused by the increased need to operate the heat exchanger at the heart of the evaporation process more efficiently. Due to the changes in the properties of milk's constituents in the heat transfer process, deposits tend to form on the heat transfer surfaces, which greatly reduce the efficiency of the heat exchanger. There are several ways by which the fouling can occur within the evaporator tubes. Precipitation fouling, chemical reaction fouling, biological fouling and corrosion fouling are examples for different mechanisms of fouling.

The requirement for operation of the evaporator tubes is to have a complete film during evaporation. The film breaks up at low flow rates, forming rivulets exposing the tube surface to the air/vapour atmosphere. Due to the low heat

transfer coefficient of air to heat transfer, the temperature of the wall at these points will be increased. If the dry patches persist, the milk will be more concentrated and become still at these hot points. This may initiate the fouling process via any of the first three mechanisms. To avoid this, the evaporator tubes should be supplied with high flow rates of milk. But to optimise the evaporation process, flow should be the minimum possible. Hartley and Murgatroyd (1964) and Hoke and Chen (1992) have proposed methods to

estimate the minimum peripheral flow at which a hot surface should be supplied to avoid film break-up problems.

2.7 Hartley and Murgatroyd force criteria

The insufficient flows within the evaporator tubes cause the film to break and dry patches are formed. The behaviour of a dry patch formed on the surface can be one of three categories:

1. The dry patch will be stable and remained indefinitely.
2. The dry patch will be slowly swept and taking more time for the film to completely reform.
3. The dry patch will be quickly swept with the film reforming.

If the dry patch behaviour were in either category 1 or 2 then the fouling would be likely to occur. To avoid this fouling, the peripheral flow in a falling-film evaporator should exceed the threshold at which stable dry patches can occur. This threshold can be predicted from the Hartley and Murgatroyd force criterion.

Hartley and Murgatroyd have presented several analyses of the criteria for film break-up. Their force criterion considers the stability of dry patches (Figure 3) on a vertical plate. To permit the existence of a stable dry patch, the upward forces on the film at the stagnation point of a dry patch must exceed those required to sustain the pressure difference across the liquid/vapour interface. This pressure difference will increase as the peripheral flow (mass flow per unit width) increases.

The maximum peripheral flow, Γ ($kgm^{-1}s^{-1}$), at which dry patches are stable, is shown to be given by:

$$\Gamma_{H\&M} = 1.69\left(\frac{\mu\rho}{g}\right)^{\frac{1}{5}}\left(\sigma(1-Cos\theta)\right)^{\frac{3}{5}} \qquad (9)$$

Where μ -Liquid viscosity ($kgm^{-1}s^{-1}$) ρ -Liquid density (kgm^{-3})

σ -Surface tension (Nm^{-1})

θ -Advancing contact angle (^{o})

g -Acceleration due to gravity (ms^{-2})

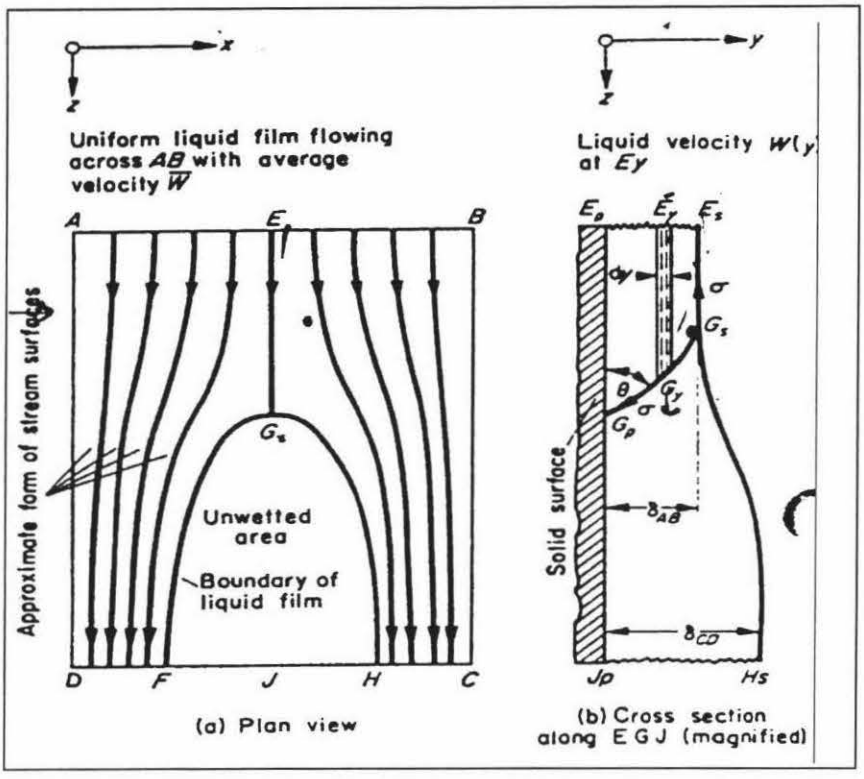

Figure5: Dry patch formation in liquid layers flowing over a solid body
Hartley and Murgatroyd (1964)

To avoid dry patches becoming stable and hence the likely onset of fouling, the peripheral flows in the evaporator tubes should exceed this threshold value. Previous experimental studies (Paramalingam, 1999) on minimum flow revealed that the Hartley and Murgatroyd (1964) model predicts the minimum flow well at low concentrations but overestimates at high concentrations of milk. Figure 6 shows the predicted flows using the Hartley and Murgatroyd (1964) model and

measured minimum flows. The Hoke and Chen (1992) model will be shown to eliminate this discrepancy at high concentration.

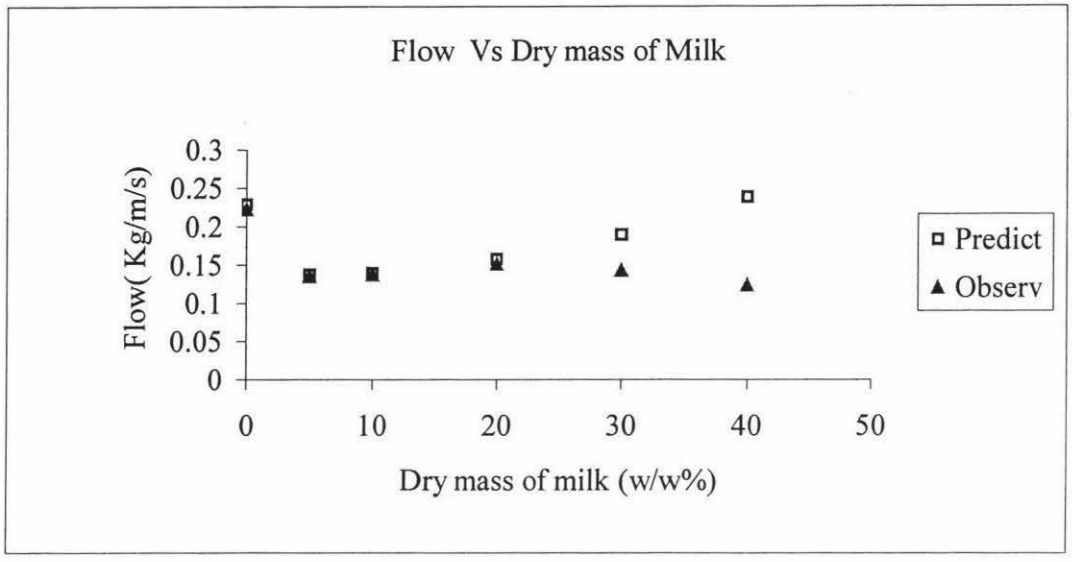

Figure 6: Comparison of observed and predicted minimum flow (Paramalingam, 1999)

2.8 Hoke and Chen force criteria

The Hartley and Murgatroyd (1964) model assumes that the wall shear force cancels the weight of the liquid above the dry patch. This is not true at high concentrations because Hoke and Chen (1992) relax this assumption by adding extra terms to incorporate wall shear and the weight. The film thickness and the minimum liquid loading equations of the Hartley and Murgatroyd model are modified to:

$$\sigma[1-\cos(\theta)] = \frac{\rho.g}{4}\left[\frac{\delta}{1-\cos(\theta)}\right]^2[2.\theta-\sin(2.\theta)]+\frac{\rho^3.g^2.\delta^5}{15.\mu^2} \qquad (10)$$

And

$$\Gamma_{H\&C} = \frac{\rho^2.g.\delta^3}{3.\mu} \qquad (11)$$

δ - film thickness (m)

The symbols are the same as for the Hartley and Murgatroyd equation. Figure 7 shows the predicted flows using the Hoke and Chen (1992) model and the measured minimum flows.

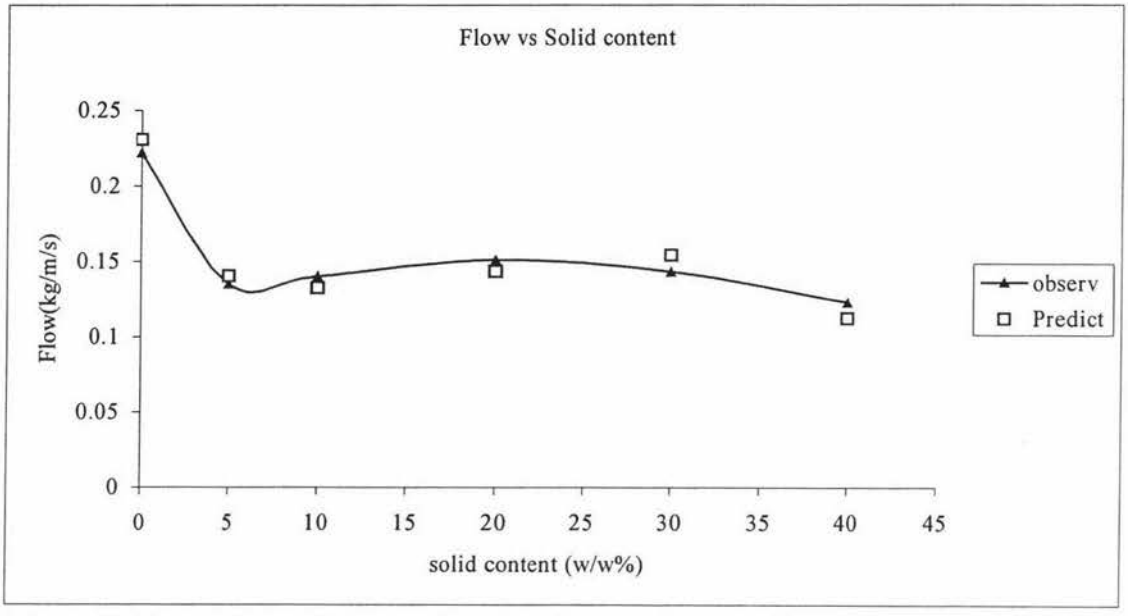

Figure 7: Comparison of observed and predicted minimum flow

Winchester (2000)

3. METHODOLOGY

3.1 Introduction

The models used in minimum flow estimation are strongly dependent on the physical properties of milk. These are density, viscosity, surface tension and advancing contact angle for milk products over a range of concentration and temperature. There are some theoretical models in the literature to estimate density and viscosity (Brenmuhl, 1999; Winchester, 2000; Fernandez, 1972) but no model is available for surface tension and contact angle. Therefore the experimental technique from previous studies (Paramalingam, 1999) has been used to find the surface tension and advancing contact angle.

There is a significant difference in minimum flow rate between flow on a wet surface and flow on a dry surface. This difference is due to the different contact angle which milk makes with the surface when the surface is wet and dry. The angle that the milk makes when the surface is wet is called the *retarding contact angle* and the angle made when the surface is dry is known as the *advancing contact angle*. The difference between the advancing and retarding contact angle is known as *hysteresis* in the contact angle. For water on stainless steel, the *hysteresis* has been found to be around 40-50° (Adamson, 1976). This value is not available for milk, but researchers have assumed the retarding contact angle for milk on stainless steel to be around 40°. Since the flow within the evaporator should not allow dry patches to occur, the minimum flow estimation should be based on the advancing contact angle. That is, the flow should sweep away the dry patch. Note that using the retarding contact angle will produce a smaller minimum flow below which, it is believed, dry patches will begin to form. The two minimum flows are called the advancing minimum flow and the retarding minimum flow respectively.

In this study the sessile drop profile method and capillary rise method are used in finding both advancing contact angle and the surface tension. The viscosity and density of reconstituted milk are also measured in the laboratory to check the values obtained from the theoretical models. Having found all these physical properties, the

minimum peripheral flows for different milk products was estimated. These peripheral flows give an idea of the flow rates at which the evaporator tubes should be supplied with different milk products to avoid fouling due to film break-up.

3.2 Advancing contact angle and surface tension

Advancing contact angle and surface tension are very important parameters in force analysis at the stagnation point of a stable dry patch. The technique from previous studies was used to evaluate these parameters. The sessile drop profile equation (11) and capillary rise on a vertical plate, equation (12), were simultaneously solved for two unknown parameters, surface tension and advancing contact angle (Paramalingam, 1999).

$$\sin\frac{\theta}{2} = \frac{h_s}{2a} - \frac{a}{3r}\left(\frac{1-Cos^3\frac{\theta}{2}}{Sin\frac{\theta}{2}}\right) \qquad (12)$$

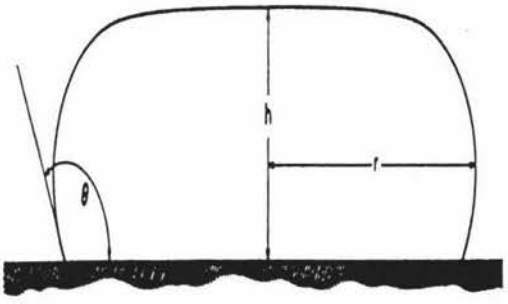

Figure 8: Sessile drop on a horizontal plate

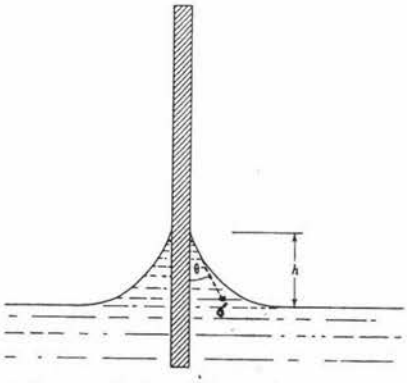

Figure 9: Capillary rise on a vertical Plate

$$Sin\theta = 1 - \left(\frac{h_c}{a}\right)^2 \qquad (13)$$

Where, $a = \left(\frac{\sigma}{\Delta\rho}\right)^{\frac{1}{2}}$

θ - Advancing contact angle (^{o})

σ - Surface tension (Nm^{-1})

$\Delta\rho$ - Different in liquid to vapour density (kgm^{-3})

r - Radius of sessile drop (m)

h_c - height of capillary rise (m)

h_s - height of sessile drop (m)

Experimental Method with sessile drop

The steel plate, on which the contact angle of milk is to be measured, was cleaned and dried. Then the steel plate was placed on an adjustable bed and the knobs of the bed were adjusted till the plate was perfectly flat. The flatness was ensured with a spirit level. A large sessile drop of liquid was formed on the plate using a syringe. Care was taken to ensure that the liquid did not oscillate and that the perimeter of the drop was bounded by dry plate. This ensured that the angle formed between the surface of the drop and the plate, at the boundary, was the advancing contact angle. When the sessile drop formed was large enough, readings of the height were taken using a travelling microscope as shown in Figure 10.

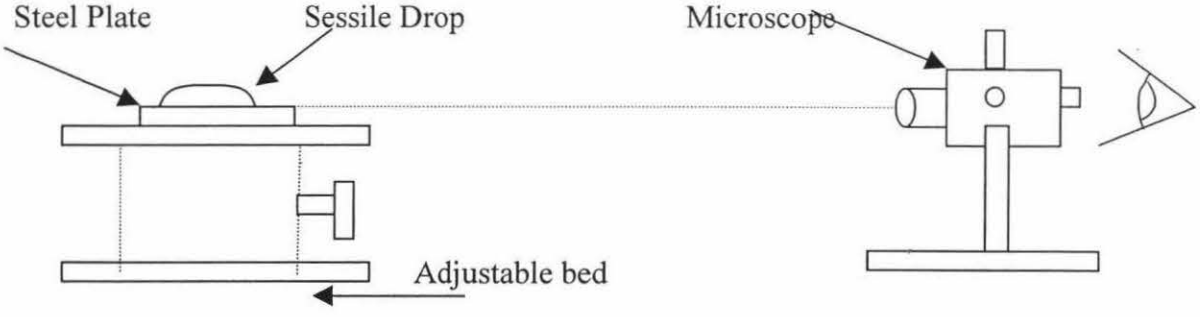

Figure 10:Apparatus set up for sessile drop profile measurements

First the microscope was focused to the top edge of the steel plate and the initial reading was taken. Then the microscope was moved gently to focus on the apex of the sessile drop and the second reading was taken. The difference between these two readings was recorded as the height of the sessile drop. Four such readings were taken to give the average height. A vernier caliper was used to measure the diameter of the sessile drop. Two samples from each concentration of milk and four sets of readings on each sample were taken.

Experimental Method with capillary rise on a vertical plate

The same type of plate used for the sessile drop tests was also used to measure the capillary rise. The dry plate was immersed in a glass beaker with a known concentration of milk. The plate was clamped firmly and vertically as shown in Figure 11 and the capillary rise was measured using the travelling microscope. Four sets of readings were taken with each sample. Tests were performed at 20°C and elevated temperatures for various concentrations of milk on #304 stainless steel.

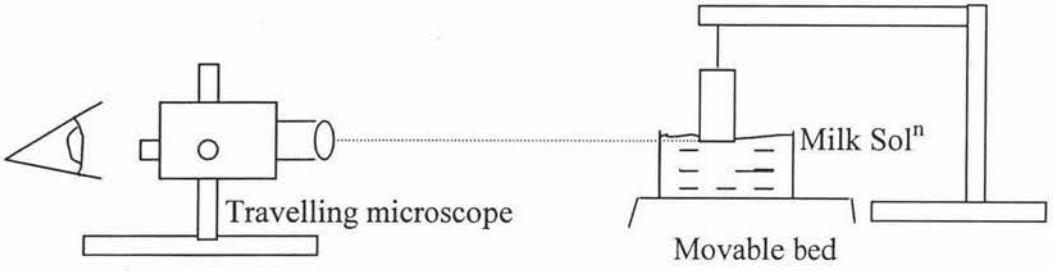

Figure 11:Apparatus set up for capillary rise measurement

The measurements were done at the laboratory for Whole milk and Sophi-Lo. Height and radius were measured with the sessile drop method, and the rise of liquid on a vertical plate was measured with capillary rise method. Both the sessile drop height method and the capillary rise method readings are listed in Appendix A. Equations 5 and 6 were simultaneously solved for contact angle and surface tension.

3.3 Experimental measurement of density

A hydrometer was used to measure the density of milk in the laboratory. The milk hydrometer was designed for non-concentrated milk. There are hydrometers with a wide range of densities, which will allow measuring the density of concentrated solutions. The hydrometers are calibrated to a specific temperature, e.g 27°C. Higher temperature measurements need the hydrometer to be calibrated against a known standard such as water.

The milk solution was filled in a glass-measuring cylinder. The hydrometer was lightly dropped in to the solution and at the same time it was given a spin. When it

had stopped bobbing up and down the number on the stem which corresponded to the level reached by the liquid was read. This was repeated with different concentrations of milk solutions at room temperature. The measurements with the hydrometer were done with Whole milk only.

3.4 Experimental measurement of viscosity

The RM 180 Rheomat, shown in Figure 12, was used to measure the viscosity of concentrate of reconstituted milk powders produced under different heating regimes. The RM 180 is a rotational viscometer. Its open, concentric measurement system allows measurements by immersion. The measuring head and measuring tube are rigidly coupled; a direct-current motor drives the measuring unit. The measuring rod rotates within a fixed surrounding tube, defining a specific geometry. The flow resistance of the sample in the measuring gap causes a retarding torque that is measured electronically from the motor current. The viscosity is the measured torque divided by the applied shear rate.

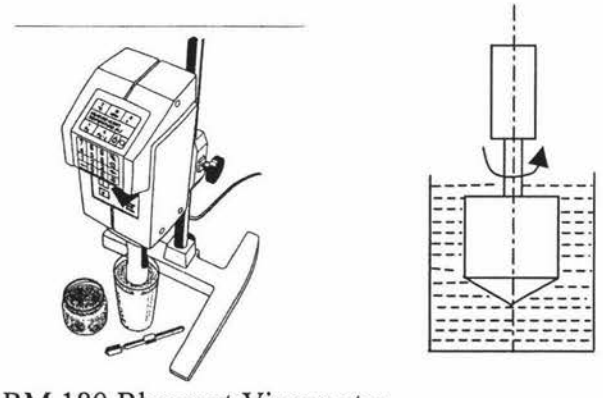

Figure 12:RM 180 Rheomat Viscometer

Samples of milk were filled in to a measuring system (beaker). The RM180 was turned on, and there was a delay until the display showed the measure mode. Then the message from the menu on the instrument was followed to obtained the desired readings. This was repeated with all samples of different concentration.

3.5 Minimum flow and Heat transfer coefficient test at Powder 3-A Plant

The flows after each pass at Kiwi Co-op Dairies Ltd., Powder 3 plant were checked for minimum flow violation at current operating conditions. Experiments were carried out with Whole milk and Sophie-Lo. The total solid contents were measured after each pass and flow by simple mass balance calculations across the passes. Also, the steady state model predictions were checked against the experimental results. The model inputs were taken from the stored data for that particular run, except the condensate flow to the plate heat exchanger, which was measured. The results are described in chapter 5.

One of the reasons why the steady state model showed deviation from the experimental results (section 5.4) with the time of a run could have been caused by not having incorporated the changes in the heat transfer coefficient with time. The heat transfer coefficients at all passes of a run at different times during the run were estimated with the following assumptions.

1. Temperature difference across the tube wall is constant.
2. The latent heat of evaporation is constant.
3. The surface area available for evaporation in each pass is constant.

The following equation was used to estimate the average heat transfer coefficient within the evaporation unit.

$$U = \frac{M_{evap} \times \lambda}{A \times \Delta\theta} \tag{14}$$

Where,

U - Overall Heat transfer coefficient ($W/m^2.k$)

M_{evap} - Mass of evaporation (kg)

A - Surface area available for evaporation (m^2)

λ - Latent heat for evaporation (KJ/kg)

$\Delta\theta$ -Temperature difference (K)

The tests were carried out with Whole milk and Sohpie-Lo in the Powder 3 Plant. The significance of the heat transfer coefficient changes with time and the effect of mass of steam injected in the DSI (Direct Steam Injection) unit on the heat transfer coefficient are described in chapter 6.

The historical data were checked for a violation minimum flow. Due to the fact that the flows after each pass were not available from past data, Winchester's (2000) model was used to find the flows after each pass for minimum flow tests. The film break-up at low flows and the heat transfer coefficient changes with the time of a run are validated with the historical data available with water at the Powder 3 Plant. The results are shown and discussed in chapter 7.

4. THEORETICAL ESTIMATION OF MINIMUM FLOW

4.1 Introduction

To maintain a complete film along the evaporator tubes, the milk should be supplied at a flow rate above a minimum flow based on the physical properties of both milk and stainless steel. This minimum flow is of two types, one is flow on a wet surface and the other is flow on a dry surface. The first one is normally referred as *flow on the wet surface* and the second is known as the *re-wetting process*. The requirements within the evaporator tubes are to maintain the complete film and, if film break-up happened to occur, it should be eliminated by the milk flow. Hence the flow should be sufficient to wet a dry surface. This is mandatory in the evaporation process to avoid fouling due to film break-up.

Brenmuhl (1999) has estimated the theoretical minimum peripheral flows based on the retarding contact angle. This chapter describes the theoretical estimation of viscosity, density and minimum peripheral flows based on advancing contact angles. All calculations were done at 65°C and 55°C. This is because the evaporators in the MVR section at Kiwi Co-op Dairies Ltd. operate at 65°C and the TVR at 55°C. The maximum concentration after the MVR is 40% and after the TVR is 50%.

4.2 Density

The density of Whole milk and Sophie-Lo were calculated for a range of total solid contents and temperatures. The sample calculation for 10% solid content of Whole milk is shown in Appendix B. The results are also tabulated in Appendix B. The density measurements were done in the laboratory for reconstituted Whole milk. The measurement results are shown in Appendix B.

Figures 14 and 15 show the density variation with total solid content for Whole milk and Sophie-Lo respectively. The graphs show the density values at 65°C up to 10-40% and at 55°C from 25-55%. The figures also show that the model-predicted density

varies linearly with total solids. The experimental results of whole milk are plotted against the model prediction values in Figure 13. This validates the model at 22°C.

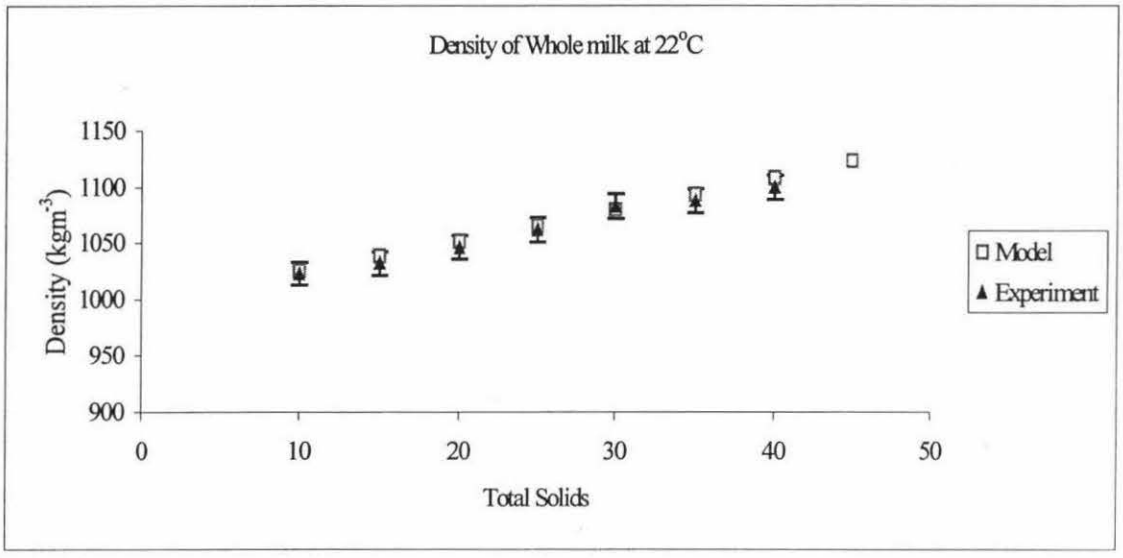

Figure: 13 Experimental and model density values of Whole milk with total solids.

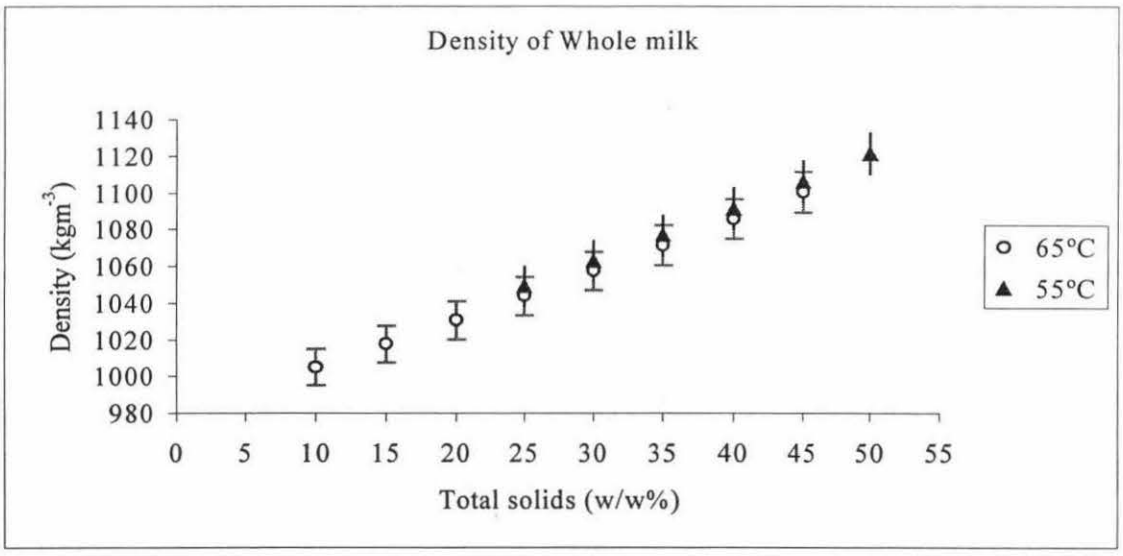

Figure: 14 Density of Whole milk with total solids and temperature.

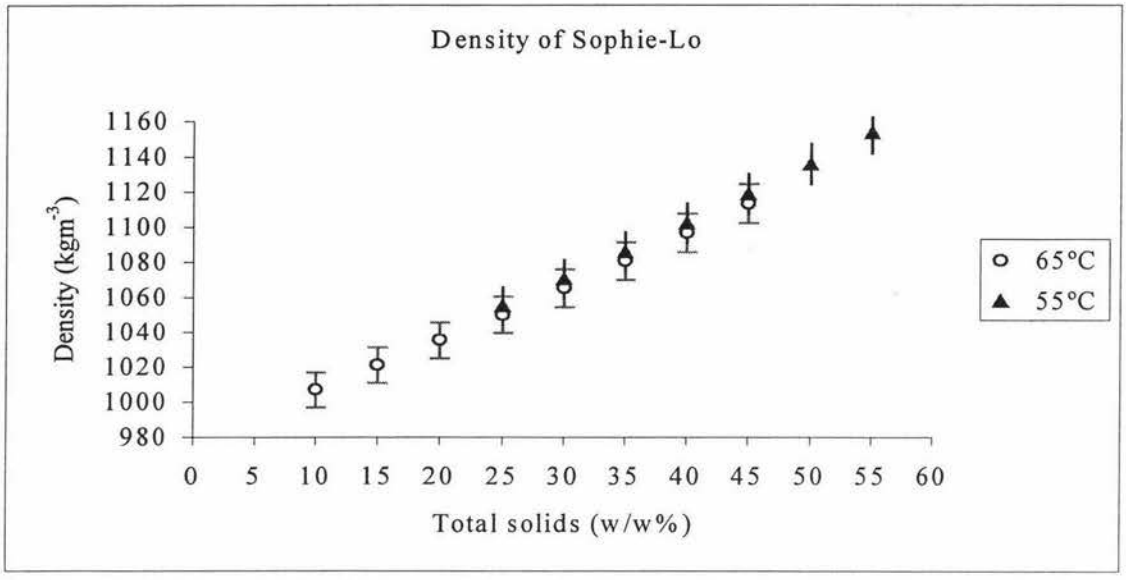

Figure 15: Density of Sophie-Lo with total solids and temperature

4.3 Viscosity

The viscosity of whole milk and Sophi-Lo were calculated for a range of total solid contents and temperatures. The sample calculation using the analytical method with 10% solid content of Whole milk is shown in Appendix C. The results of both Whole milk and Sophie-Lo are also tabulated in Appendix C (Table 2).

The viscosity is estimated for milk solutions at evaporator operating conditions, since the minimum flows are required at these conditions. Figure 16 shows the viscosity variation with total solid content for Whole milk and Sophie-Lo at 65°C, and Figure 17 shows the viscosity values at 55°C. Figures 16 and 17 also show the numerical solution of the viscosity model (Chapter 2) and the experimental values for both Whole Milk and Sophie-Lo. The experimental results at 22°C were also compared with the model prediction in Figure 18 at two shear rates $1200s^{-1}$ and $0s^{-1}$.

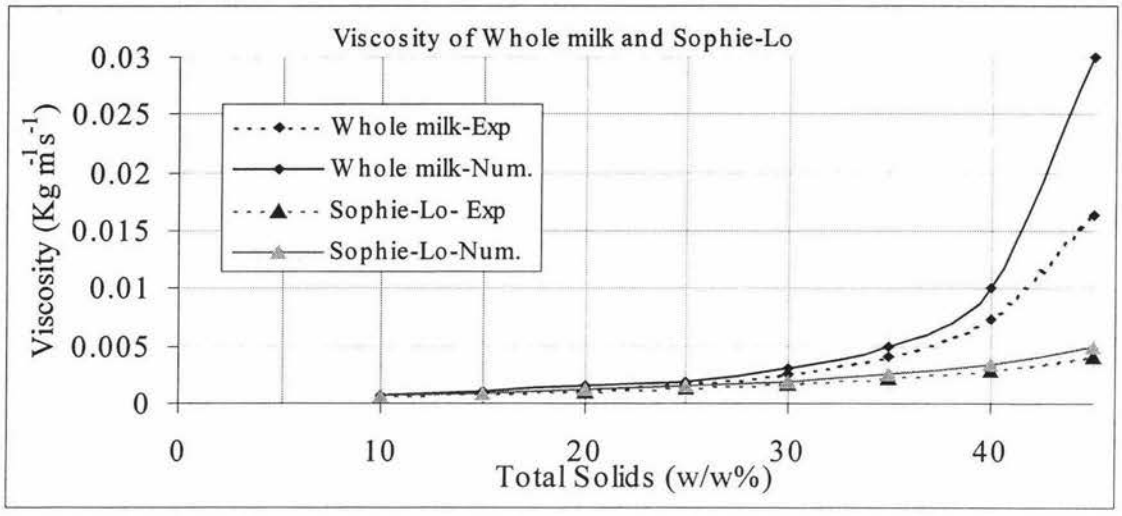

Figure 16: Viscosity variation with total solids for both Whole milk and Sophie-Lo at 65°C

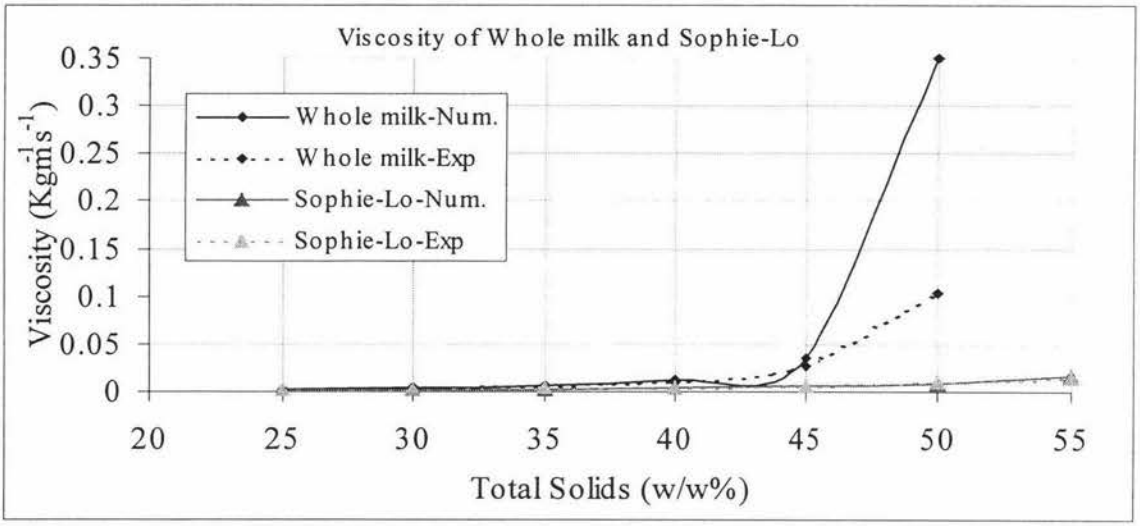

Figure 17: Viscosity variation with Total Solids for Whole milk and Sophi-Lo at 55°C

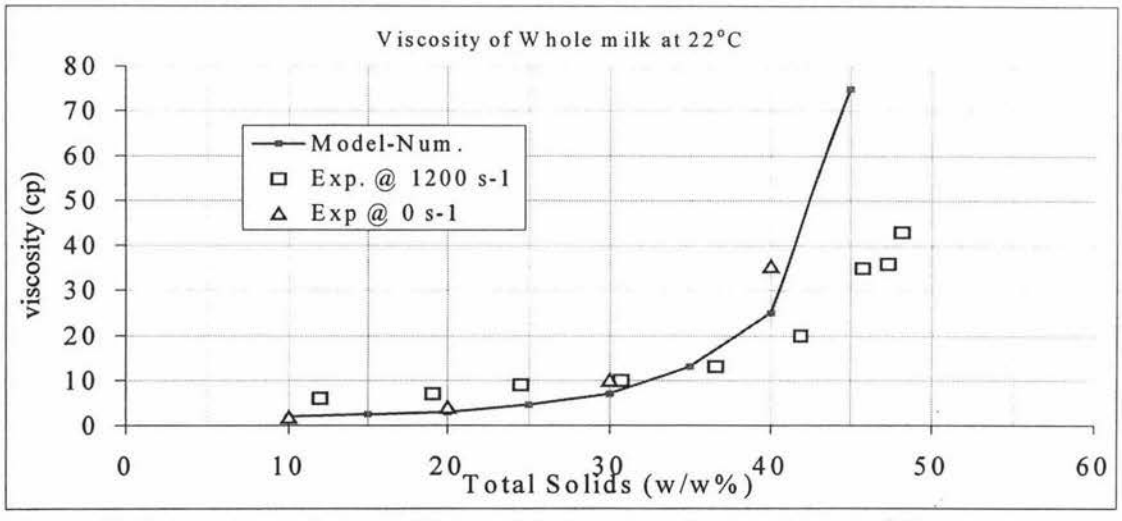

Figure 18: Viscosity variation with Total Solids for Whole milk at 22°C

Figures show that the numerical solutions of the viscosity model are accurate at low concentrations (10-30%w/w), and that above 30% solid content model underestimates the viscosity. It is clear from the figure 18 that the RM 180 Rheomat overestimates the viscosity at lower concentration and underestimates the viscosity at high concentration. This due to the effect of shear rate ($1200s^{-1}$) on absolute viscosity. Therefore the numerical solution of the viscosity model was taken as the viscosity values for the following reasons.:

1. The minimum peripheral flow is strongly affected by viscosity at low concentrations.
2. At high concentrations, milk weight at the stagnation point of a dry patch becomes significant and lowers the minimum peripheral flow (Hoke & Chen, 1992).
3. The numerical solution of the viscosity model at 22°C showed less deviation from the absolute viscosity ($0\ s^{-1}$ shear rate).
4. No absolute viscometer, which could be used simply and quickly, was available at either at Kiwi Co-op Dairies Ltd. or Massey University.

4.4 Advancing contact angle and surface tension

Four different sessile drops were measured and four different capillary rise experiments were conducted. Samples at different concentrations were prepared and measured twice, giving 32 estimates for contact angle and surface tension. The experiment measurements of Whole milk and Sophie-Lo are listed in Appendix A. Sample calculations and a table of results are shown in Appendix D (Table 1 and Table 2). The measurement errors associated with contact angle and surface tension are also tabulated in Appendix D (Table 3).

The measurements were done at elevated temperatures with high total solids milk. This is due to the highly viscous nature of milk at high total solids content. At Kiwi

Co-op Dairies Ltd., the MVR section operates at 65°C and the TVR at 55°C. Ponter et al. (1967) found that the contact angle of water on copper decreased with increases in temperature by approximately 0.1°per °C. Similar changes could be assumed for concentrated milk-derived products. The surface tension at elevated temperatures for concentrated milk was estimated from the measured surface tension of concentrated milk at 30°C (σ_w^{20}), the surface tension of raw milk at 30°C (σ_{raw}^{20}) and at elevated temperature, T (σ_w^T) (Bertsch, 1983) by,

$$\sigma_w^T = \frac{\sigma_{raw}^T}{\sigma_{raw}^{30}} \sigma_w^{30} \tag{14}$$

The plots of calculated contact angle and surface tension with total solids for both Whole milk and Sophie-Lo are shown in Figures 19 and 20.

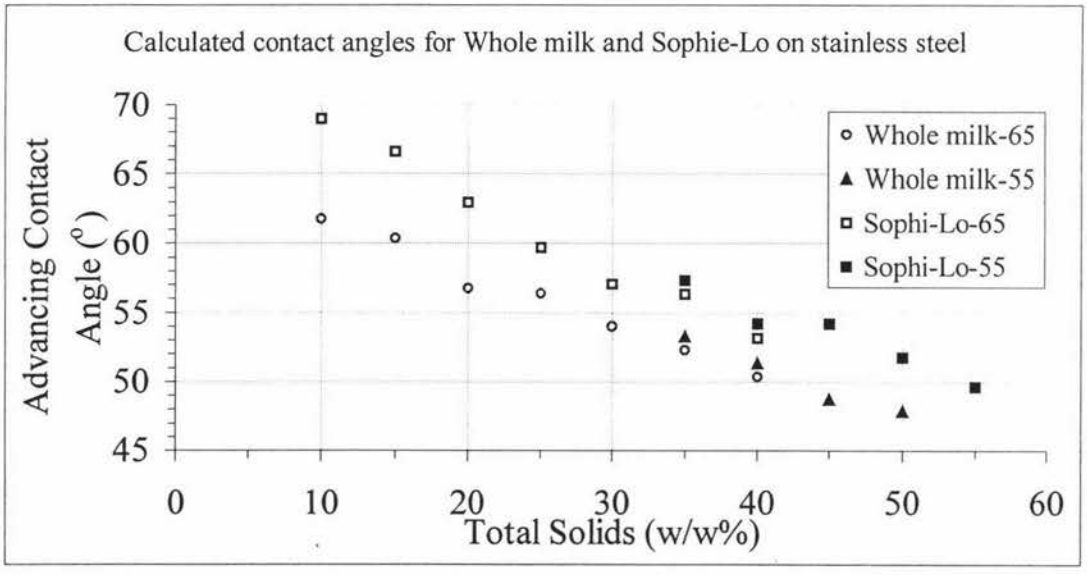

Figure 19: Advancing contact angle with total solids for whole milk and Sophie-Lo

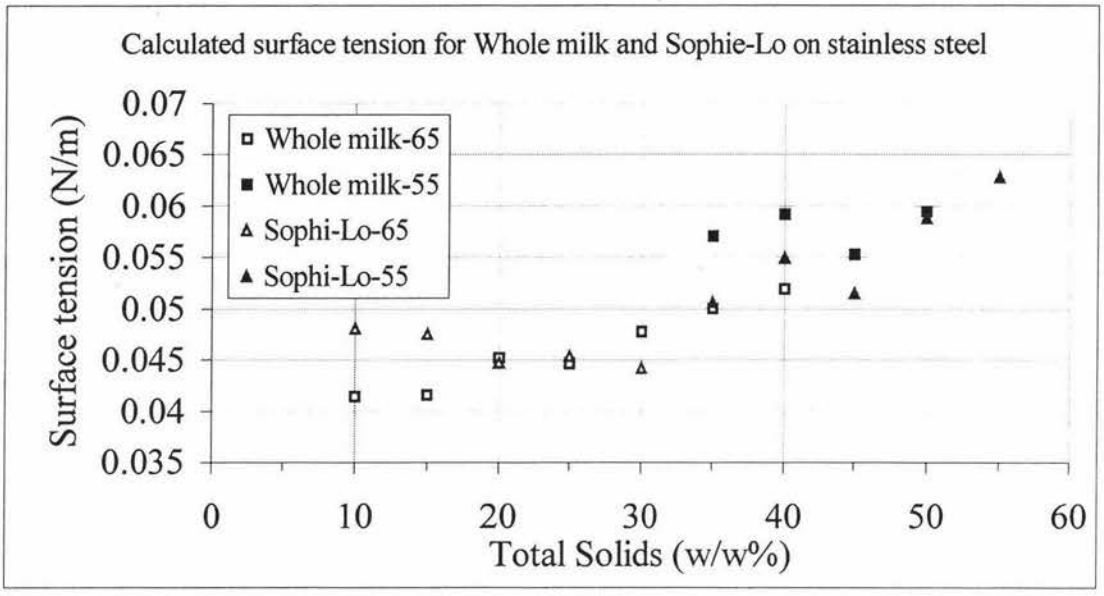

Figure 20: Surface tension with total solids for Whole milk and Sophie-Lo

4.5 Minimum flow from proposed models

Hartley and Murgatroyd (1964) and Hoke and Chen (1992) models were proposed to estimate the minimum flow required in evaporator tubes to overcome stable dry patches. The Hartley and Murgatroyd method was used with water, and both the Hartley and Murgatroyd and Hoke and Chen models were used with milk products. This is due to the fact that weight of the stagnant liquid at a dry patch becomes significant with concentrated milk products. Sample calculations for both methods are shown in Appendix E. The results are also tabulated in Appendix E (Table 1 and Table 2).

Figure 21 shows the minimum flows of water required in each pass of the falling film evaporators to avoid dry patches at milk operating conditions. Figures 22 and 23 show the minimum flow variation with total solids for both Whole milk and Sophie-Lo respectively. Also, the Figures show the discrepancy between the Hartley and Murgatroyd (1964) and Hoke and Chen (1992) models at high total solids of milk products.

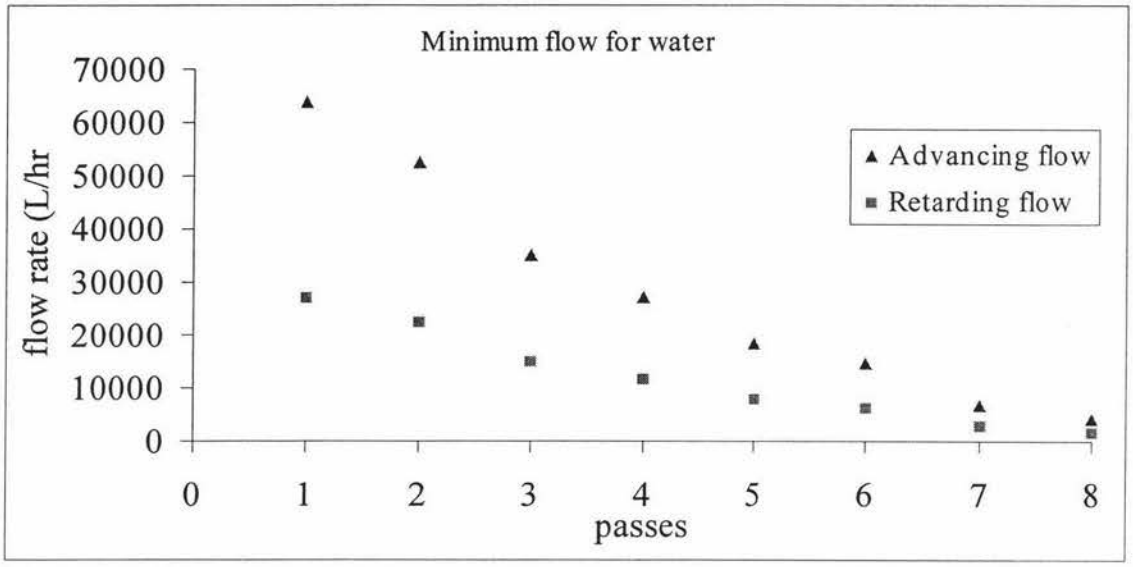

Figure 21: Advancing and retarding minimum flow of water in each pass at Kiwi Co-op Dairies Ltd. Powder 3 plant

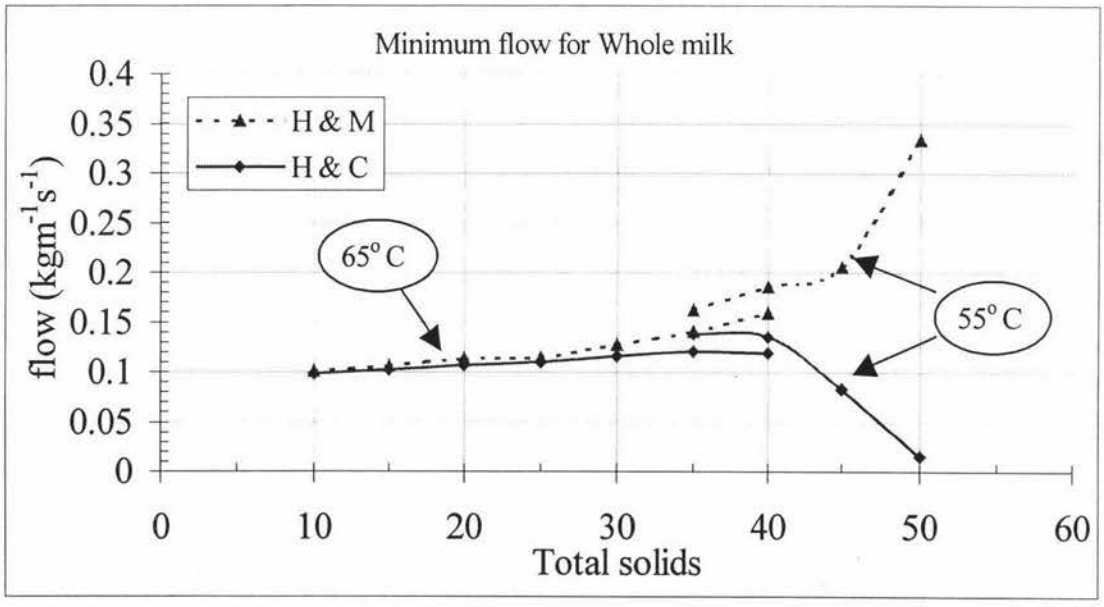

Figure 22: Minimum flow as a function of total solids concentration for Whole milk

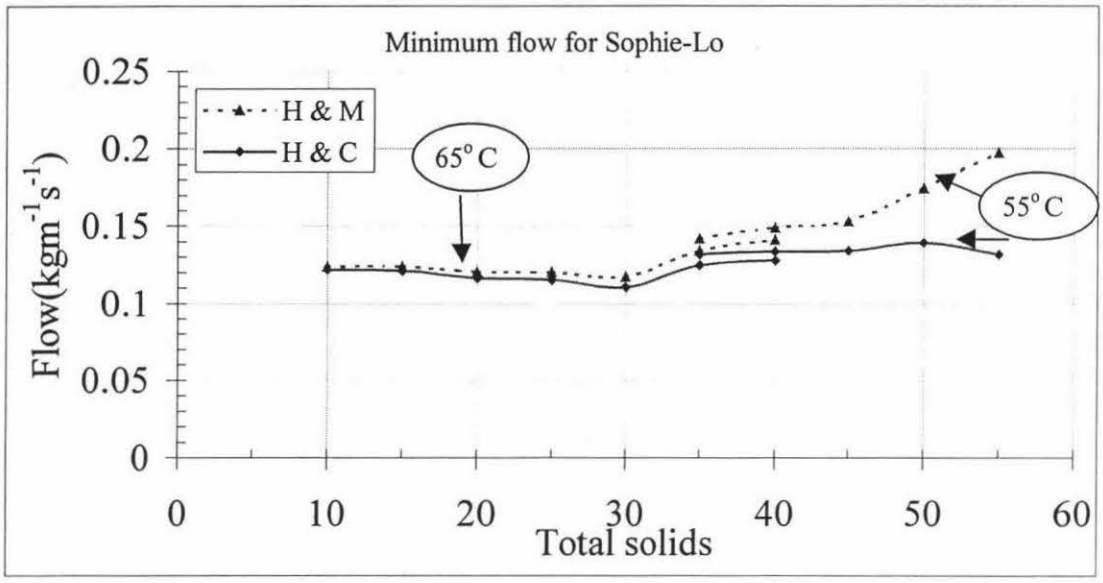

Figure 23: Minimum flow as a function of total solids concentration for Sophie-Lo

The Hoke and Chen (1992) model estimates minimum flows lower than that of the Hartley and Murgatroyd model. This is due to the fact that the weight of the stagnant fluid of a dry patch is incorporated in the Hoke and Chen force analysis. This addition of weight force will increase the resultant downward force at the stagnation point lowering the minimum peripheral flow.

At high concentrations of Whole milk a sudden increase in minimum flow is observed with the Hartley and Murgatroyd (1964) model, whereas a sudden drop is observed with the Hoke and Chen (1992) model. This is due to the higher viscosity gradient at high concentrations of Whole milk. This is not so with Sophi-Lo because the viscosity predictions do not show the same shape as the Whole milk does at high concentrations. This emphasises the fact that the accurate study of the viscosity of milk products is vital.

It can be seen from Figures 22 and 23 that the weight of the stagnation point becomes significant above 25% (w/w). The minimum flow calculation with the Hartley and Murgatroyd model is simple compared to that using the Hoke and Chen model. The weight of the stagnation point of a dry patch becomes significant in the force analysis above 25%(w/w). Therefore, in the following analysis, below 25% the minimum flows

were estimated using the Hartley and Murgatroyd model and above 25% using the Hoke and Chen model.

5. TESTS FOR MINIMUM FLOW IN THE POWDER 3 PLANT

5.1 Introduction

Avoiding possible fouling within the evaporator tubes can extend the evaporator run and minimise the cost of cleaning. One of the causes to fouling is the film break-up within the evaporator tubes. This could be overcome with sufficient flow that can sweep a dry patch away within the evaporator tubes. To sweep a dry patch the minimum flow should be estimated based on the advancing contact angle as shown in Chapter 4. The flow to the evaporator could be lowered, or the evaporation rate in the MVR section could be increased, to increase the energy efficiency of the evaporation unit. Both of these operations in the evaporation unit will cause the flows at the end of each pass to be lowered. There is a minimum flow for the evaporator tubes below which the breakdown of the falling film is spontaneous. If the flow is above the minimum flow based on the advancing contact angle, the dry patch will be swept. If the flow below the minimum flow based on the retarding contact angle, then film break-up is definite. In between these two there is a risk of film break-up occurring which will then result in a stable dry patch. This indicates that operation should always be above advancing minimum flow but that dry patches forming and fouling may not be seen until retarding minimum flow is reached.

With the minimum flows based on the advancing contact angle as discussed in Chapter 4, and the minimum flow estimated by Brenmuhl (1999) based on the retarding contact angle, the Powder 3 Plant was tested for current operating flows after each pass. Then, using the experimental data, the steady state model was tested for accuracy of flows and total solid content predictions after each pass.

5.2 Measurements

The samples were taken at the start and end of a run with both Whole milk and Sophie-Lo. Four samples were collected at each pass and the Refractometer readings

were taken to avoid the effect of fluctuation in flow calculation. The samples were collected at different times during a run to examine the change of evaporation rate throughout a run. The Refractometer readings were calibrated against the total solids of both Whole milk and Sophie-Lo. This enabled the total solid content to be found easily without any laboratory tests. The measurement readings and the calibration results from the Refractometer, with both Whole milk and Sophie-Lo, are listed in Appendix F.

5.3 Actual flows and total solids at the end of passes

Calculation

The Refractometer readings of the samples were converted to total solids with the calibration results obtained (section 5.2). Knowing the total solids after each pass, the flows after each pass were then calculated with a simple mass balance across each pass. Similar calculations were carried out with both Whole milk and Sophie-Lo.

The changes in advancing contact angle on a protein-adsorbed surface were studied by Yang et al (1991). A reduction of 20^{o} was observed with water on stainless steel. It is estimated that this reduction causes the advancing minimum flow of water to drop by approximately 20%. This is assumed to be the same with the advancing minimum flows with milk products when protein is adsorbed to the solid surface. The reduction in the retarding minimum flow was not taken into account because the actual retarding contact angles for milk products were not known. Therefore only the reduction in the advancing minimum flows due to protein adsorption are shown in the following figures.

Experimental results and comparison with theoretical estimation

The Figures below show the comparison of the experimental flows with the theoretical flows at the end of each pass in the Powder 3A evaporator.

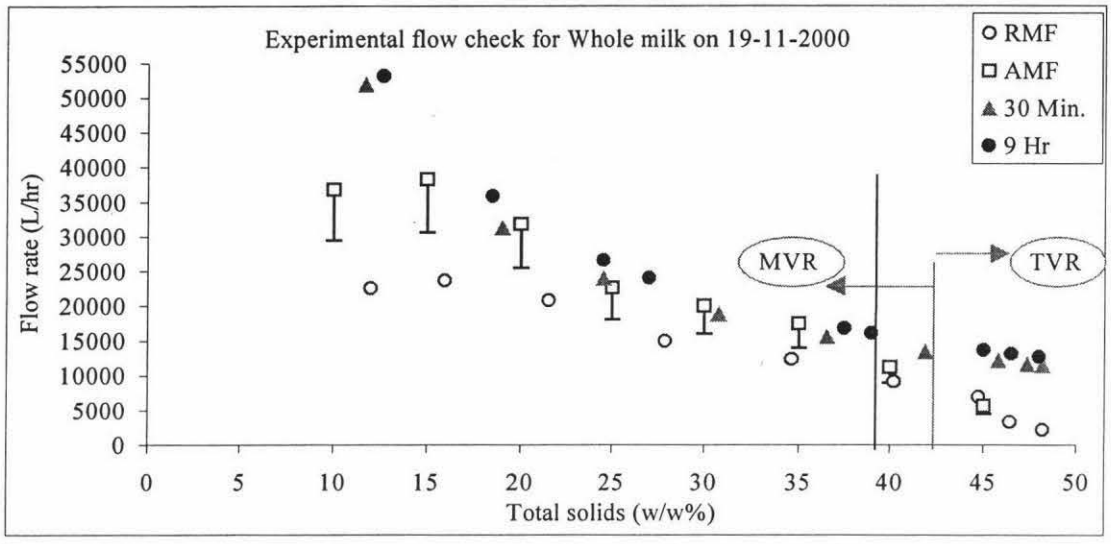

Figure 25: Experimental flows compared with the advancing and retarding minimum flows with Whole milk. RMF- Retarding minimum flow, AMF-Advancing minimum flow. 30 Min., 9 Hr - flows after 30 Minutes and 9hour runs respectively.

Figure 25 show that the flows at the start of a run are consistently lower than later in the run. Therefore they are, for some passes, below the advancing minimum flows. The Figures show also the variation of actual flows and total solids after each pass with time. This variation is due to the changes in the inputs to the evaporator and the changes in the heat transfer coefficient within the passes. This is because the changes in feed flow and in feed concentration during the run on 19/11/2000 are significant (F=50541 to 51779L/hr, X_F =11.7 to 12.7). Therefore, the changes in total solids and flows during the run on 19/11/2000 could be explained by changes in the Heat transfer coefficient.

Figure 26 shows the comparison of experimental and the theoretical minimum flows with Sophie-Lo.

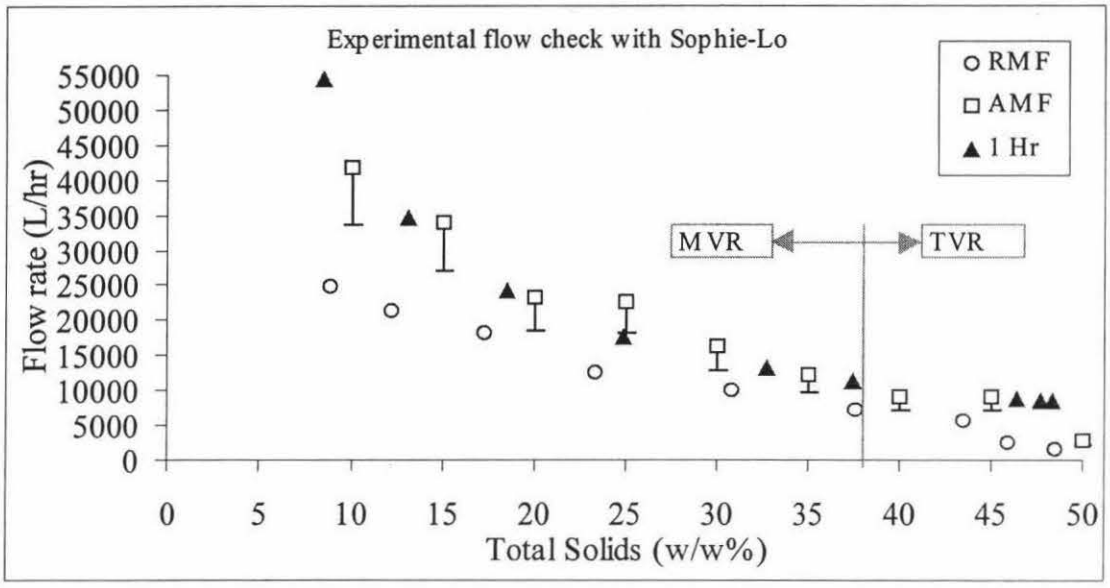

Figure 26: Experimental flows on 07-12-2000 at Kiwi Co-op Dairies Ltd., Powder 3 Plant compared with theoretical minimum flows. RMF- Retarding minimum flow, AMF-Advancing minimum flow. 1Hr- flows after 1 hour run.

It can be seen from the above figure that the operating flows with Sophie-Lo in the MVR section in the Powder 3 Plant were lower than the advancing flows, but well above the retarding flows. These flows were sufficient to maintain complete film within the evaporator tubes, but not sufficient to sweep off dry patches if they arose in the MVR section. The operating flows in the TVR section satisfy the flow requirements and this safety margin will be increased if the minimum flows in the MVR are satisfied.

5.4 Validation of Steady state model prediction

The steady state model of the Powder 3 Plant was developed from the basic principles of thermodynamics, mass transfer and heat transfer. This model was used to predict the flows and the total solids after each pass of the evaporation unit, and the accuracy of the model prediction was tested using the experimental results. The figures below show the model prediction and how close those predictions were to the actual values.

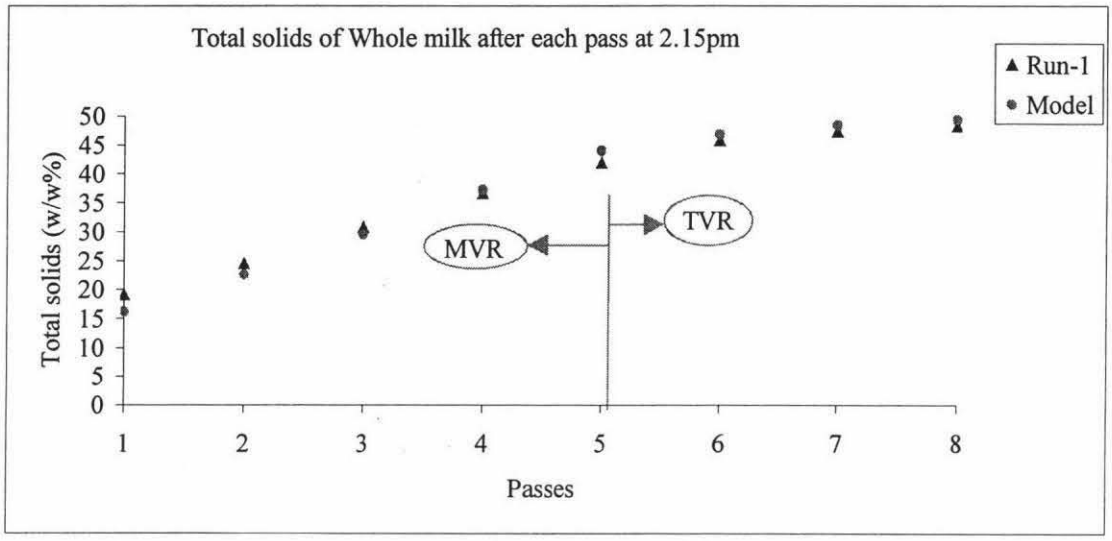

Figure 27: Comparison of total solids prediction with the steady state model and the experimental values on 19/11/2000 at 2.15pm

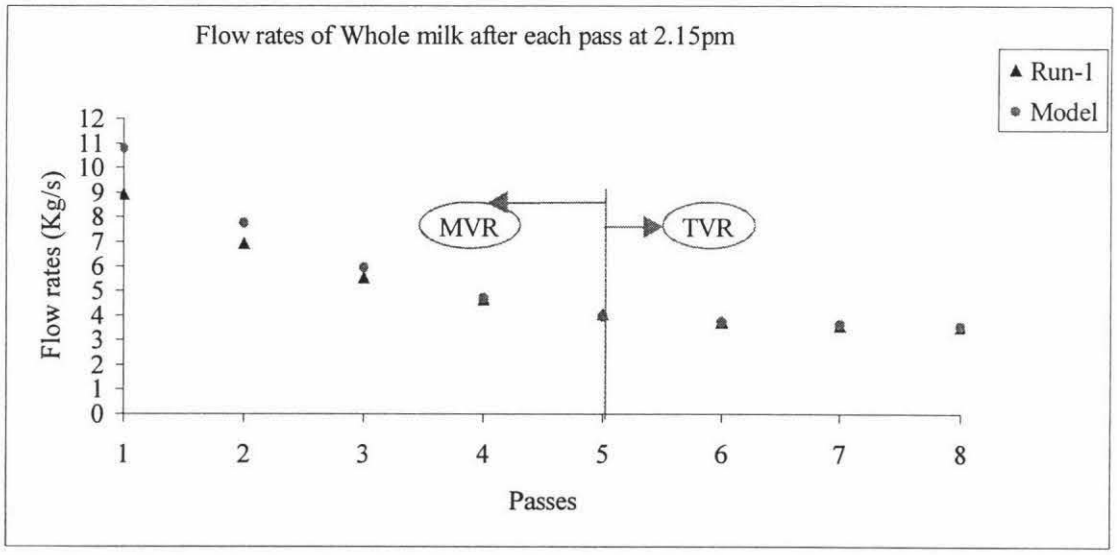

Figure 28: Comparison of flow predictions and the experimental values on 19/11/2000 at 2.15pm

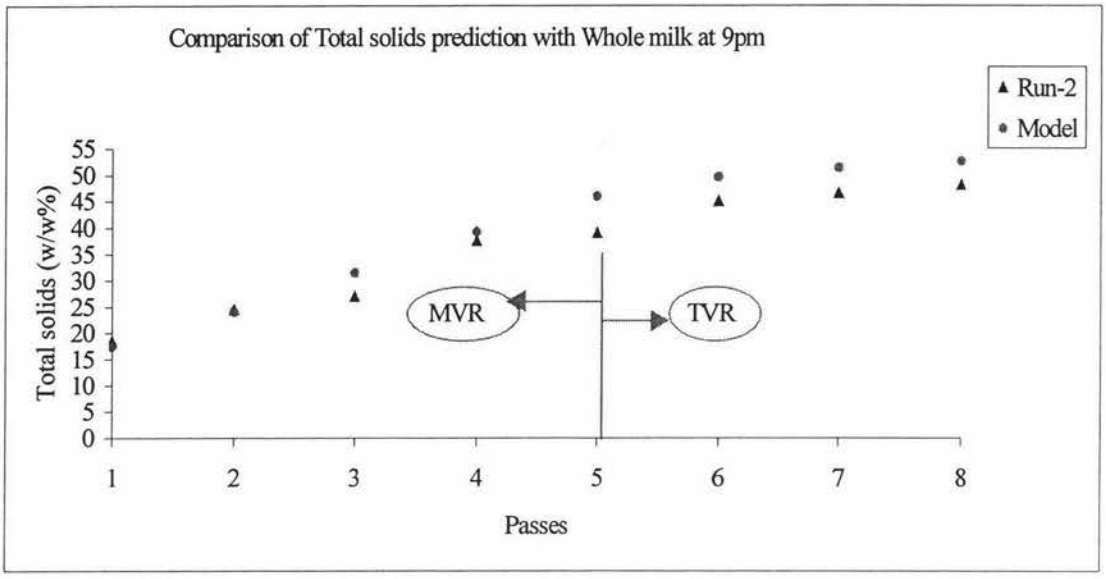

Figure 29: Comparison of total solids predictions with the steady state model and the experimental values on 19/11/2000 at 9pm

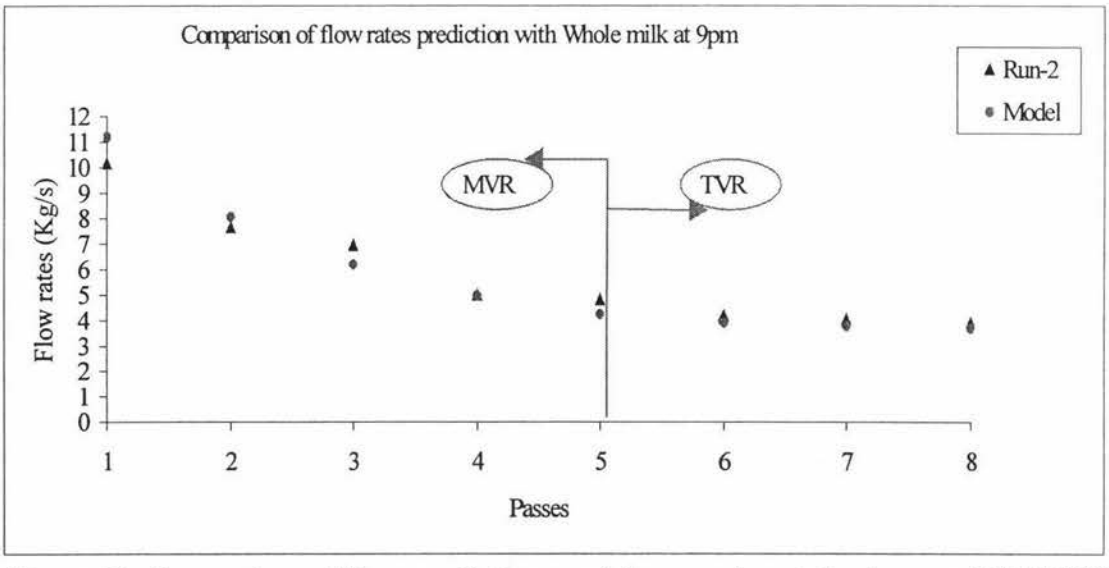

Figure 30: Comparison of flow predictions and the experimental values on 19/11/2000 at 9pm

The model predictions were tested against experimental results at different times during a run with Whole milk. Figures 27 and 28 show the model predictions and

experimental values close to the start of the run. Figures 29 and 30 show the values after 7 hours of the same run.

The model predictions close to the start of the run match the experimental results except for the first two passes. The reason for this is that the actual heat transfer coefficient in the first two passes at the start of the run is higher than that predicted by the heat transfer coefficient model for these passes. After 7 hours of the run the total solids and flows after the first two passes match the experimental results-but the predictions with all other passes show deviation from the experimental results.

The reasons why the model predictions deviate from the experimental results:

1. The calculated heat transfer coefficients from the dry matter measurements were plotted against the feed total solid concentrations for the corresponding passes instead of the average total solids. This effect is significant at low concentrations due to high heat transfer coefficients. The figure below shows the difference in heat transfer coefficient when plotted against the feed and the average concentration.

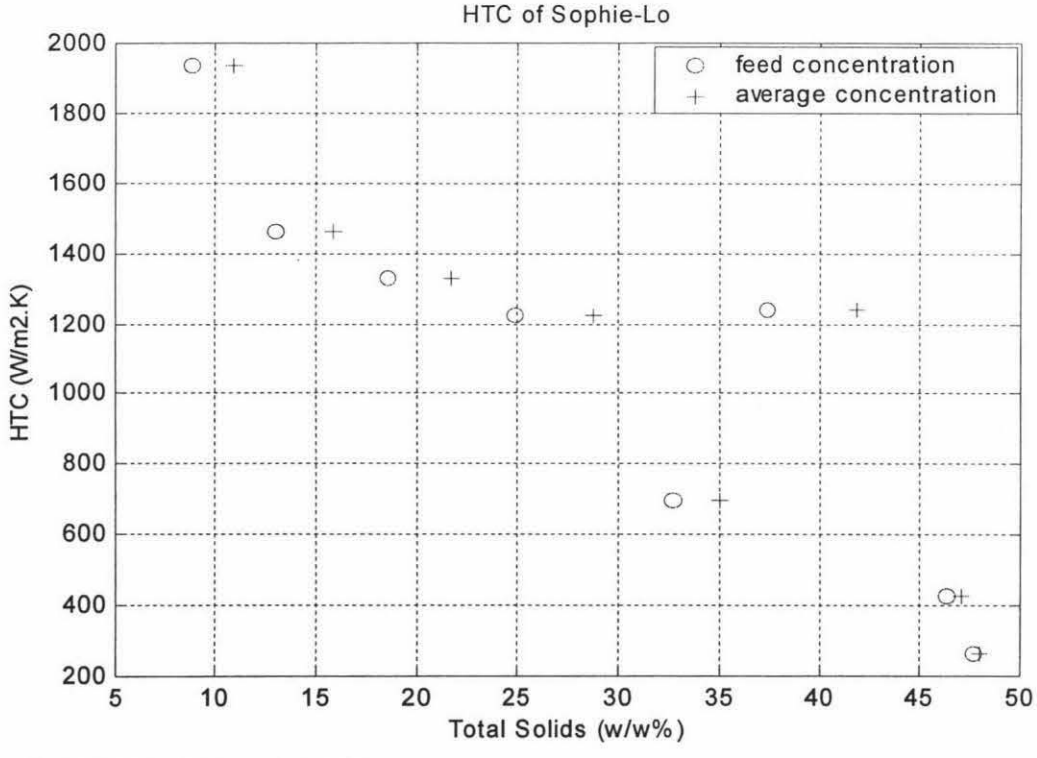

total solids concentrations.

2. The model does not incorporate the changes in heat transfer coefficient during a run (Reduction in heat transfer coefficient not only with total solids but also with time). This is significant with concentrated milk because the increase in resistance to heat with time is high (Chapter 6).

These indicate that the steady state model can only be used close to start of a run. To predict at later times the heat transfer coefficients would need to be calculated.

6. TIME VARYING HEAT TRANSFER COEFFICIENTS

6.1 Introduction

The factors determining the heat transfer coefficients of falling films are very complex. But it is necessary to understand their behaviour to increase the energy efficiency of the evaporation process. There are many models in the literature for calculating the heat transfer coefficient within the falling film evaporators (Mackereth, 1993; Winchester, 2000; Hong, 1992). All these models are based on the physical and chemical properties of the evaporating liquid, condensing steam on the shell side and the evaporator tube material. It was observed at the Powder 3 Plant not only that the heat transfer coefficient changed within the passes but also that it changed with time. No data are available in the literature on time-variant heat transfer coefficients. Here the average heat transfer coefficient of Whole milk within all passes at the Powder 3 Plant were estimated based on the mass of evaporation. The heat transfer coefficients and their changes were calculated from the operational (stored) data. The TVR steam pressure and the MVR fan speed increases with time indicates the drop in the heat transfer coefficient with time having all other parameters (feed concentration and feed flow) operated at fixed values.

6.2 Heat transfer coefficient of Whole milk

The heat transfer coefficient can be calculated from the mass of evaporation, temperature difference and the effective area of heat transfer (equation 14). Here the HTC is estimated with the assumption that the effective area for heat transfer is constant during the run (This may not be true if dry patches form in the tubes thereby reducing the heat transfer area). The shell temperature in the Powder 3 Plant is measured after the compressor and the effect temperature is measured at the separator. These measurements allow the heat transfer coefficient to be estimated based on the average temperature difference along the tubes.

The mass of steam from the DSI unit was added to the mass of evaporation in the first pass. Both the pressure drops along the tube and the boiling point elevations with total solids were taken into account in evaluating the temperature difference across the wall. The pressure drop along the tube reduces the temperature difference, while the boiling point elevation increases the temperature difference. The sample calculation of mass of steam injected in the DSI unit is shown in Appendix G. The results of heat transfer coefficients are also listed in Appendix G. Figure 33 shows the heat transfer coefficient and its changes during a run with Whole milk.

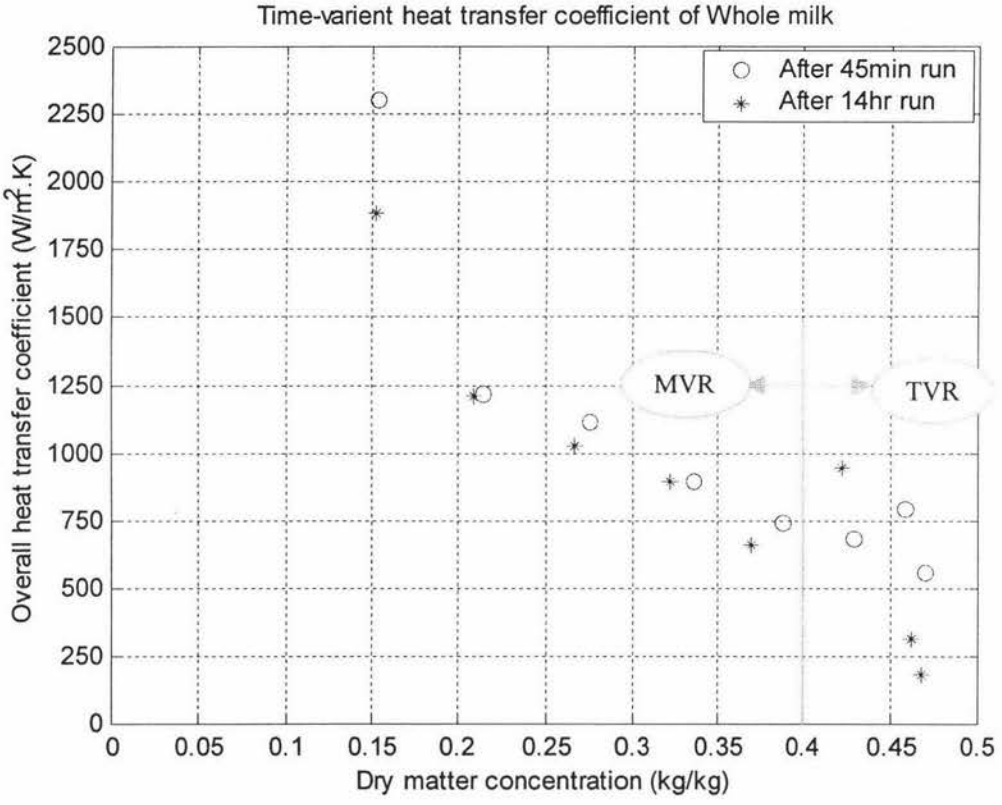

Figure 33: Average heat transfer coefficient and its changes during the run with Whole milk on 05-12-2000

The changes in heat transfer coefficients are significant in all passes. The heat transfer coefficient of Whole milk in the passes close to start match with the values given by Pisecky (1997). Since the shell temperature in the 2nd effect is not measured at the Powder 3 Plant, Winchesters' (2000) steady state model was used to find the temperature. The average heat transfer coefficient values shown in Figure 33 were

not calculated at the same operating conditions. This is because after 14 hours of the run with Whole milk, the compressor fan speed and the TVR steam pressure had to increase to meet the product specifications. If no changes had been made in the operating conditions during the run, actual heat transfer coefficients would have been observed.

6.3 Effect of Cleanliness of the surface on the HTC

Many researchers (including Bewing & Zisman, 1965; White & Drobek, 1966) have suggested that impurities on the surface of a tube wall would change the contact angle that a liquid will make on a solid surface. This will have a direct affect on the minimum flow. The affect may be to either reduce or increase the minimum flow depending upon the type of impurities on the surface (Paramalingam, 1999). Adsorption of protein particles from milk solutions is the major cause for the change in the contact angles and thus the minimum flows in the falling film evaporators. Yang, McGuire and Kolbe (1991) noted that the protein adsorption onto a surface caused a significant reduction in the contact angle. e.g., the contact angle of water measured between clean and β-lactoglobulin film-covered stainless steel surface showed a difference of $22^{o} \pm 3.47$. Therefore, it can be assumed that the affect of protein adsorption on the surfaces of the tubes on minimum flows is significant. The more the adsorption the larger the difference in contact angles, and thus the difference in minimum flows, which can be observed (section 5.3). The non-cleanliness of the surface and more protein adsorption during the run could be the reasons for the lower heat transfer coefficient observed at the later part of a run with milk.

The heat transfer coefficient reduction will be more significant in the TVR section due to the fact that concentrated milk is in contact with the wall of the evaporator tube. Since the shell temperature in the 2^{nd} effect is not measured, the calculations of heat transfer coefficient become difficult in the 2^{nd} effect.

This reduction in heat transfer coefficient—and thus the reduction in the amount of evaporation—will be higher with longer runs, as more protein will be adsorbed and

the formation of a thin layer along the evaporator tube wall will become significant. The fouled surfaces have also been shown to have smaller heat transfer coefficients. This is due to either substance being precipitated on the tube wall or to the evaporator tubes being only partially wetted. In the latter case the reduction in surface area appears as a reduction in heat transfer coefficient, since the surface area is assumed to be constant.

7. HISTORICAL DATA CHECK FOR MINIMUM FLOW VIOLATION

7.1 Introduction

Falling film evaporators should be supplied with sufficient flow to avoid dry patches arising within the evaporator tubes. The falling film evaporators could be run with a flow above the retarding minimum flow without dry patches if no disturbances occur within the tubes. This flow will not sweep off dry patches if they occur within the tubes. If flows within the passes are above the advancing mWinchester (2000) inimum flow, then dry patches will be swept off. Therefore, the risk of not re-wetting dry patches increases as the flow decreases from the advancing minimum flow to the retarding minimum flow. The occurrence of the dry patches within the tubes of falling-film evaporators was identified using historical data from the Powder Plant. First, the heat transfer coefficient variation when the falling film evaporator was running with water was used to validate the film break-up at low flows. Secondly the operating flows with milk in the Powder Plant were tested for minimum flow violations.

7.2 Film break-up and heat transfer coefficient of water

Due to the fact that the heat transfer coefficient is very lower between air and vapour relative to water and vapour, a low heat transfer coefficient will be observed when films break and allow the surface to be exposed. The variation in the heat transfer coefficient of water in MVR section at the Powder 3 Plant was observed. Not all passes could be analysed because the flows after the other passes were not being measured in Powder 3 Plant.

The heat transfer coefficients calculations were based upon the mass of evaporation in the MVR section. Due to the fact that properties of vapour (viscosity, density, thermal conductivity) are much lower than that of water, the actual falling film heat transfer coefficient when the surface of tubes is exposed to vapour will be very low.

Therefore a decrease in heat transfer coefficient is expected. The Figures below show the results of an experimental run on water. They show the flows and the heat transfer coefficient variation with water in the MVR section.

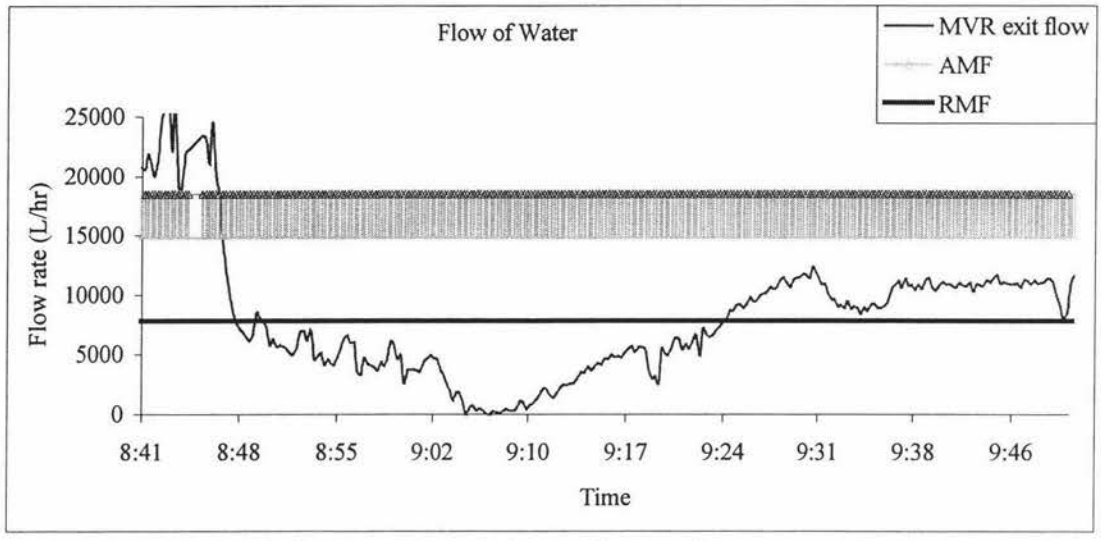

Figure 34: MVR exit flow and the minimum flows with water on 27-10-2000. RMF-Retarding minimum flow, AMF-Advancing minimum flow band.

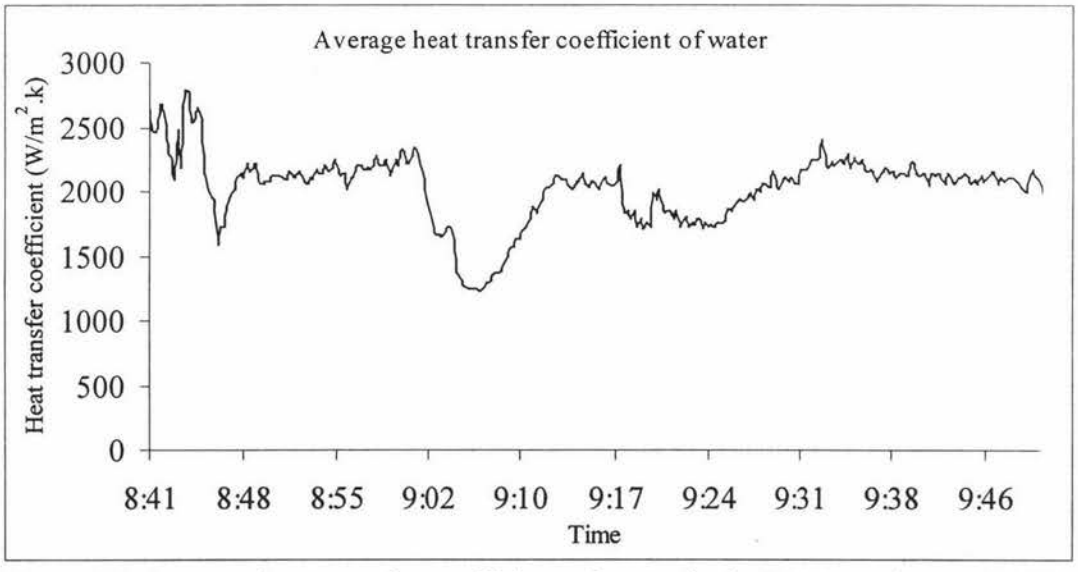

Figure 35: Average heat transfer coefficient of water in the MVR section on 27-10-2000.

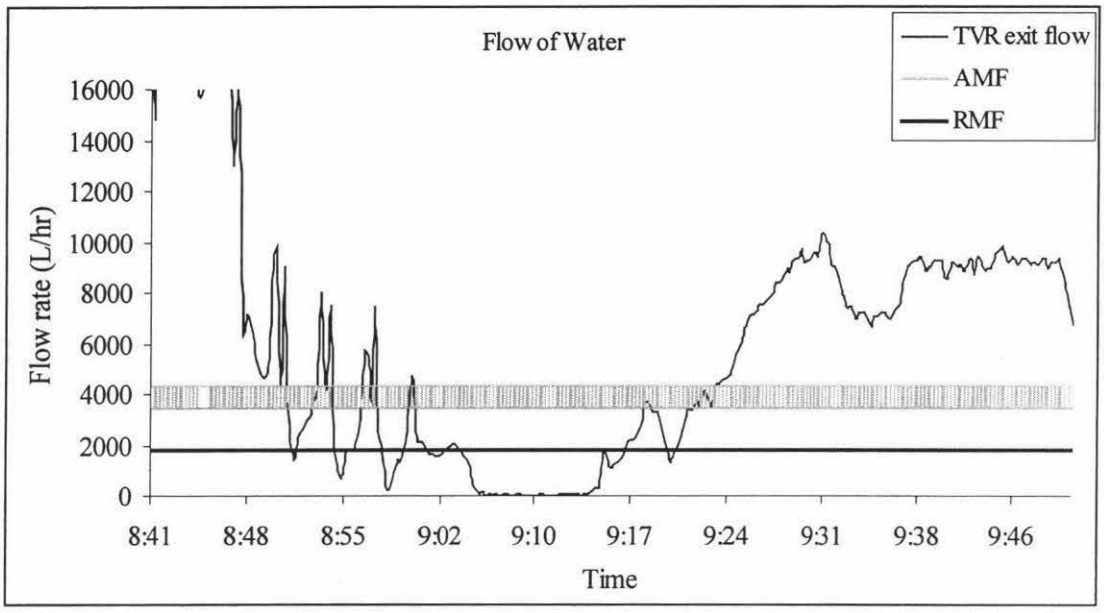

Figure 36: TVR exit flow and the minimum flows with water on 27-10-2000. RMF-Retarding minimum flow, AMF-Advancing minimum flow band.

Figure 34 shows that the MVR exit flow initially reduced to below the retarding minimum flow and was not increased to the advancing minimum flow. The TVR exit flow (Figure 36) followed the same pattern, but was increased well above the advancing minimum flow. This means that the dry patches formed in the MVR section would not have been eliminated by the water flow while the TVR section would have developed dry patches that would have then be swept off. Figure 35 shows that the average heat transfer coefficient in the MVR section did not fully recover. This further verifies the existence of dry patches.

If the flows after each pass were measured, it would be possible to show exactly the passes in which the film breakdown would have occurred. Figure 37 shows the initial film breakdown in the passes of the MVR section. The flows after each pass were calculated by assuming the mass of evaporation in each pass is proportional to the total surface area in that pass in the MVR section.

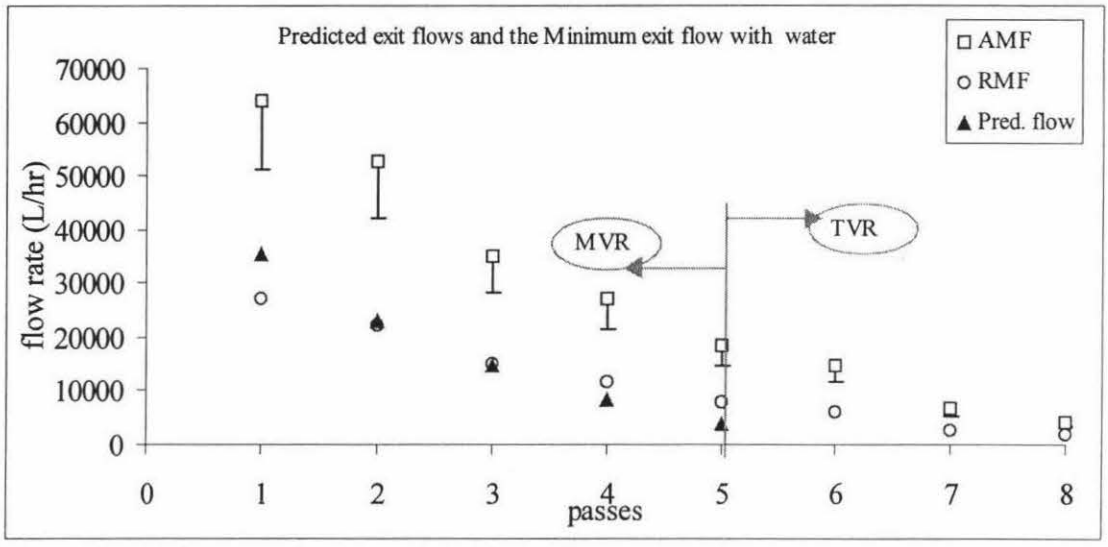

Figure 37: Minimum flows and predicted flows out of each pass on 27-10-2000 with water. RMF- Retarding minimum flow, AMF-Advancing minimum flow.

It can be seen from Figure 37 that the film breakdown could have occurred at the end of the 5th and the 4th passes. The flow at the top of the 4th pass is sufficient, but not sufficient at the bottom. Also the flow at the top of the 5th pass is sufficient, but not sufficient at the bottom. When the flow goes further down from the retarding minimum flow, the area of the tube wall that is exposed to vapour increases. As described in section 6.3, the minimum flows may have been affected by the protein adsorption onto the wall of the evaporator tubes. If the flows after each pass were to be measured, then the actual change in the overall heat transfer coefficient in each pass could have been observed.

The minimum flow violations in the 1st pass in the TVR section were tested. Figure 38 shows the violation of minimum flow in the 1st pass in the TVR section. Figure 39 shows the variation of 2nd effect temperature at this low flow to the TVR. This shows a dramatic increase in temperature, which is presumably due to reduced heat transfer in the pass caused, in turn, by film break-up. This suggests the occurrence of film break-up in the 1st pass of TVR. It is important also to note that the 2nd effect temperature increases to 76°C at a steam supply pressure of 5 bar. Therefore, the temperature variation with steam supply pressure in the shell of the 2nd effect should

be known for better control and to avoid fouling due to hot spots in the 1st pass of the TVR section.

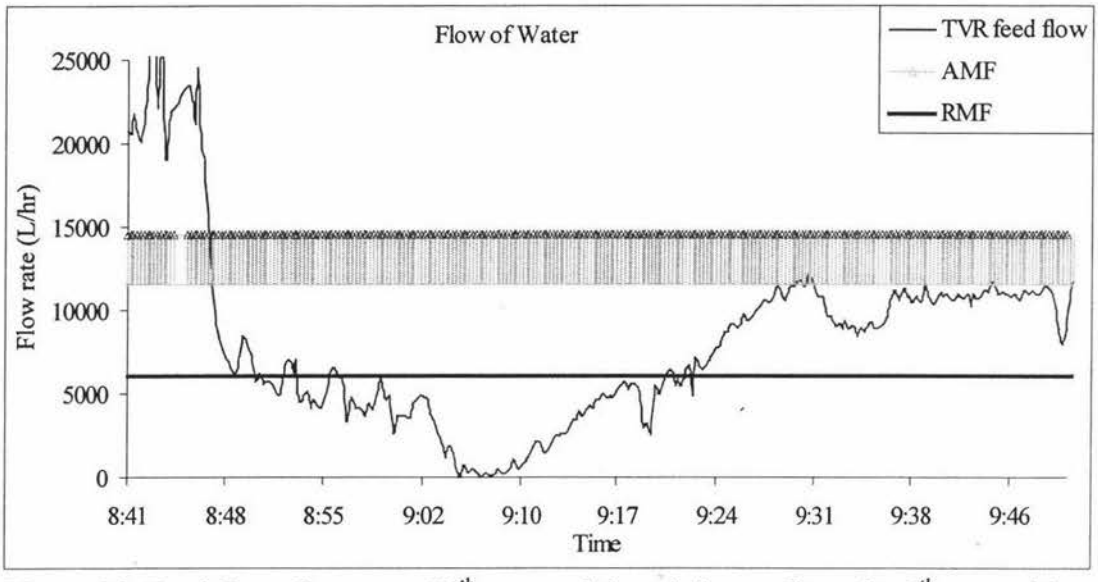

Figure 38: Feed flow, flow out of 6th pass and the minimum flows for 6th pass with water on 27-10-2000. RMF- Retarding minimum flow, AMF-Advancing minimum flow band.

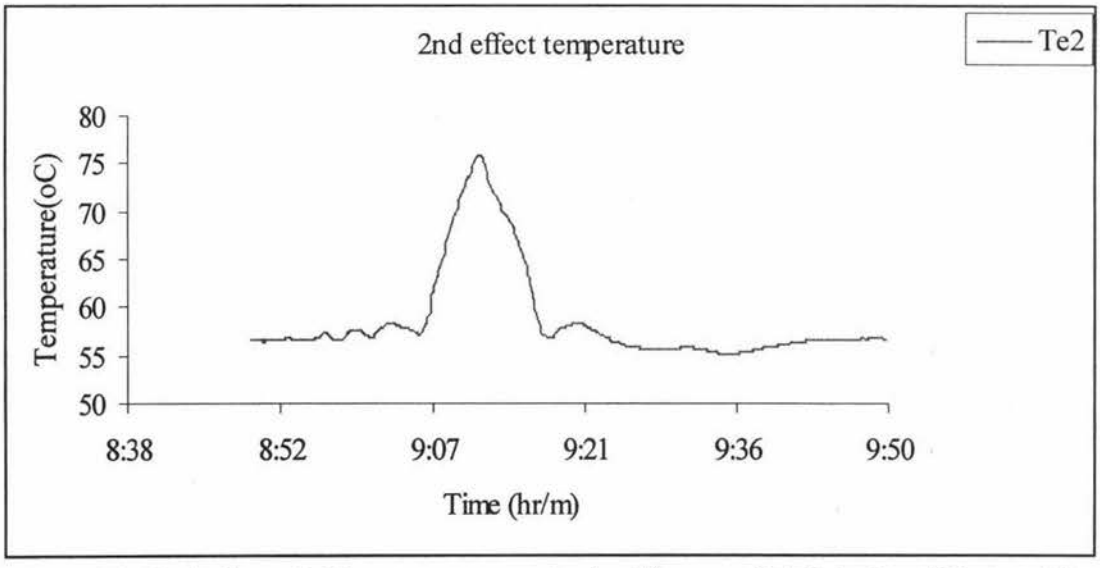

Figure 39: Variation of effect temperature in the 1st pass of TVR before Whole milk was turned on 27-10-2000. Te2- 2nd effect temperature.

7.3 Minimum flow violations with milk product

In this section the historical data of the Powder 3 Plant at Kiwi Co-op Dairies Ltd. was checked for minimum flow violations. Since the operating conditions and the control strategies now at this plant are steady and better than those of two years ago, only the year 2000 data were examined for minimum flow violation.

One test with each product may represent all runs, as the operating flows with each product in the Powder 3 Plant were almost the same for all runs. The steady state model was used in evaluating the flows after each pass because the flows in between the passes are not measured at the plant. Some of the worst situations with both milk products when the flows violate the minimum flow requirement are described here.

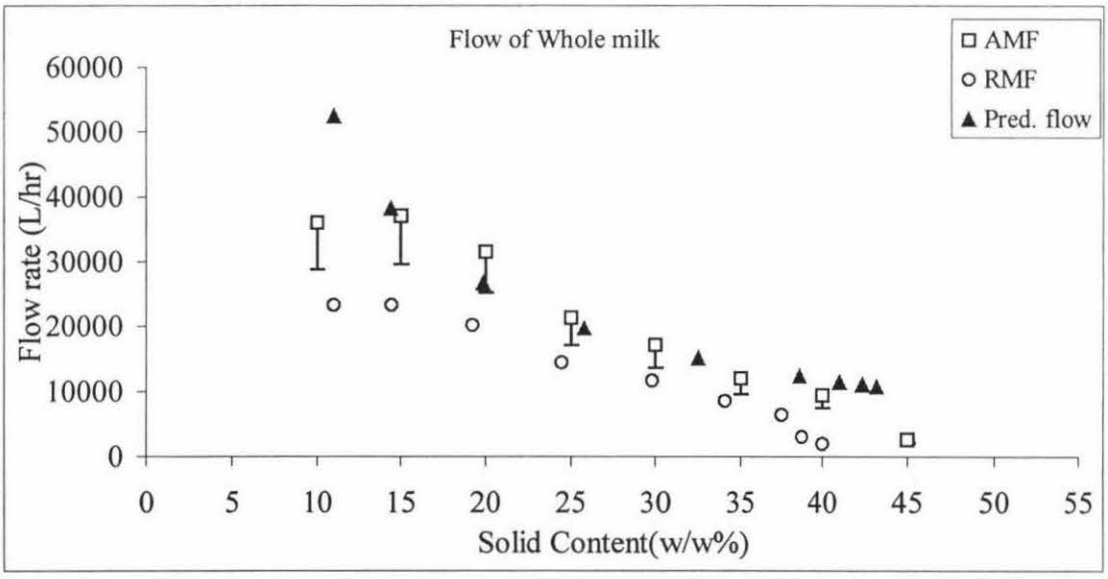

Figure 40: Comparison of model predicted flows (08-09-00) and minimum flows with Whole milk. RMF- Retarding minimum flow, AMF-Advancing minimum.

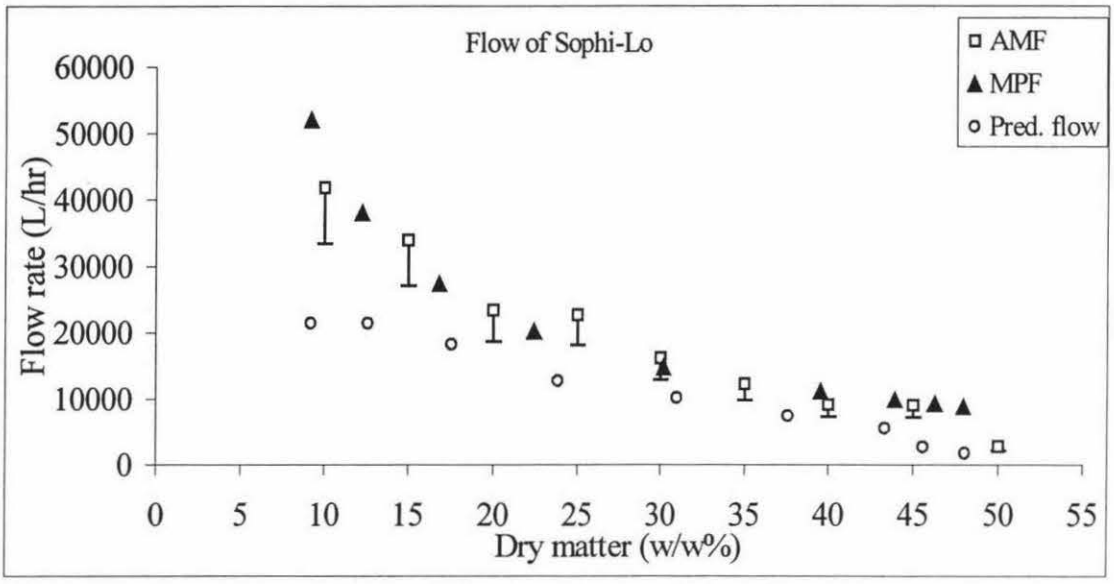

Figure 41: Comparison of model predicted flows (17-09-00) and minimum flows with Sophie-Lo. RMF- Retarding minimum flow, AMF-Advancing minimum.

Figures 41 and 42 show the operating flows and the theoretical minimum flows with Whole milk and Sophie-Lo respectively. The flows with Whole milk in the Powder 3 Plant satisfy the advancing minimum flows in all passes except in the 2nd pass (20%w/w). The flows with Sophie-Lo do not satisfy the advancing minimum flows in the 2nd and 3rd passes (15%w/w and 25%w/w). This does not mean that there will be fouling with all runs in these passes, but it could happen if dry patches formed since the flows are not sufficient to sweep them off.

The milk could be overheated at the leading front when it encounters a dry surface. This can happen when the flow of water is very low prior to the arrival of the product. This situation can be seen frequently in the historical data. The flows and the total solids variation exiting from the MVR section during the start-up are analysed with both Whole milk and Sophie-Lo. These start-up flows are then tested for minimum flow violations. The total solids content of milk out of MVR section close to start of a run increase rapidly but not in a similar pattern with all runs. Figures 42 to 49 illustrate the low water operating flows prior to milk and how that affects the milk product in the falling film evaporators.

Whole Milk

Figures 42 and 43 show the low flows with water prior to whole milk and figures 44 and 45 shows how these low flows affect the whole milk in the evaporator

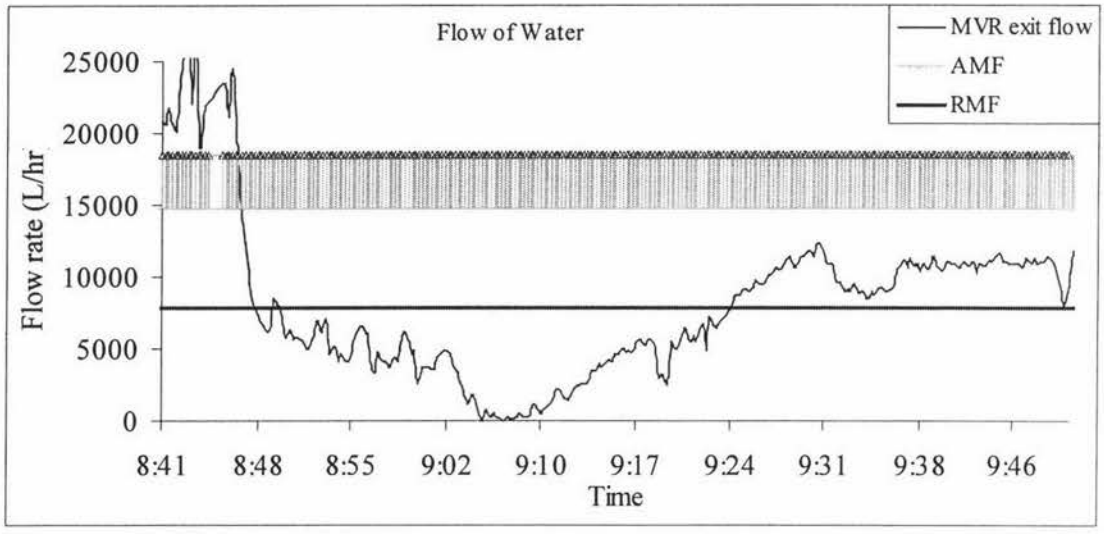

Figure 42: MVR exit flow and the minimum flows with water. RMF- Retarding minimum flow, AMF-Advancing minimum flow band.

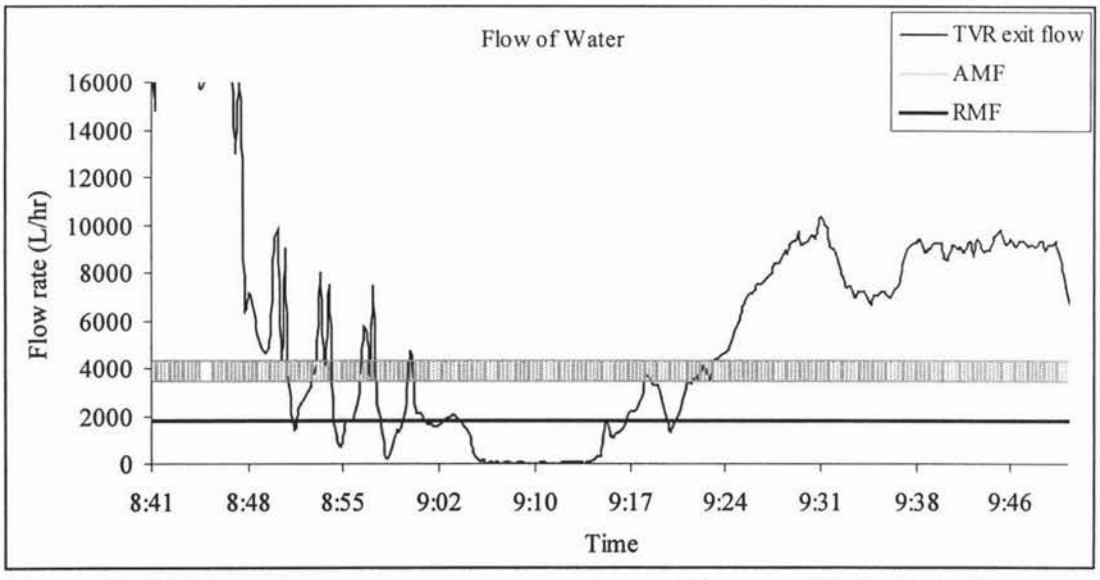

Figure 43: TVR exit flow and the minimum flows with water. RMF- Retarding minimum flow, AMF-Advancing minimum flow band.

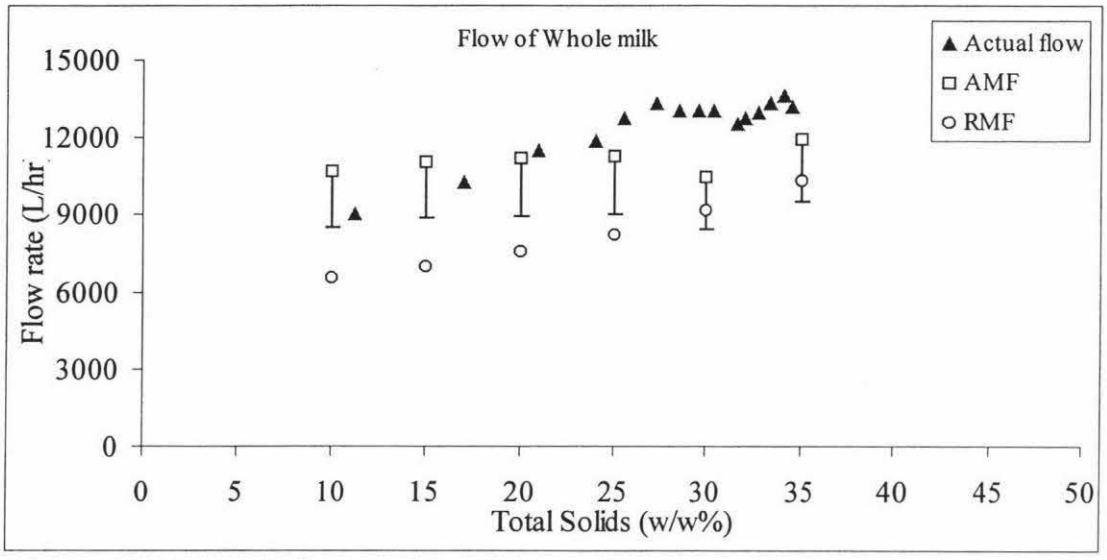

Figure 44: MVR exit flows and the minimum flows just after the product was turned on. RMF- Retarding minimum flow, AMF-Advancing minimum.

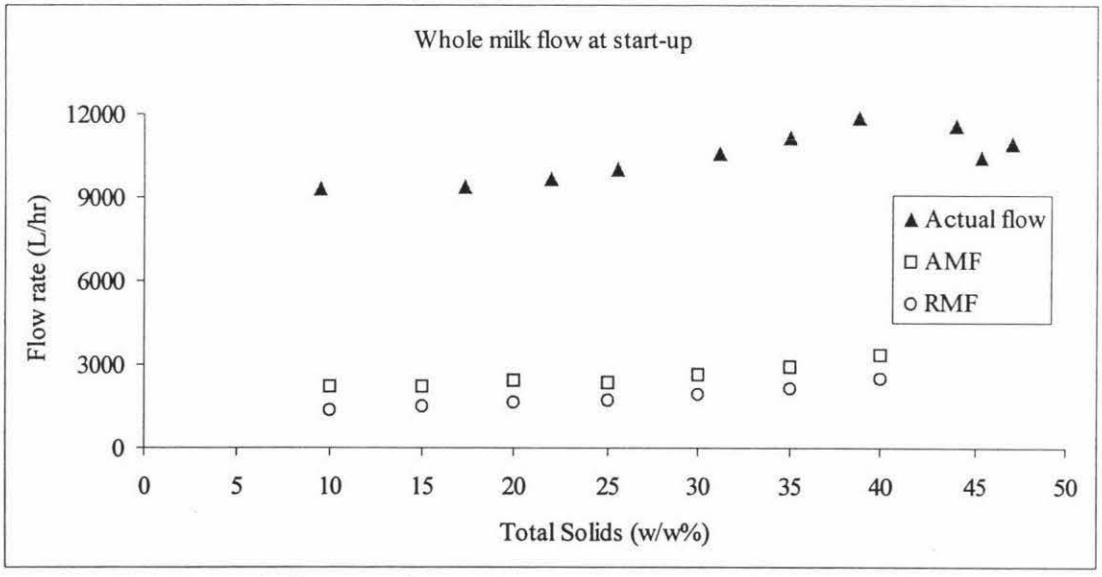

Figure 45: TVR exit flows and the minimum flows just after the product was turned on. RMF- Retarding minimum flow, AMF-Advancing minimum.

The exit water flows from both MVR and TVR before the Whole milk run, went down below the retarding minimum flow and the exit water flow from the MVR remained the same whereas the exit flow from the TVR increased above the advancing minimum flow (Figures 42 & 43). Therefore, the dry patches, which

occurred, in the last pass of MVR section would not have been swept off and the Whole milk would have been encountered the dry surface in the MVR section. The dry patches formed in the last pass in the TVR section would have been swept off prior to the arrival of milk as the flow of water increased above the advancing minimum flow for that pass.

The Whole milk flow rates exiting from both the MVR and the TVR, a few minutes after the evaporator was fed with milk, were examined. Figure 44 and 45 show the comparison of Whole milk with the minimum flows at various total solids concentrations. It can be seen from the figure 44 that close to start of the run with Whole milk on 27-10-2000 operates close to, and above, the advancing minimum flows for the last pass of the MVR section. This means the dry patches formed in the last pass of the MVR were more likely to be stable at low concentrations. The milk in the last pass of the TVR section could not have encountered hot surfaces as the water flow prior to the milk arrival and the milk flows were above the advancing minimum flow (Figures 43 & 45).

Sophie-Lo

Figures 46 and 47 show the low flows with water prior to Sophie-Lo and figures 48 and 49 show how these low flows affect the Sophie-Lo in the evaporator.

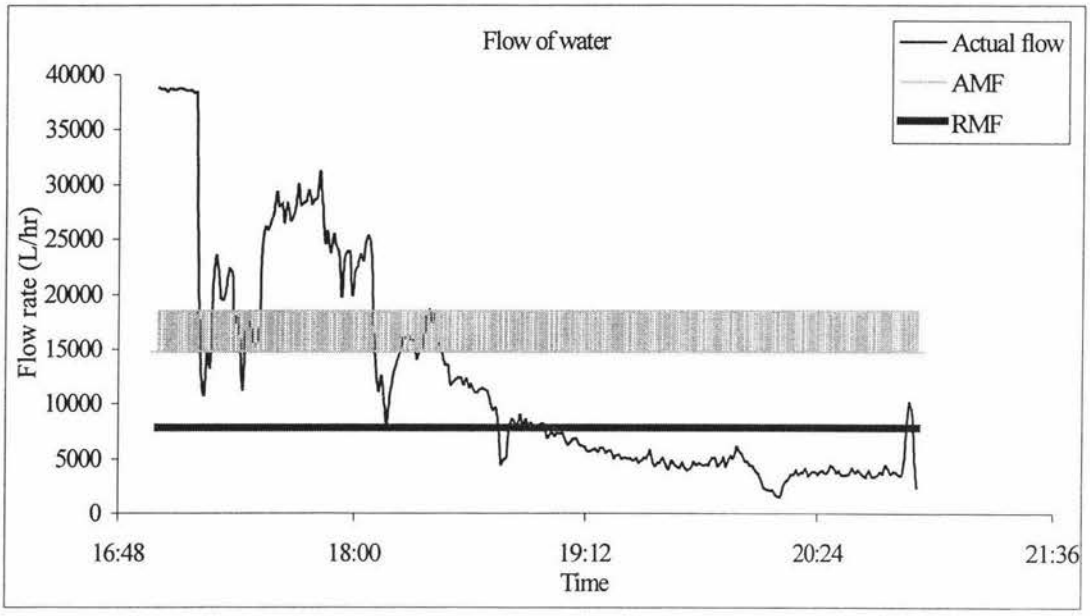

Figure 46: MVR exit flows (11-08-00) and the minimum flows prior to Sophie-Lo run. RMF- Retarding minimum flow, AMF-Advancing minimum flow band.

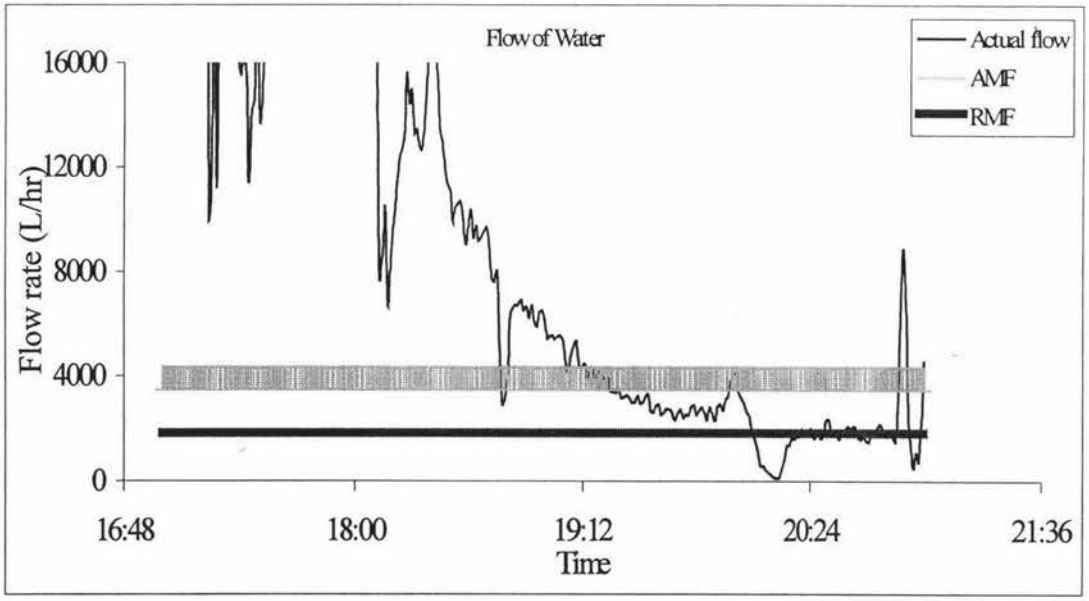

Figure 47: TVR exit flows (11-08-00) and the minimum flows prior to Sophie-Lo run. RMF- Retarding minimum flow, AMF-Advancing minimum flow band.

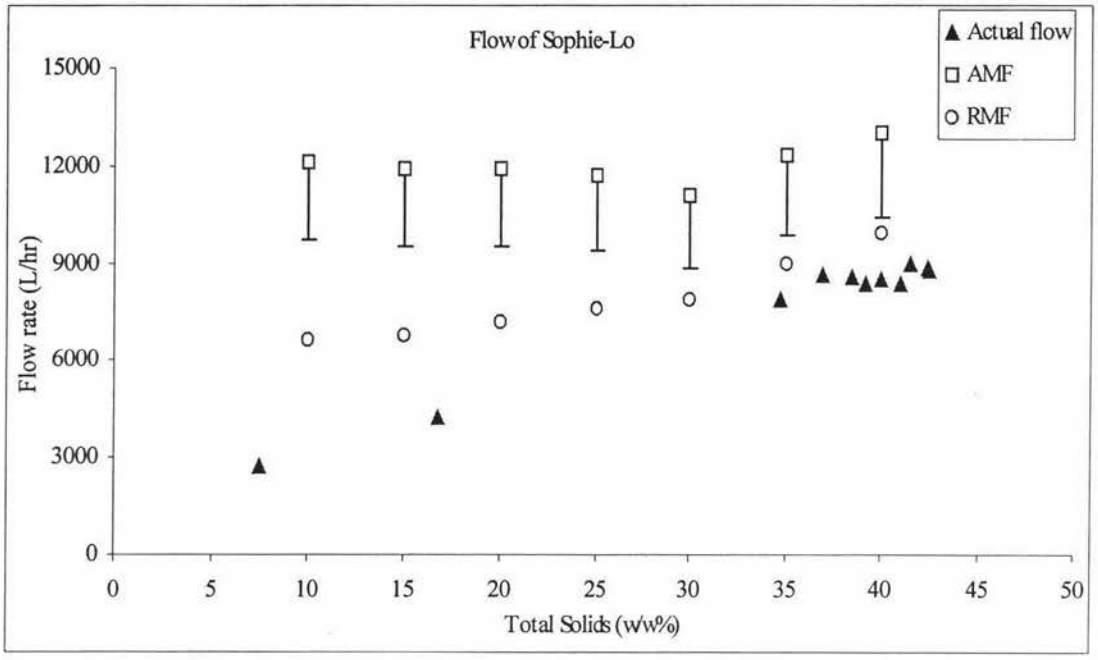

Figure 48: MVR exit flows (11-08-00) and the minimum flows just after the product was turned on. RMF- Retarding minimum flow, AMF-Advancing minimum

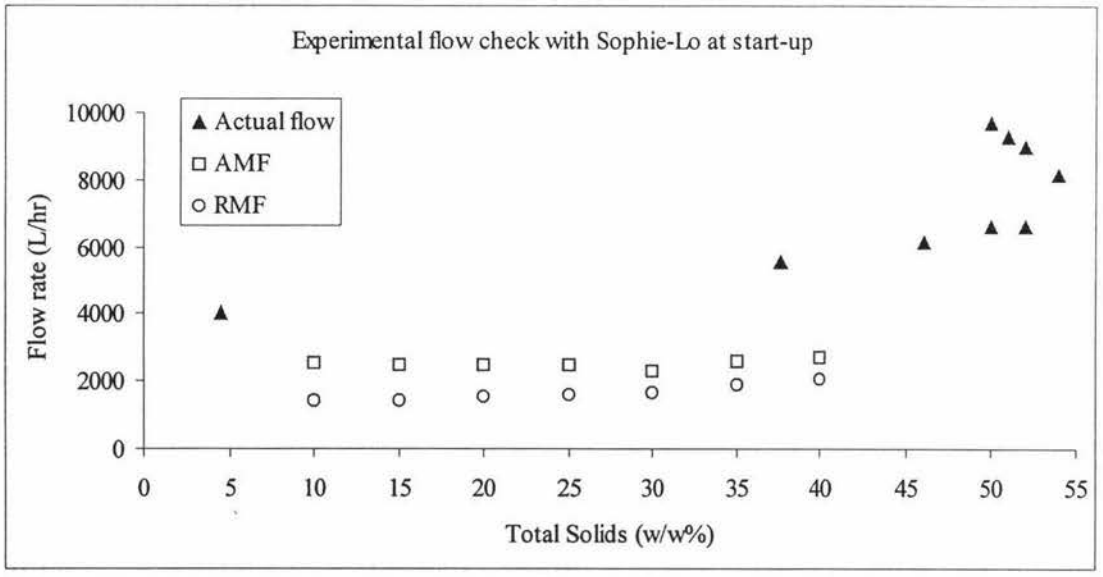

Figure 49: TVR exit flows (11-08-00) and the minimum flows just after the product was turned on. RMF- Retarding minimum flow, AMF-Advancing minimum

The exit flow rates from both MVR and TVR sections with water before the Sophie-Lo run went down below the retarding flow. Since the exit water flow from both sections remained the same and below the advancing minimum flow, the dry patches, which occurred, would not have been swept off. Therefore, the Sophie-Lo should have been exposed to hot surfaces in both the MVR and TVR sections.

Figures 48 and 49 show the flows with Sophie-Lo just after the product was turned on. It can be seen also from the figures that the MVR exit flows on 11-08-2000 with Sophie-Lo were lower than the retarding minimum flows, whereas the TVR exit flows were above the advancing minimum flows. Therefore the dry patches formed prior to the milk arrival in the last pass of the MVR section would not have been swept off by the milk flow. The milk could have been overheated in this section and possibly fouling. The dry patches formed in the last pass of the TVR section when running with water would have been swept off by the milk flow as the flows were above the advancing minimum flows.

8. CONCLUSION

Re-wetting is of great interest in the falling film evaporators, as the advancing minimum flow is sufficient to sweep off any stable dry patches occurring in falling films. The retarding minimum flow below which the dry patches can occur spontaneously is also important information for the sake of the safe operation of the falling film evaporators. Both Hartley and Murgatroyd and Hoke and Chen models are used to predict these minimum flows.

The Hartley and Murgatroyd (1964) model predicts well with low total solids of milk products and water, and the Hoke and Chen (1992) model is best fitted to high total solids milk products and high viscosity liquids. To estimate the advancing and retarding flows for milk and water by either model, physical properties of different milk products—advancing contact angle, retarding contact angle, surface tension, viscosity and density—are needed.

The viscosity and density of "milk-drive products" were estimated from composition and temperature based models. These models based on the assumption of an ideal mixture, which is not exactly correct in the case of milk. However, the ideal mixture models are comparatively simple and their accuracy can be improved by model identification. No details of the advancing contact angle or surface tension of milk products were found in the open literature. An experimental technique developed from previous studies (Paramalingam, 1999) was used to obtain those data. The retarding contact angle was assumed to be 40° for both milk products and water. Further studies on retarding contact angle with milk products would improve the accuracy in retarding minimum flow predictions. Having found the physical properties, the advancing and the retarding minimum flows for different milk products and for water were estimated.

The minimum flows were estimated at the evaporators' operating conditions, with the physical properties being converted to evaporator operating conditions. The predictions with milk products and water were compared with experimental measurements after each pass at the Powder 3 Plant. The comparison conclusions are,

- The operating flows with Whole milk satisfy the minimum flow requirements in all passes except in the 2nd pass—where it is very close to the constraint.

- The operating flows with Sophie-Lo violate or are less than the minimum flows in the 2nd and 3rd passes.

- The flows with water were found to violate both advancing and retarding flows on several occasions.

- The steady state model predictions deviate from the experimental results after several hours run with milk. The reason was found to be the assumption of a constant heat transfer coefficient in the steady state model.

- The average overall heat transfer coefficient calculation in the MVR section from the on line data when operating with water was used to validate the breakdown of falling films at lower flows.

The attractive features of both the Hartley and Murgatroyd (1964) and Hoke and Chen (1992) models are their simplicity and negligible measurement errors. These models relax some of the forces that are complex to analyse and shown (Paramalingam, 2000) to be insignificant. The advancing contact angle and surface tension measurements do not take into account the chemical and physical changes in milk and other possible factors that may prevail in the falling film evaporators. However, the validation results when evaporators running with water show the accuracy in the flow predictions. Though the concentrations—and thus the flows—vary along the evaporator tubes, the minimum flow does exist at the end of the tubes. Therefore, with the knowledge of advancing and retarding minimum flows, the operational flows after each pass could be controlled and eventually could avoid fouling due to film break-up. Also, knowledge of the ways in which the heat transfer coefficient differs in the various passes, their changes during a run and thus the adjustments that should be made in the operating conditions would be beneficial to the falling film evaporator plants.

9. RECOMMENDATIONS AND AREAS FOR FUTURE WORK

9.1 Viscosity

The viscosity of milk concentrates is one of the most important process input variables in the manufacture of milk powders. Also it shows a significant effect in the minimum flows at high concentrations of milk products, as the weight force at the stagnant point of a dry patch is high. Therefore, availability of the absolute viscosity measurements at Kiwi Co-op Dairies Ltd. would improve the optimisation studies. Also developing a viscosity model that incorporated the effects of total solids, the heat treatment, the composition, the holding time and the temperature on the viscosity of milk would improve the minimum flow predictions.

9.2 Heat transfer coefficient

Heat transfer coefficients of falling films within the evaporators should be identified reasonably accurately for both milk and water to improve the steady state model predictions and the controllability of the model predictive controller in the Powder 3 Plant. It has been found that the heat transfer coefficient not only varies within the passes in the evaporator but also during the run. In order to calculate the apparent heat transfer coefficients of both water and milk in each pass at Kiwi Co-op Dairies Ltd., the flows after each pass, feed total solids concentration and the 2^{nd} effect shell temperature should be measured. The pressure drop calculation in both the shell side and in the effect side would improve the accuracy in estimating the driving force in the evaporation and thus the heat transfer coefficient (Chapter 6).

9.3 Current operating flows

The current operating flows with Sophie-Lo were found to have more minimum flow violations than those with Whole milk. Either the feed flows with milk should be increased or the initial evaporation in the MVR should be decreased to satisfy the minimum flow requirements, as the heat transfer coefficient of milk products is high

at the start-up of a run. It can be seen from Chapter 5 (Figure 25) that the increased feed flow with Whole milk brought the flows after each pass above the minimum flow requirements.

Some of the worst situations were found with milk operating flows at the start up of the run. The flows after the 5th pass with Sophie-Lo (Figures 39 and 40, Chapter 7) were found to be lower than that which is necessary to hold a complete film within the tubes. This was not so with Whole milk (Figure 41, Chapter7) because the heat transfer coefficient of Sophie-Lo is higher than the heat transfer coefficient of Whole milk at low concentrations. These problems could be avoided with a high flow of water just before the products are turned on.

Many cases were found (Figures 42 and 44) with insufficient flow of water within the evaporator tubes, especially just before the products are fed in. The hot spots formed due to the low flow with water could overheat the oncoming milk and may lead to fouling. To avoid this either the water flow should be increased, or the water flow and the MVR fan speed should be adjusted in such a way that the flows from the passes never fall below the retarding minimum flows for water. This water flow control just before the product is turned on and just after the product is turned off, would minimise the cleaning length and thus the chemicals used in cleaning.

9.4 Measure of fouling

The quality control of the product at the end of the process at Kiwi Co-op Dairies Ltd. would satisfy the market, but it is not sufficient to solve the problems occurring within the process. There should be some sort of measurements (Turbidity measurements using HILLS) to judge the fouling after the important units in the powder processing (e.g., after the Preheat section, after the MVR section, after the TVR section and at the feed to the Spray Drier). It is well known that a direct link exists between fouling and the heat-denaturation of proteins when milk products are processed above 70°C. It should be noted that the feed temperatures to the Spray Drier are 70°C with Whole milk and 80°C with Sophie-Lo. The fouling that related to the operating conditions

could be analysed if some form of fouling measure were to be made available at various units in the plant. This could be fed to the model for better control.

10 NOMENCLATURE

Nomenclature	Description	Units
ρ	Density of liquid	kg/m^3
σ	Surface tension	N/m
θ	Advancing Contact angle	^{o} (degree)
δ	Film thickness	m
g	Acceleration due to gravity	m/s^2
μ	Viscosity of liquid	kg/m/s
h_S	Sessile drop height	m
r	radius of the sessile drop	m
d_V	Density of vapour	kg/m^3
h_C	Height of capillary rise	m
T	Temperature	^{o}C
$\Gamma_{H\&M}$	Minimum flow from Hartley & Murgatroyd	kg/m/s
$\Gamma_{H\&C}$	Minimum flow from Hoke & Chen	kg/m/s
M_{evap}	Rate of Mass of evaporation	kg/s

λ	Latent heat of evaporation	kJ/kg
$\Delta\theta$	Temperature difference	^{o}C
A	Surface area of evaporator tubes	m^2
U	Overall Heat transfer coefficient	$W/m^2.k$

11. REFERENCES

Adamson W, Physical Chemistry of Surfaces, 3rd edition, 1976, John Wiley & Sons, Inc, USA

Bertsch A J, Surface Tension of Whole and Skim-milk between 18oC and 135oC, Journal of Dairy Research, 1983, Vol.50, pp. 259-267

Bewing K W and Zisman W A, Journal of Physical chemistry, 1965,Vol.69, p. 4238

Bloore C G and Boag I F, Some factors affecting the viscosity of concentrated skim milk, New Zealand Journal of Dairy Science and Technology, 1981, Vol. 16, pp. 143-154

Brenmuhl M M, Model based study of Energy utilisation in milk evaporation, M.Tech thesis, 1999, Massey University, Palmerston North, New Zealand

Chun M H and Kim K T, Assessment of the new and existing correlation for laminar and turbulent film condensation on a vertical wall, International communications in Heat and Mass Transfer, 1990, Vol. 17, pp. 421-441

Chung J C and Bankoff S G, Initial breakdown of a heated liquid film in concurrent two-component annular flow, Chem. Eng. Communication, 1979, Vol. 4, pp. 455-470

Emily T, Investigation into CIP of Powder evaporators, 2000, Project report, Kiwi Co-op Dairies Ltd

Fernandez-Martin F, Influence of temperature and composition on some physical properties of milk and milk concentrates, Journal of dairy research, 1972, Vol. 39, pp. 75-82

Hartley D E and Murgatroyd W, Criteria for the break-up of thin liquid layers flowing isothermally over solid surfaces, International Journal of Heat and Mass Transfer, 1964, Vol.7, pp. 1003-1015

Hoke B C and Chen J C, Thermocapillary breakdown of subcooled falling liquid films, Industrial Engineering and Chemistry Research, 1992, Vol. 31, pp. 688-694

Hong C, Factors affecting heat transfer in the falling film evaporator, M.Tech, 1992, Massey University, Palmerston North, New Zealand.

Hughes D T, Bott T R, The break up of falling films inside small diameter tubes, Chemical engineering science, 1991, Vol. (46-7), pp. 1795-1805

Jam Pisecky, Handbook of Milk Powder Manufacture, 1997, Copenhagen, Denmark

Kruif C G, Van lersel E M F and Vrij A, Viscosity as a function of shear rate and volume fraction, Journal of Chemical Physics, 1985, Vol. 83, pp. 4717-4725

Mackereth A R, Thermal and Hydraulic Aspects of Falling-film evaporation, Ph.D. thesis, 1993, University of Canterbury, Christchurch, New Zealand

Paramalingam S, The Wetting Constraint in Falling Film Evaporators, Dip.Tech. Dissertation, 1999, Massey University, Palmerston North, New Zealand

Paramalingam S, Winchester J, Marsh C, On the fouling of falling-film evaporators due to film break-up, Transaction of the Institute of Chemical Engineers, 1999, Vol.78, pp. 79-84

Ponter A B, Davis G A, Beaton W and Ross T K, The measurement of Contact angles under conditions of heat Transfer when a liquid film breaks on a vertical surface, Journal of Heat and Mass Transfer, 1967, Vol.10, pp. 1633-1636

Snoeren T H M, Damman A J, Klok H J, The viscosity of skim-milk concentrates, Netherlands milk dairy Journal, 1982, Vol. 36, pp. 305-316

White M L and Drobek J, Journal of Physical Chemistry, 1966, Vol. 70, pp. 3432

Winchester J A, Model based Analysis of the Operation and Control of falling film evaporators, 2000, PhD thesis, Massey University, Palmerston North, New Zealand

Yang J, McGuire J and Kolbe E, Use of Equilibrium contact angle as an index of Contact surface cleanliness, Journal of Food Protection, 1991, Vol.9, pp.879-884

Zuber N and Staub F W, Stability of dry patches forming in liquid films flowing over heated surfaces, International Journal of Heat and Mass Transfer, 1966, Vol. 9, pp. 897-905

Appendix

Appendix A : Experimental data for contact angle and surface tension

Appendix B : Density

Appendix C : Viscosity

Appendix D : Contact angle and surface tension results

Appendix E : Minimum flows

Appendix F : Experimental data and results at Powder Plant

Appendix G : Heat transfer coefficients

APPENDIX-A

The measurement readings from sessile drop and capillary rise methods are tabulated here for milk concentrations 5% to 50% in step of 5. Whole milk data is in table A-1 and Sophie-Lo is in table A-2. The last two columns of the tables give the contact angle and the surface tension values from the simultaneous solution of equations 4 and 5.

Table A-1 10% Whole Milk

Sample	Temp (°C)	h_c (mm)	H_s (mm)	r(cm)		θ(°)	σ (N/m)
1	28	0.87	2.44	2.45		67.5258	0.0459
			2.38	2.35		65.8579	0.0434
			2.40	2.50		66.2472	0.0449
			2.41	2.55		67.3340	0.0452
		0.89	2.44	2.45		66.1079	0.0464
			2.38	2.35		65.6325	0.0446
			2.40	2.50		65.8262	0.0453
			2.41	2.55		65.9141	0.0457
		0.95	2.44	2.45		64.8806	0.0479
			2.38	2.35		64.3889	0.0461
			2.40	2.50		64.5898	0.0468
			2.41	2.55		64.6808	0.0472
		0.93	2.44	2.45		65.2854	0.0474
			2.38	2.35		64.7990	0.0456
			2.40	2.50		64.9975	0.0463
			2.41	2.55		65.0875	0.0467
2	29	0.96	2.43	2.50		64.6185	0.0479
			2.41	2.50		64.4650	0.0474
			2.40	2.45		64.3729	0.0470
			2.42	2.40		64.5121	0.0475
		0.99	2.43	2.50		64.0216	0.0487
			2.41	2.50		65.8659	0.0481
			2.40	2.45		65.7724	0.0478
			2.42	2.40		63.9134	0.0483
		0.92	2.43	2.50		65.4291	0.0469
			2.41	2.50		65.2789	0.0464
			2.40	2.45		66.1888	0.0460
			2.42	2.40		65.3253	0.0465
		0.94	2.43	2.50		65.0217	0.0474
			2.41	2.50		64.8698	0.0469
			2.40	2.45		64.7787	0.0465
			2.42	2.40		64.9165	0.0470

Whole Milk

15%

Sample	Temp. (°C)	h_c (mm)	H_s (mm)	r(cm)		θ(°)	σ (N/m)
1	30	0.98	2.37	2.45		63.7340	0.0472
			2.36	2.40		63.6385	0.0469
			2.39	2.35		63.8613	0.0477
			2.35	2.25		63.5076	0.0464
		0.97	2.37	2.45		63.9354	0.0470
			2.36	2.40		63.8403	0.0466
			2.39	2.35		64.0621	0.0474
			2.35	2.25		63.7102	0.0462
		0.94	2.37	2.45		64.5459	0.0462
			2.36	2.40		64.4523	0.0459
			2.39	2.35		64.6710	0.0467
			2.35	2.25		64.3246	0.0454
		0.95	2.37	2.45		64.3413	0.0465
			2.36	2.40		64.2437	0.0461
			2.39	2.35		64.4669	0.0469
			2.35	2.25		64.1187	0.0457
2	31	0.97	2.36	2.60		63.8981	0.0468
			2.35	2.55		63.8042	0.0465
			2.34	2.65		63.7502	0.0463
			2.38	2.55		64.0435	0.0474
		0.97	2.36	2.60		63.8981	0.0468
			2.35	2.55		63.8042	0.0465
			2.34	2.65		63.7502	0.0463
			2.38	2.55		64.0435	0.0474
		1.00	2.36	2.60		63.2973	0.0476
			2.35	2.55		63.2019	0.0473
			2.34	2.65		63.1474	0.0471
			2.38	2.55		63.4446	0.0481
		0.98	2.36	2.60		63.6968	0.0471
			2.35	2.55		63.6024	0.0468
			2.34	2.65		63.5481	0.0466
			2.38	2.55		63.8428	0.0476

Whole Milk

20%

Sample	Temp. (°C)	h_c (mm)	h_s (mm)	r(cm)		θ(°)	σ (N/m)
1	30	1.20	2.34	2.45		59.3029	0.0528
			2.31	2.35		58.9991	0.0518
			2.32	2.45		59.1251	0.0522
			2.32	2.40		59.1073	0.0521
		1.15	2.34	2.45		60.2123	0.0514
			2.31	2.35		59.9137	0.0504
			2.32	2.45		60.0373	0.0508
			2.32	2.40		60.0200	0.0508
		1.14	2.34	2.45		60.3971	0.0511
			2.31	2.35		60.0995	0.0501
			2.32	2.45		60.2226	0.0505
			2.32	2.40		60.2054	0.0505
		1.15	2.34	2.45		60.2123	0.0514
			2.31	2.35		59.9137	0.0504
			2.32	2.45		60.0373	0.0508
			2.32	2.40		60.0200	0.0508
2	28	1.12	2.33	2.50		60.6996	0.0504
			2.35	2.35		60.8208	0.0508
			2.35	2.35		60.8208	0.0508
			2.32	2.40		60.5794	0.0500
		1.12	2.33	2.50		60.6996	0.0504
			2.35	2.35		60.8208	0.0508
			2.35	2.35		60.8208	0.0508
			2.32	2.40		60.5794	0.0500
		1.15	2.33	2.50		60.1417	0.0512
			2.35	2.35		60.2637	0.0516
			2.35	2.35		60.2637	0.0516
			2.32	2.40		60.0200	0.0508
		1.12	2.33	2.50		60.6996	0.0504
			2.35	2.35		60.8208	0.0508
			2.35	2.35		60.8208	0.0508
			2.32	2.40		60.5794	0.0500

Whole Milk

25%

Sample	Temp. (°C)	h_c (mm)	h_s (mm)	r(cm)		θ(°)	σ (N/m)
1	27	1.16	2.26	2.40		58.5121	0.0531
			2.31	2.35		58.5789	0.0534
			2.27	2.25		58.3265	0.0525
			2.29	2.30		58.2258	0.0522
		1.15	2.26	2.40		58.3342	0.0535
			2.31	2.35		58.4011	0.0538
			2.27	2.25		58.1478	0.0529
			2.29	2.30		58.0469	0.0526
		1.15	2.26	2.40		59.6918	0.053
			2.31	2.35		59.7585	0.0532
			2.27	2.25		59.507	0.0524
			2.29	2.30		59.4067	0.052
		1.14	2.26	2.40		58.3342	0.0535
			2.31	2.35		58.4011	0.0538
			2.27	2.25		58.1478	0.0529
			2.29	2.30		58.0469	0.0526
2	29	1.13	2.32	2.45		60.4090	0.0509
			2.30	2.55		60.2652	0.0504
			2.26	2.60		59.9218	0.0493
			2.29	2.65		60.2062	0.0502
		1.13	2.32	2.45		60.4090	0.0509
			2.30	2.55		60.2652	0.0504
			2.26	2.60		59.9218	0.0493
			2.29	2.65		60.2062	0.0502
		1.15	2.32	2.45		60.0373	0.0514
			2.30	2.55		59.8927	0.0509
			2.26	2.60		59.5471	0.0498
			2.29	2.65		59.8335	0.0507
		1.14	2.32	2.45		60.2226	0.0511
			2.30	2.55		60.0784	0.0507
			2.26	2.60		59.7339	0.0495
			2.29	2.65		60.0193	0.0505

Whole Milk

30%

Sample	Temp. (°C)	h_c (mm)	H_s (mm)	r(cm)		θ(°)	σ (N/m)
1	30	1.26	2.25	2.55		57.4469	0.0531
			2.27	2.40		57.5822	0.0535
			2.30	2.25		57.8006	0.0543
			2.22	2.30		57.0687	0.0519
		1.27	2.25	2.55		57.2714	0.0534
			2.27	2.40		57.4070	0.0538
			2.30	2.25		57.6257	0.0545
			2.22	2.30		56.8921	0.0522
		1.24	2.25	2.55		57.8005	0.0525
			2.27	2.40		57.9356	0.0530
			2.30	2.25		58.1531	0.0537
			2.22	2.30		57.4247	0.0514
		1.28	2.25	2.55		57.0970	0.0537
			2.27	2.40		57.2327	0.0541
			2.30	2.25		57.4517	0.0548
			2.22	2.30		56.7164	0.0525
2	30	1.25	2.28	2.50		57.8873	0.0537
			2.31	2.45		58.1458	0.0545
			2.28	2.45		57.8698	0.0536
			2.27	2.25		57.6990	0.0531
		1.26	2.28	2.50		57.7116	0.0540
			2.31	2.45		57.9707	0.0548
			2.28	2.45		57.6939	0.0539
			2.27	2.25		57.5225	0.0534
		1.28	2.28	2.50		57.3629	0.0545
			2.31	2.45		57.6231	0.0554
			2.28	2.45		57.3450	0.0545
			2.27	2.25		57.1723	0.0539
		1.29	2.28	2.50		57.1899	0.0548
			2.31	2.45		57.4507	0.0557
			2.28	2.45		57.1719	0.0548
			2.27	2.25		56.9986	0.0542

Whole Milk

35%

Sample	Temp. (°C)	h_c (mm)	h_s (mm)	r(cm)		θ(°)	σ (N/m)
1	30	1.33	2.25	2.45		56.2025	0.0557
			2.25	2.40		56.1835	0.0556
			2.26	2.35		56.2597	0.0559
			2.23	2.30		55.9498	0.0549
		1.35	2.25	2.45		55.8650	0.0563
			2.25	2.40		55.8459	0.0562
			2.26	2.35		55.9222	0.0565
			2.23	2.30		55.6109	0.0555
		1.36	2.25	2.45		55.6976	0.0566
			2.25	2.40		55.6783	0.0565
			2.26	2.35		55.7548	0.0567
			2.23	2.30		55.4428	0.0558
		1.37	2.25	2.45		55.5311	0.0569
			2.25	2.40		55.5117	0.0568
			2.26	2.35		55.5882	0.0570
			2.23	2.30		55.2756	0.0561
2	28	1.38	2.26	2.50		55.4811	0.0575
			2.26	2.60		55.4811	0.0575
			2.23	2.55		55.2066	0.0567
			2.25	2.55		55.4021	0.0573
		1.34	2.26	2.50		56.1478	0.0563
			2.26	2.60		56.1826	0.0565
			2.23	2.55		55.8753	0.0555
			2.25	2.55		56.0693	0.0561
		1.36	2.26	2.50		55.8127	0.0569
			2.26	2.60		55.8477	0.0570
			2.23	2.55		55.5392	0.0561
			2.25	2.55		55.7340	0.0567
		1.35	2.26	2.50		55.9798	0.0566
			2.26	2.60		56.0147	0.0567
			2.23	2.55		55.7068	0.0558
			2.25	2.55		55.9012	0.0564

Whole Milk

40%

Sample	Temp. (°C)	h_c (mm)	H_s (mm)	r(cm)		θ(°)	σ (N/m)
1	30	1.42	2.21	2.45		54.3154	0.0578
			2.23	2.50		54.5335	0.0585
			2.21	2.45		54.3154	0.0578
			2.20	2.50		54.2339	0.0576
		1.46	2.21	2.45		53.6722	0.0590
			2.23	2.50		53.8919	0.0597
			2.21	2.45		53.6722	0.0590
			2.20	2.50		53.5905	0.0588
		1.44	2.21	2.45		53.9921	0.0584
			2.23	2.50		54.2110	0.0591
			2.21	2.45		53.9921	0.0584
			2.20	2.50		53.9105	0.0582
		1.44	2.21	2.45		53.9921	0.0584
			2.23	2.50		54.2110	0.0591
			2.21	2.45		53.9921	0.0584
			2.20	2.50		53.9105	0.0582
2	29	1.45	2.20	2.60		53.7863	0.0586
			2.19	2.55		53.6670	0.0582
			2.18	2.45		53.5274	0.0578
			2.21	2.45		53.8317	0.0587
		1.47	2.20	2.60		53.4683	0.0592
			2.19	2.55		53.3485	0.0588
			2.18	2.45		53.2083	0.0584
			2.21	2.45		53.5135	0.0593
		1.44	2.20	2.60		53.9466	0.0583
			2.19	2.55		53.8275	0.0579
			2.18	2.45		53.6882	0.0575
			2.21	2.45		53.9921	0.0584
		1.45	2.20	2.60		53.7863	0.0586
			2.19	2.55		53.6670	0.0582
			2.18	2.45		53.5274	0.0578
			2.21	2.45		53.8317	0.0587

Whole Milk

45%

Sample	Temp. (°C)	h_c (mm)	H_s (mm)	r(cm)		θ(°)	σ (N/m)
1	46	1.51	2.05	2.47		51.1969	0.0560
			2.00	2.58		50.6744	0.0546
			2.03	2.25		50.8810	0.0551
			2.00	2.2		50.5183	0.0542
		1.50	2.05	2.47		51.3544	0.0557
			2.00	2.58		50.8323	0.0543
			2.03	2.25		51.0390	0.0548
			2.00	2.2		50.6768	0.0539
		1.52	2.05	2.47		51.0404	0.0563
			2.00	2.58		50.5175	0.0549
			2.03	2.25		50.7239	0.0554
			2.00	2.2		50.3608	0.0545
		1.50	2.05	2.47		51.3544	0.0557
			2.00	2.58		50.8323	0.0543
			2.03	2.25		51.0390	0.0548
			2.00	2.2		50.6768	0.0539
2	45	1.52	2.05	2.18		50.9136	0.0560
			1.98	2.43		50.2313	0.0541
			1.99	2.2		50.2463	0.0542
			2.01	2.3		50.5207	0.0549
		1.49	2.05	2.18		51.3873	0.0550
			1.98	2.43		50.7061	0.0532
			1.99	2.2		50.7220	0.0533
			2.01	2.3		50.9952	0.0540
		1.51	2.05	2.18		51.0706	0.0557
			1.98	2.43		50.3887	0.0538
			1.99	2.2		50.4040	0.0539
			2.01	2.3		50.6780	0.0546
		1.51	2.05	2.18		51.0706	0.0557
			1.98	2.43		50.3887	0.0538
			1.99	2.2		50.4040	0.0539
			2.01	2.3		50.6780	0.0546

Whole Milk

50%

Sample	Temp. (°C)	h_c (mm)	H_s (mm)	r(cm)		θ(°)	σ (N/m)
1	45	1.58	1.99	2.5		49.4486	0.0571
			2.02	2.35		49.7310	0.0579
			2.00	2.6		49.6009	0.0575
			2.00	2.55		49.5827	0.0575
		1.59	1.99	2.5		49.2974	0.0574
			2.02	2.35		49.5798	0.0582
			2.00	2.6		49.4499	0.0578
			2.00	2.55		49.4316	0.0578
		1.60	1.99	2.5		49.1470	0.0577
			2.02	2.35		49.4294	0.0585
			2.00	2.6		49.2997	0.0582
			2.00	2.55		49.2814	0.0581
		1.58	1.99	2.5		49.4486	0.0571
			2.02	2.35		49.7310	0.0579
			2.00	2.6		49.6009	0.0575
			2.00	2.55		49.5827	0.0575
2	44	1.57	2.08	2.45		50.5942	0.0596
			2.05	2.35		50.2204	0.0585
			2.10	2.5		50.8324	0.0603
			2.05	2.5		50.2819	0.0587
		1.60	2.08	2.45		50.1428	0.0605
			2.05	2.35		49.7676	0.0595
			2.10	2.5		50.3817	0.0612
			2.05	2.5		49.8298	0.0596
		1.59	2.08	2.45		50.2925	0.0602
			2.05	2.35		49.9178	0.0591
			2.10	2.5		50.5311	0.0609
			2.05	2.5		49.9797	0.0593
		1.59	2.08	2.45		50.2925	0.0602
			2.05	2.35		49.9178	0.0591
			2.10	2.5		50.5311	0.0609
			2.05	2.5		49.9797	0.0593

SOPHIE-LO

Table A-2 10%

Sample	Temp (°C)	h_c (mm)	h_s (mm)	r(cm)		θ(°)	σ (N/m)
1	20	0.65	2.90	2.45		73.8566	0.0547
			2.88	2.45		73.7648	0.0541
			2.90	2.55		73.8779	0.0548
			2.85	2.35		73.6020	0.0530
		0.68	2.90	2.45		73.2252	0.0526
			2.88	2.45		73.1305	0.0548
			2.90	2.55		73.2473	0.0556
			2.85	2.35		72.9625	0.0538
		0.63	2.90	2.45		74.2825	0.0542
			2.88	2.45		74.1927	0.0547
			2.90	2.55		74.3032	0.0543
			2.85	2.35		74.0335	0.0525
		0.66	2.90	2.45		73.6451	0.0549
			2.88	2.45		73.5524	0.0543
			2.90	2.55		73.6667	0.0551
			2.85	2.35		73.3878	0.0533
2	19	0.64	2.88	2.50		73.9889	0.0539
			2.90	2.60		74.1000	0.0546
			2.85	2.35		73.8172	0.0528
			2.84	2.55		73.8143	0.0527
		0.68	2.88	2.50		73.1418	0.0549
			2.90	2.60		73.2577	0.0557
			2.85	2.35		72.9625	0.0538
			2.84	2.55		72.9599	0.0537
		0.69	2.88	2.50		72.9325	0.0552
			2.90	2.60		73.0496	0.0559
			2.85	2.35		72.7513	0.0540
			2.84	2.55		72.7488	0.0540
		0.65	2.88	2.50		73.7756	0.0541
			2.90	2.60		73.8879	0.0549
			2.85	2.35		73.6020	0.0530
			2.84	2.55		73.5991	0.0530

SOPHIE-LO

15%

Sample	Temp (°C)	h_c (mm)	h_s (mm)	r(cm)		θ(°)	σ (N/m)
1	21	0.73	2.80	2.65		71.7295	0.0546
			2.78	2.50		71.5911	0.0538
			2.75	2.55		71.4425	0.0530
			2.78	2.25		71.5263	0.0534
		0.75	2.80	2.65		71.3152	0.0551
			2.78	2.50		71.1742	0.0543
			2.75	2.55		71.0230	0.0535
			2.78	2.25		71.1079	0.0540
		0.73	2.80	2.65		71.7295	0.0546
			2.78	2.50		71.5911	0.0538
			2.75	2.55		71.4425	0.0530
			2.78	2.25		71.5263	0.0534
		0.73	2.80	2.65		71.7295	0.0546
			2.78	2.50		71.5911	0.0538
			2.75	2.55		71.4425	0.0530
			2.78	2.25		71.5263	0.0534
2	20	0.77	2.68	2.60		70.2211	0.0519
			2.72	2.45		70.4146	0.0529
			2.74	2.50		70.5398	0.0536
			2.80	2.35		70.8310	0.0552
		0.76	2.68	2.60		70.4314	0.0516
			2.72	2.45		70.6234	0.0526
			2.74	2.50		70.7475	0.0533
			2.80	2.35		71.0365	0.0549
		0.75	2.68	2.60		71.0365	0.0549
			2.72	2.45		70.8333	0.0524
			2.74	2.50		70.9563	0.0531
			2.80	2.35		70.8231	0.0525
		0.73	2.68	2.60		71.2430	0.0547
			2.72	2.45		70.8333	0.0524
			2.74	2.50		70.9563	0.0531
			2.80	2.35		71.2430	0.0547

SOPHIE-LO

20%

Sample	Temp (°C)	h_c (mm)	h_s (mm)	r(cm)		θ(°)	σ (N/m)
1	22	0.86	2.53	2.55		67.3902	0.0503
			2.55	2.80		67.5834	0.0512
			2.51	2.60		67.2664	0.0498
			2.55	2.60		67.5376	0.0510
		0.85	2.53	2.55		67.5978	0.0501
			2.55	2.80		67.7896	0.0509
			2.51	2.60		67.4747	0.0495
			2.55	2.60		67.7441	0.0507
		0.86	2.53	2.55		67.3902	0.0503
			2.55	2.80		67.5834	0.0512
			2.51	2.60		67.2664	0.0498
			2.55	2.60		67.5376	0.0510
		0.87	2.53	2.55		67.1964	0.0506
			2.55	2.80		67.3784	0.0515
			2.51	2.60		67.0591	0.0501
			2.55	2.60		67.3321	0.0512
2	21	0.85	2.53	2.60		67.6102	0.0501
			2.52	2.55		67.5302	0.0498
			2.54	2.60		67.6774	0.0504
			2.52	2.50		67.5173	0.0497
		0.86	2.53	2.60		67.4028	0.0504
			2.52	2.55		67.3222	0.0500
			2.54	2.60		67.4704	0.0507
			2.52	2.50		67.3092	0.0500
		0.87	2.53	2.60		67.1964	0.0506
			2.52	2.55		67.1153	0.0503
			2.54	2.60		67.2645	0.0509
			2.52	2.50		67.1022	0.0502
		0.84	2.53	2.60		67.8187	0.0499
			2.52	2.55		67.7393	0.0495
			2.54	2.60		67.8854	0.0502
			2.52	2.50		67.7265	0.0495

SOPHIE-LO

25%

Sample	Temp (°C)	h_c (mm)	h_s (mm)	r(cm)		θ(°)	σ (N/m)
1	23	0.98	2.45	2.75		64.4394	0.0519
			2.43	2.40		64.1891	0.0509
			2.44	2.60		64.3245	0.0515
			2.41	2.50		64.0646	0.0505
		0.97	2.45	2.75		64.6371	0.0517
			2.43	2.40		64.3883	0.0507
			2.44	2.60		64.5229	0.0512
			2.41	2.50		64.2643	0.0502
		0.98	2.45	2.75		64.4394	0.0519
			2.43	2.40		64.1891	0.0509
			2.44	2.60		64.3245	0.0515
			2.41	2.50		64.0646	0.0505
		0.95	2.45	2.75		65.0356	0.0511
			2.43	2.40		64.7898	0.0501
			2.44	2.60		64.9227	0.0507
			2.41	2.50		64.6669	0.0497
2	20	0.97	2.43	2.40		64.3883	0.0507
			2.45	2.65		64.6120	0.0516
			2.40	2.55		64.2007	0.0500
			2.42	2.50		64.3416	0.0505
		0.99	2.43	2.40		63.9910	0.0512
			2.45	2.65		64.2173	0.0521
			2.40	2.55		63.8018	0.0505
			2.42	2.50		63.9440	0.0510
		1.00	2.43	2.40		63.7939	0.0515
			2.45	2.65		64.0215	0.0524
			2.40	2.55		63.6040	0.0508
			2.42	2.50		63.7468	0.0513
		1.00	2.43	2.40		63.7939	0.0515
			2.45	2.65		64.0215	0.0524
			2.40	2.55		63.6040	0.0508
			2.42	2.50		63.7468	0.0513

SOPHIE-LO

30%

Sample	Temp (°C)	h_c (mm)	h_s (mm)	r(cm)		θ(°)	σ (N/m)
1	43	1.11	2.34	2.52		60.98	0.0504
			2.31	2.32		60.6528	0.0493
			2.32	2.17		60.6811	0.0494
			2.32	2.23		60.7055	0.0495
		1.1	2.34	2.52		61.1686	0.05
			2.31	2.32		60.8418	0.0489
			2.32	2.17		60.8707	0.049
			2.32	2.23		60.8949	0.0491
		1.12	2.34	2.52		60.7924	0.0506
			2.31	2.32		60.4633	0.0495
			2.32	2.17		60.4916	0.0496
			2.32	2.23		60.5162	0.0496
		1.13	2.34	2.52		30.3288	0.05
			2.31	2.32		60.2759	0.0498
			2.32	2.17		60.3041	0.0499
			2.32	2.23		60.3288	0.05
2	41	1.13	2.33	2.2		60.4032	0.0502
			2.31	2.08		60.1763	0.0494
			2.32	2.42		60.3988	0.0501
			2.31	2.32		60.2754	0.0497
		1.12	2.33	2.2		60.5914	0.05
			2.31	2.08		60.3654	0.0492
			2.32	2.42		60.5867	0.05
			2.31	2.32		60.4638	0.0496
		1.14	2.33	2.2		60.2171	0.0505
			2.31	2.08		59.9893	0.0498
			2.32	2.42		60.2129	0.0505
			2.31	2.32		60.089	0.0501
		1.12	2.33	2.2		60.5914	0.05
			2.31	2.08		60.3654	0.0492
			2.32	2.42		60.5867	0.05
			2.31	2.32		60.4638	0.0496

SOPHIE-LO

35%

Sample	Temp (°C)	h_c (mm)	h_s (mm)	r(cm)		θ(°)	σ (N/m)
1	41	1.20	2.37	2.50		59.5830	0.0561
			2.30	2.60		58.9947	0.0540
			2.41	2.45		59.9092	0.0573
			2.35	2.30		59.3352	0.0552
		1.22	2.37	2.50		59.2276	0.0567
			2.30	2.60		58.6360	0.0546
			2.41	2.45		59.5557	0.0579
			2.35	2.30		58.9779	0.0558
		1.28	2.37	2.50		58.1833	0.0585
			2.30	2.60		57.5827	0.0564
			2.41	2.45		58.5165	0.0597
			2.35	2.30		57.9281	0.0576
		1.28	2.37	2.50		58.1833	0.0585
			2.30	2.60		57.5827	0.0564
			2.41	2.45		58.5165	0.0597
			2.35	2.30		57.9281	0.0576
2	40	1.21	2.39	2.45		59.5608	0.0570
			2.40	2.60		59.6969	0.0575
			2.36	2.50		59.3175	0.0561
			2.32	2.35		58.9090	0.0547
		1.20	2.39	2.45		59.7385	0.0567
			2.40	2.60		59.8740	0.0572
			2.36	2.50		59.4959	0.0558
			2.32	2.35		59.0887	0.0544
		1.23	2.39	2.45		59.2081	0.0576
			2.40	2.60		59.3452	0.0581
			2.36	2.50		58.9634	0.0567
			2.32	2.35		58.5523	0.0552
		1.29	2.39	2.45		58.1713	0.0593
			2.40	2.60		58.3116	0.0599
			2.36	2.50		57.9230	0.0585
			2.32	2.35		57.5043	0.0570

SOPHIE-LO

40%

Sample	Temp (°C)	h_c (mm)	h_s (mm)	r(cm)		θ(°)	σ (N/m)
1	42	1.41	2.32	2.60		55.5997	0.0618
			2.34	2.55		55.7691	0.0624
			2.32	2.45		55.5445	0.0616
			2.35	2.55		55.8618	0.0627
		1.43	2.32	2.60		55.2790	0.0624
			2.34	2.55		55.4489	0.0630
			2.32	2.45		55.2232	0.0622
			2.35	2.55		55.5420	0.0633
		1.40	2.32	2.60		55.7613	0.0614
			2.34	2.55		55.9304	0.0620
			2.32	2.45		55.7063	0.0613
			2.35	2.55		56.0230	0.0624
		1.41	2.32	2.60		55.5997	0.0618
			2.34	2.55		55.7691	0.0624
			2.32	2.45		55.5445	0.0616
			2.35	2.55		55.8618	0.0627
2	41	1.42	2.32	2.40		55.3635	0.0618
			2.31	2.60		55.3445	0.0617
			2.32	2.80		55.5041	0.0623
			2.34	2.50		55.5900	0.0626
		1.39	2.32	2.40		55.8493	0.0609
			2.31	2.60		55.8298	0.0608
			2.32	2.80		55.9879	0.0614
			2.34	2.50		56.0742	0.0617
		1.43	2.32	2.40		55.2032	0.0621
			2.31	2.60		55.1843	0.0621
			2.32	2.80		55.3444	0.0626
			2.34	2.50		55.4302	0.0629
		1.38	2.32	2.40		56.0129	0.0606
			2.31	2.60		55.9932	0.0605
			2.32	2.80		56.1509	0.0610
			2.34	2.50		56.2373	0.0613

SOPHIE-LO

45%

Sample	Temp (°C)	h_c (mm)	h_s (mm)	r(cm)		θ(°)	σ (N/m)
1	53	1.44	2.23	2.47		54.1996	0.0591
			2.25	2.58		54.4379	0.0599
			2.21	2.25		53.9074	0.0582
			2.2	2.2		53.7834	0.0578
		1.43	2.23	2.47		54.3605	0.0588
			2.25	2.58		54.5982	0.0596
			2.21	2.25		54.069	0.0579
			2.2	2.2		53.9452	0.0575
		1.45	2.23	2.47		54.0401	0.0596
			2.25	2.58		54.2789	0.0604
			2.21	2.25		53.7472	0.0587
			2.2	2.2		53.6229	0.0583
		1.43	2.23	2.47		54.3605	0.0588
			2.25	2.58		54.5982	0.0596
			2.21	2.25		54.069	0.0579
			2.2	2.2		53.9452	0.0575
	54	1.42	2.21	2.18		54.1986	0.0575
			2.2	2.43		54.2072	0.0575
			2.19	2.48		54.1254	0.0572
			2.2	2.45		54.215	0.0575
		1.4	2.21	2.18		54.5269	0.0571
			2.2	2.43		54.5348	0.0571
			2.19	2.48		54.4532	0.0568
			2.2	2.45		54.5425	0.0571
		1.43	2.21	2.18		54.036	0.0578
			2.2	2.43		54.0449	0.0578
			2.19	2.48		53.9631	0.0575
			2.2	2.45		54.0527	0.0578
		1.4	2.21	2.18		54.5263	0.0569
			2.2	2.43		54.5343	0.0569
			2.19	2.48		54.4527	0.0566
			2.2	2.45		54.542	0.0569

SOPHIE-LO

50%

Sample	Temp (°C)	h_c (mm)	h_s (mm)	r(cm)		θ(°)	σ (N/m)
1	55	1.58	2.25	2.50		52.2465	0.0657
			2.28	2.60		52.5833	0.0668
			2.21	2.45		51.8212	0.0643
			2.23	2.40		52.0036	0.0649
		1.61	2.25	2.50		51.8029	0.0667
			2.28	2.60		52.1412	0.0678
			2.21	2.45		51.3760	0.0653
			2.23	2.40		51.5589	0.0659
		1.63	2.25	2.50		51.5109	0.0674
			2.28	2.60		51.8501	0.0685
			2.21	2.45		51.0830	0.0659
			2.23	2.40		51.2661	0.0666
		1.59	2.25	2.50		52.0979	0.0660
			2.28	2.60		52.4352	0.0672
			2.21	2.45		51.6721	0.0646
			2.23	2.40		51.8546	0.0652
2	54	1.63	2.25	2.65		51.5686	0.0676
			2.24	2.30		51.3218	0.0667
			2.21	2.50		51.1037	0.0660
			2.26	2.45		51.5905	0.0676
		1.62	2.25	2.65		51.7141	0.0672
			2.24	2.30		51.4678	0.0664
			2.21	2.50		51.2497	0.0657
			2.26	2.45		51.7362	0.0673
		1.58	2.25	2.65		52.3032	0.0659
			2.24	2.30		52.0596	0.0651
			2.21	2.50		51.8415	0.0644
			2.26	2.45		52.3260	0.0660
		1.60	2.25	2.65		52.0072	0.0666
			2.24	2.30		51.7622	0.0657
			2.21	2.50		51.5441	0.0650
			2.26	2.45		52.0296	0.0666

SOPHIE-LO

55%

Sample	Temp (°C)	h_c (mm)	h_s (mm)	r(cm)		θ(°)	σ (N/m)
1	57	1.71	2.20	2.55		49.8778	0.0694
			2.21	2.60		50.0014	0.0698
			2.22	2.60		50.1048	0.0701
			2.20	2.50		49.8574	0.0693
		1.75	2.20	2.55		49.3236	0.0708
			2.21	2.60		49.4477	0.0712
			2.22	2.60		49.5513	0.0715
			2.20	2.50		49.3029	0.0707
		1.75	2.20	2.55		49.3236	0.0708
			2.21	2.60		49.4477	0.0712
			2.22	2.60		49.5513	0.0715
			2.20	2.50		49.3029	0.0707
		1.74	2.20	2.55		49.4611	0.0704
			2.21	2.60		49.5851	0.0708
			2.22	2.60		49.6887	0.0712
			2.20	2.50		49.4405	0.0703
2	59	1.76	2.22	2.65		49.4340	0.0719
			2.23	2.60		49.5179	0.0722
			2.20	2.55		49.1867	0.0711
			2.22	2.40		49.3297	0.0716
		1.76	2.22	2.65		49.4340	0.0719
			2.23	2.60		49.5179	0.0722
			2.20	2.55		49.1867	0.0711
			2.22	2.40		49.3297	0.0716
		1.70	2.22	2.65		50.2638	0.0698
			2.23	2.60		50.0698	0.0698
			2.20	2.55		50.0182	0.0690
			2.22	2.40		50.1616	0.0695
		1.74	2.22	2.65		49.7078	0.0712
			2.23	2.60		49.7917	0.0715
			2.20	2.55		49.4611	0.0704
			2.22	2.40		49.6043	0.0709

APPENDIX- B

The density model coefficients for Whole milk, Sophie-Lo and water are listed in table 1 and 3 respectively. Table 2 consist of density constants for milk constituents. Sample calculation with 10%(w/w) Whole milk is shown and the results with both Whole milk and Sophie-Lo are listed in the table 4.

Table 1: Density model coefficients

Milk	Fat (%)	Lactose (%)	Protein (%)	Salt (%)	Experimental (a_{ts})	55°c Model (a_{ts})	65°c Model (a_{ts})
Whole	27.7	38.4	27.9	6	0.24187	0.2242	0.2258
Sophie-Lo	24.6	52	17.4	6	0.26518	0.2396	0.2544

Table 2: Density constants of milk constituents

CONSTANT	Fat (%)	Lactose (%)	Protein (%)	Salt (%)
a_i	925.59	1599.1	1329.9	2423.8
b_i	-0.31046	-0.31046	-0.5184	-0.28063

Table 3: Density constants of water

$$A_{water} = 1000.59343115042$$

$$B_{water} = -0.07053672161237$$

$$C_{water} = -0.00359723304621$$

Sample calculation

Product type : Whole milk
T : 65°C
w_{TS} : 10%

$\rho_{water} = A_{water} + B_{water}T + C_{water}T^2$ Where, $A_{water} = 1000.59343115042$

$B_{water} = -0.07053672161237$

$\rho_{water} = 980.4$ kgm^{-3} $C_{water} = -0.00359723304621$

$$\rho = \frac{\rho_{water}}{(1 - a_{TS}.w_{TS})}$$

From the table 1, $a_{TS} = 0.24187$

$$\rho = \frac{980.4}{(1 - 0.24187x0.01)}$$

$\rho = 1005.1$ kgm^{-3}

Table 4: Density of Whole milk and Sophie-Lo from model prediction

TOTAL SOLIDS (%)	WHOLE MILK (KGM^{-3})		SOPHIE-LO(KGM^{-3})	
	65°C	55°C	65°C	55°C
10	1005.121	-	1007.09	-
15	1017.734	-	1020.996	-
20	1030.668	-	1035.291	-
25	1043.934	1049.28	1049.993	1055.28
30	1057.547	1062.962	1065.118	1070.481
35	1071.519	1077.006	1080.685	1086.127
40	1085.866	1091.426	1096.714	1102.237
45	1100.601	1106.237	1113.226	1118.832
50	-	1121.456	-	1135.934
55	-	-	-	1153.567

APPENDIX C

The specific volumes of the milk constituents that are used in the viscosity calculations are given in table 1. Sample calculation with 10% Whole milk is shown and the viscosity results with both Whole milk and Sophie-Lo are tabulated in table 2.

Table 1: Specific volumes of milk components.

Milk constituents	Inverse of specific density (l/kg)	Experimental specific volume (l/kg)
Milkfat	1.039	-
Casein protein	0.784	3.57
Whey protein	0.784	1.07
Denatured whey protein	0.784	3.09

Sample calculation

Milk product : Whole milk
T : 65°C
Solid content : 10%

From Table 1, Protein : 27.9%
Fat : 27.7%
Lactose : 38.4%

From Table 3, v_{cas} : 3.57
v_{whey} : 3.09 (Denatured whey protein)
v_{fat} : 1.039

And $d_1=1$, $a_{TS} = 0.24187$, $\mu_{water} = 0.4$ CP, $\phi_{\max} = 0.79$

$$\mu_{TS} = v_{cas}.x_{cas} + v_{whey}.x_{whey} + v_{fat}.x_{fat}$$

$$\mu_{TS} = (3.57 * (0.83 * 0.279) + 3.09 * (0.17 * 0.279) + 1.039 * 0.277) \div 1000$$

$$\mu_{TS} = 0.001261$$

$$\Phi = \mu_{TS}.w_{TS}.\rho$$

$$\mu = \mu_{water}\left[1 + d_1.w_{TS}\right]\left[1 + \frac{1.25\mu_{TS}.w_{TS}.\rho_{water}}{1 - \left(a_{TS} + \frac{\mu_{TS}.\rho_{water}}{\Phi_{\max}}\right)w_{TS}}\right]^2$$

$$\mu = 0.0004\left[1 + 1 * 0.01\right]\left[1 + \frac{1.25 * 0.001261 * 0.01 * 978.7312}{1 - \left(0.24187 + \frac{0.001261 * 978.7312}{0.79}\right) * 0.01}\right]^2$$

$$\mu = 0.0006213 \text{ Kg m}^{-1} \text{ s}^{-1}$$

Table 2: Viscosity of Whole milk and Sophie-Lo from model prediction

Total solids (%)	Whole milk ($kgm^{-1}s^{-1}$)		Sophie-lo($kgm^{-1}s^{-1}$)	
	65°C	55°C	65°C	55°C
10	0.0007	-	0.0007	-
15	0.001	-	0.00085	-
20	0.00148	-	0.0012	-
25	0.0019	0.0023	0.0015	0.0017
30	0.003	0.0035	0.0018	0.0023
35	0.005	0.006	0.0025	0.003
40	0.01	0.013	0.0034	0.004
45	0.03	0.035	0.005	0.006
50	-	0.35	-	0.009
55	-	-	-	0.017

APPENDIX-D

The sample calculation of surface tension and contact angle is shown here 10% Whole milk. The results of contact angle, surface tension and measurement errors with both Whole milk and Sophie-Lo are tabulated in tables 1, 2, and 3 respectively. The values are estimated at evaporator operating temperatures.

Sample Calculation

Product type : Whole Milk
T : 28°C
Total Solids : 10%
$h_C = 0.00087$ m $h_S = 0.00244$ m r =0.0 245 m $\Delta\rho = 1010 kg/m^3$
$\rho_v = 0.1825 kg/m^3$

From Capillary rise method (5),

$$Sin\theta = 1 - \left(\frac{h_c}{a}\right)^2$$

Sessile drop profile method (4),

$$Sin\frac{\theta}{2} = \frac{h_s}{2a} - \frac{a}{3r}\left(\frac{1 - Cos^3\frac{\theta}{2}}{Sin\frac{\theta}{2}}\right)$$

Where, $a = \left(\frac{\sigma}{\Delta\rho}\right)^{\frac{1}{2}}$

The above two equations were solved simultaneously for two unknowns θ and σ

$$\theta = 67.5258^{\circ} \text{ and } \sigma = 0.0459 \text{ N/m}$$

Table 1: Contact angle of Whole milk and Sophie-Lo at 65°C and at 55°C.

TOTAL SOLIDS (%)	WHOLE MILK (°)		SOPHIE-LO(°)	
	65°C	55°C	65°C	55°C
10	61.7658	-	69.03499	-
15	60.3821	-	66.63308	-
20	56.72739	-	62.96298	-
25	55.35912	-	59.72162	-
30	53.99129	-	57.06478	-
35	52.27193	53.27193	56.32191	57.32191
40	50.34544	51.34544	53.17388	54.17388
45	-	48.76635		53.21621
50	-	47.84799	-	51.77904
55	-	-	-	49.60258

Table 2: Surface tension of Whole milk and Sophie-Lo at 65°C and at 55°C.

TOTAL SOLIDS (%)	WHOLE MILK (N/m)		SOPHIE-LO(N/m)	
	65°C	55°C	65°C	55°C
10	0.041396	-	0.04809	-
15	0.041543	-	0.047596	-
20	0.045209	-	0.044718	-
25	0.044643	-	0.045362	-
30	0.047765	-	0.044193	
35	0.050079	0.057095	0.050609	0.050609
40	0.051917	0.05919	0.054983	0.054983
45	-	0.055339		0.051495
50	-	0.0595	-	0.058793
55	-	-	-	0.062867

Table 3: Measurement errors associated with Contact angle and Surface tension for Whole milk and Sophie-Lo at 65°C

SOLIDS (W/W%)	WHOLE MILK		SOPHIE-LO	
	Contact angle	Surface tension	Contact angle	Surface tension
10	2.538315	0.003487	1.365732	0.002813
15	1.139577	0.001844	1.271457	0.002884
20	1.565417	0.002009	0.665399	0.001661
25	0.924047	0.001884	1.116918	0.002028
30	1.072651	0.002956	2.861891	0.001336
35	0.841036	0.001818	2.173288	0.004737
40	0.900074	0.001581	0.885753	0.002151
45	0.974007	0.002461	0.824947	0.003045
50	1.342588	0.003686	1.154253	0.003165
55	-	-	0.896462	0.002592

APPENDIX-E

Sample calculations of minimum peripheral flow with 10% Whole milk using both Hartley and Murgatroyd are shown here. The results with both Whole milk and Sophie-Lo are tabulated in table 1 using Hartley and Murgatroyd model and the results using Hoke and Chen model are listed in table 2.

Sample calculation: Hartley and Murgatroyd:

Product type : Whole milk
Solid content : 10%(w/w)
T : 65°C

From previous results,

$\rho = 1005.121 kgm^{-3}$ $\mu = 0.0006212 kgm^{-1}s^{-1}$ $\theta = 61.77^{o}$
$\sigma = 0.0414 Nm^{-1}$

$$\Gamma_{H\&M} = 1.69\left(\frac{\mu\rho}{g}\right)^{\frac{1}{5}}\left(\sigma(1-Cos\theta)\right)^{\frac{3}{5}}$$

$$\Gamma_{H\&M} = 1.69\left(\frac{0.0006212\times 1005.121}{9.81}\right)^{0.2}\left(0.0414\times(1-Cos61.77)\right)^{0.6}$$

$$\Gamma_{H\&M} = 0.100552 kgm^{-1}s^{-1}$$

Sample calculation: Hoke and Chen:

Product type : Whole milk
Solid content : 10%(w/w)
T : 65°C

From previous results,

$\rho = 1005.121 kgm^{-3}$ $\mu = 0.0006212 kgm^{-1}s^{-1}$ $\theta = 61.77^{o}$
$\sigma = 0.0414 Nm^{-1}$

$$\sigma[1-\cos(\theta)] = \frac{\rho.g}{4}\left[\frac{\delta}{1-\cos(\theta)}\right]^{2}[2.\theta-\sin(2.\theta)] + \frac{\rho^{3}.g^{2}.\delta^{5}}{15.\mu^{2}}$$

The above equation was solved for film thickness knowing all physical properties.

$\delta = 0.2751 mm$

$$\Gamma_{H\&C} = \frac{\rho^2.g.\delta^3}{3.\mu}$$

$$\Gamma_{H\&C} = \frac{1005.121^2 * 9.81 * 0.0002751^3}{3 * 0.0006212}$$

$$\Gamma_{H\&C} = 0.098256 kgm^{-1}s^{-1}$$

Table 1: Minimum peripheral flow for Whole milk and Sophie-Lo from Hartley and Murgatroyd model.

TOTAL SOLIDS (%)	WHOLE MILK (Kg/m/s)		SOPHIE-LO(Kg/m/s)	
	65°C	55°C	65°C	55°C
10	0.100552	-	0.123928	-
15	0.105855	-	0.123676	-
20	0.112782	-	0.120472	-
25	0.114834	-	0.120325	-
30	0.127776	-	0.117222	
35	0.140815	0.161533	0.134234	0.142083
40	0.158911	0.185405	0.141185	0.14905
45	-	0.205429		0.152814
50	-	0.333751	-	0.174575
55	-	-	-	0.197296

Table 2: Minimum peripheral flow for Whole milk and Sophie-Lo from Hoke and Chen model.

TOTAL SOLIDS (%)	WHOLE MILK (Kg/m/s)		SOPHIE-LO(Kg/m/s)	
	65°C	55°C	65°C	55°C
10	0.098256	-	0.121881	-
15	0.102374	-	0.121097	-
20	0.107239	-	0.116527	-
25	0.110235	-	0.115056	-
30	0.116047	-	0.110608	-
35	0.120886	0.137987	0.124789	0.131634
40	0.119055	0.135201	0.127613	0.133462
45	-	0.08335	-	0.133869
50	-	0.015639	-	0.139057
55	-	-	-	0.131695

APPENDIX F

The experimental measurements at Kiwi Co-op Dairies Ltd. Powder 3A Plant are listed here. The results of refractometer calibration and the flows after each pass with both Whole milk and Sophie-Lo are also tabulated.

Table 1: Calibration of Refractometer readings against Total solids

NUMBER OF PASSES	*WHOLE MILK*		*SOPHIE-LO*	
	R. Index Reading	T.Solids (w/w%)	R.Index Reading	T.Solids (w/w%)
0	10	12	9	8.95
1	13.5	17	13	13.03
2	20.5	23	19	19.31
3	23.5	26	24	25.13
4	29	32	32	32.99
5	36.5	39	37.5	37.26
6	42.5	44	45.5	46.42
7	43.5	45	-	-
8	45.5	46	49.5	48.14

Table 2: Measurements with Sophie-Lo on 07-12-2000 at 1.45pm

NUMBER OF PASSES	SAMPLE 1	SAMPLE 2	SAMPLE 3	SAMPLE 4
0	9	8.7	9	9
1	13	13	13	13
2	18	19	18	18.5
3	23.5	24	23.5	24
4	30.5	32	32	32.5
5	37	38	37	38
6	45	45.5	45.5	46
7	47.5	48	48	48.5
8	49	50	49.5	47

Table 3: Measurements with Whole milk on 19-11-2000 at 2.15pm

NUMBER OF PASSES	SAMPLE 1	SAMPLE 2	SAMPLE 3	SAMPLE 4
0	10	9.9	10.1	10
1	15.5	15.5	15	15.5
2	22	21.5	22.5	22
3	28	28	27.5	28.5
4	33	33	32.5	33.5
5	40	40	40	40
6	44	44.5	43.5	44
7	45.5	45	45	44.5
8	46.5	46.5	46.5	46.5

Table 4: Measurements with Whole milk on 19-11-2000 at 9pm

NUMBER OF PASSES	SAMPLE 1	SAMPLE 2	SAMPLE 3	SAMPLE 4
0	11	11	11	11
1	15	15	15.5	15.5
2	22	22.5	22	22
3	25	25.5	25	24.75
4	34	34	34	34
5	36.5	36.5	36.75	36.5
6	43.5	43.75	43.5	43.5
7	45	45	45	45.2
8	46	46.5	45.75	46

Table 5: Measurements with Whole milk on 05-12-2000 at 1.30pm

NUMBER OF PASSES	SAMPLE 1	SAMPLE 2	SAMPLE 3	SAMPLE 4
0	10.5	10.75	10.5	10.5
1	15	15	15	15.2
2	22	22	22.5	22
3	28	28.5	27.75	28
4	32	32	32.5	31.75
5	39	39	38.75	39.5
6	43.5	43.5	43.5	43.75
7	45	45	45.5	45
8	45.5	45.5	45.7	45.4

Table 6: Measurements with Whole milk on 06-12-2000 at 4.35am

NUMBER OF PASSES	SAMPLE 1	SAMPLE 2	SAMPLE 3	SAMPLE 4
0	10.75	10.75	10.75	10.5
1	14.5	14.5	14.5	14.5
2	21	21	21	20.75
3	26	26	25.75	26
4	31.5	31	31.5	31.5
5	36	36.5	36	36
6	44	43.75	44	44
7	45	45	45	45
8	45	45.5	45	45

Experimental flows with Whole milk on 19-11-2000

NUMBER OF PASSES	*2.15PM*		*9PM*	
	T.Solids (w/w%)	Flow (L/hr)	T.Solids (w/w%)	Flow (L/hr)
0	11.67709	51895.32	12.669057	53131.581
1	19.05	31250.34	18.5	35884.968
2	24.52	23943.59	24.52	26630.65
3	30.75	18786.26	27	24030.152
4	36.6	15541.53	37.5	16831.711
5	41.89	13388.54	39	16097.775
6	45.8	12055.55	45	13683.885
7	47.36	11608.19	46.5	13162.703
8	48.22	11374.6	48	12709.092

Experimental flows with Whole milk on 05-12-2000

NUMBER OF PASSES	*1.30PM*		*AFTER 14HR RUN*	
	T.Solids (w/w%)	Flow (L/hr)	T.Solids (w/w%)	Flow (L/hr)
0	12.17076	51352.58	12.44022	51245.059
1	18.5	33277.09	18	34950.431
2	24.52	24726.62	23.9	25930.57
3	30.75	19400.63	29.5	20760.862
4	36.5	16119.22	35	17202.853
5	41	14160.25	38.8	15361.768
6	45	12698.63	45.8	12706.336
7	46.6	12208.54	46.2	12581.571
8	47.36	11987.82	46.6	12460.103

Experimental flows with Sophie-Lo on 19-11-2000

NUMBER OF PASSES	*1.30PM*			
	T.Solids (w/w%)	Flow (L/hr)	T.Solids (w/w%)	Flow (L/hr)
0	8.4744701	54227.551		
1	13.03	34593.843		
2	18.515	24158.99		
3	24.815	17687.698		
4	32.745	13107.412		
5	37.375	11324.452		
6	46.3975	8854.9542		
7	47.725	8552.8644		
8	48.285	8439.6625		

Appendix G

The simple energy balance across the preheat section to estimate the mass of steam injected in to the DSI unit is shown here. The table 1 shows the average total solids contents in each pass and the Heat transfer coefficients of Whole milk close to the start-up of a run and after 14hr of the same run.

M_f=14.05 Kg/s T_{preH}=62°C T_{evpF}=76°C
C_{pw}=4.2J/Kg.k P_{DSI}=9bar Latent energy=2090KJ/Kg

From the overall energy balance across the preheat section (DSI and flash vessels)

Energy with out stream- Energy with feed = Latent energy from steam + energy due to tem. drop in steam supp.

$$(14.05+m_S)\times 4.2\times 76-14.05\times 4.2\times 62=m_S\times\left(\frac{2090}{4.2}\right)+m_S\times 4.2\times(158-95)$$

$$14.05\times(76-62)+76\times m_S=m_S\times(497.62+63.2)$$

$$m_S=0.4Kg/s$$

Mass of steam injected in DSI (m_S) When pressure is 9bar =0.4Kg/s
Mass of steam injected in DSI (m_S) When pressure is 6bar =0.38Kg/s

Table 1: Heat transfer coefficient of Whole milk close to the start-up of the run and after 14 hr run on 05-12-2000

PASSES	HTC(W/M^2.K) start of the run		HTC(W/M^2.K) After14hr run	
	Average Total Solids in the pass	*HTC*	*Average Total Solids in the pass*	*HTC*
1	15.33538	2378.513	15.22011	1941.859
2	21.51	1257.063	20.95	1244.937
3	27.635	1147.42	26.7	1058.294
4	33.625	909.4144	32.25	908.2606
5	38.75	762.8942	36.9	682.7786
6	43	708.671	42.3	985.6004
7	45.8	838.2001	46	168.7641
8	46.98	573.7137	46.4	252.1945